RADC-TR-81-170
Final Technical Report
July 1981

FIELD EMISSION COLD CATHODE DEVICES BASED ON EUTECTIC SYSTEMS

Fulmer Research Institute Ltd

Duncan Stewart
Vivian G. Rivlin
Paul D. Wilson

APPROVED FOR PUBLIC RELEASE; DISTRIBUTION UNLIMITED

SEP 3 0 1981

A

ROME AIR DEVELOPMENT CENTER
Air Force Systems Command
Griffiss Air Force Base, New York 13441

This report has been reviewed by the RADC Public Affairs Office (PA) and is releasable to the National Technical Information Service (NTIS). At NTIS it will be releasable to the general public, including foreign nations.

RADC-TR-81-170 has been reviewed and is approved for publication.

APPROVED:

JOSEPH J. HUTTA
Project Engineer

APPROVED:

FREEMAN D. SHEPHERD
Acting Director
Solid State Sciences Division

FOR THE COMMANDER:

JOHN P. HUSS
Acting Chief, Plans Office

REPORT DOCUMENTATION PAGE	READ INSTRUCTIONS BEFORE COMPLETING FORM

1. REPORT NUMBER	2. GOVT ACCESSION NO.	3. RECIPIENT'S CATALOG NUMBER
RADC-TR-81-170	AD-A104795	

4. TITLE (and Subtitle)

FIELD EMISSION COLD CATHODE DEVICES BASED ON EUTECTIC SYSTEMS

5. TYPE OF REPORT & PERIOD COVERED

Final Technical Report
1 May 77 — 31 Dec 79

6. PERFORMING ORG. REPORT NUMBER

R744/4

7. AUTHOR(s)

Duncan Stewart
Vivian G. Rivlin
Paul D. Wilson

8. CONTRACT OR GRANT NUMBER(s)

Grant AFOSR-77-3292

9. PERFORMING ORGANIZATION NAME AND ADDRESS

Fulmer Research Institute Ltd
Stoke Poges.Slough SL2 4QD. U.K.

10. PROGRAM ELEMENT, PROJECT, TASK AREA & WORK UNIT NUMBERS

62702F
46001722

11. CONTROLLING OFFICE NAME AND ADDRESS

Deputy for Electronic Technology (RADC/ESM)
Hanscom AFB MA 01731

12. REPORT DATE

Jul 1981

13. NUMBER OF PAGES

85

14. MONITORING AGENCY NAME & ADDRESS(if different from Controlling Office)

Same

15. SECURITY CLASS. (of this report)

UNCLASSIFIED

15a. DECLASSIFICATION/DOWNGRADING SCHEDULE

N/A

16. DISTRIBUTION STATEMENT (of this Report)

Approved for public release; distribution unlimited.

17. DISTRIBUTION STATEMENT (of the abstract entered in Block 20, if different from Report)

Same

18. SUPPLEMENTARY NOTES

Sponsored by AFOSR (AFSC), USAF through EOARD (London).

RADC Project Engineer: Joseph J. Hutta (ESM)

19. KEY WORDS (Continue on reverse side if necessary and identify by block number)

Field Emission	Eutectic Systems
Cold Cathode	Rod Eutectics
Electron Emitter Array	Directionally Solidified Eutectics
Multiple Emitter Cathode	Unidirectionally Solidified Eutectics
Needle Array Cathode	(see reverse)

20. ABSTRACT (Continue on reverse side if necessary and identify by block number)

A survey has been made of the performance as field emission cold cathodes of selected refractory materials fabricated as needle arrays by unidirectional solidification.

Cathodes based upon refractory metal carbides have been fabricated and tested. Performance data has been obtained using niobium, tantalum and vanadium carbides with various cathode geometries. Life times of over 1,000 hours and current densities of up to 1 Acm^{-2} have been obtained. →

Item 19 (cont'd)

Fibre Eutectic Cathode	Niobium Carbide
Segmented Cathode	Tantalum Carbide
Whisker Composites	Vanadium Carbide
In Situ Composites	Lanthanum Hexaboride
Refractory Metal Carbides	

Item 20 (cont'd)

Preliminary experiments indicated that LaB_6 can be formed into platelets by conventional cooling in an aluminum matrix and that directional solidification should produce suitable rod-like morphology.

SUMMARY

A review has been made of the published data on the physical
characteristics of various refractory compounds that could be
prepared as cold cathode needle arrays by directional solid-
ification. The literature survey was restricted to alloys
containing one or more of the non-metallic elements carbon,
boron and nitrogen together with the transition metals from
Groups IVA, VA, and VIA as well as rhenium from Group VIIA.
On the basis of the information available, it was concluded
that the six refractory compounds having the greatest promise
for cold cathode materials were Nb_2C, NbC, TaC, HfC, HfB_2 and
TaB_2. In addition in view of the reported behaviour of LaB_6
as a cathode material, the available data on this compound
were also reviewed in an Appendix.

Both stability and endurance tests have been carried
out on a number of fine needle arrays fabricated at Fulmer and
including NbC, TaC, VC and a nickel-based alloy containing molybdenum
fibres designated A77-205. The maximum current density obtained from
the four systems tested were: VC 5.8, TaC 0.5, NbC 1.3×10^{-2} and
A77-205 6.8×10^{-3} Acm^{-2}. Life tests on VC and NbC have demonstrated
operation of the carbides for 1,000 hours at current densities of 0.5 and
$4 \times 10^{-3} Acm^{-2}$ respectively. The comparatively poor performance of the
A77-205 alloy can be attributed to the irregularity of the fibre alignments
and the excessive erosion of the fibres compared with those made from the
refractory carbides. However, the conclusions from the carbide fibres may
reflect the improvements achieved during the progress of the work as much
as the real characteristics of the three refractory carbides.
In particular, the poor relative performance of the NbC fibres
is almost certainly largely due to the failure to produce fibres
with as fine tips as those in TaC and VC. The
samples of TaC eventually produced showed a considerable improvement

over earlier fibres which had a closer and more uneven fibre distribution as well as coarser fibre tips. The advantages of operation in an ultra high vacuum were also demonstrated by the use of two vacuum systems, one yielding pressures of about 10^{-9} torr and the second giving only 10^{-6} torr. The stability of the cathode in the high vacuum was considerably better. Electron spectra measurements on a TaC sample also demonstrated the need for as uniform a distribution as possible of identical needle-shaped fibres in an array.

A survey of earlier work and preliminary experiments to examine the feasibility of preparing LaB_6 in a suitable array form indicated that platelets could be obtained by conventional cooling of LaB_6 ingots. Consequently under directional solidification conditions, the LaB_6 compound may be produced with a suitable rod-like morphology.

CONTENTS

CONTENTS (continued)

iv

LIST OF TABLES

LIST OF FIGURES

LIST OF FIGURES (Continued)

LIST OF FIGURES (Continued)

1. INTRODUCTION

The advantages of operating field emission cold cathodes as substitutes for the conventional thermal cathodes was first discussed by Charbonnier et al in 1963 [1]. More recently, Considine and Balsinger [2] summarized the advantages of using field emission sources in high density, small diameter electron beams and Shelton [3] and Wardly [4] have outlined other applications for cathodes of this type. The three major advantages of cold cathodes are as follows:-

i) A cold cathode does not require a heater to emit electrons so that the associated tube technology may be simplified.

ii) The absence of a heater implies instant start thus eliminating the time delay involved in switching on a thermal cathode. In addition, failure due to heater burn-out is eliminated.

iii) The cold cathode is more robust mechanically.

Progress in the development of cold cathodes has been limited by the materials available for their construction. Earlier work [5] was concentrated on the use of tungsten as the emitting needle both in the form of a multipin array or as a single point emitter of the type used in electron microscopes and some display tubes. With tungsten however, there is the need to use an ultra-high vacuum environment of around 10^{-9} torr to reduce damage to the tip by ion bombardment. Attempts [6,7] to use carbon fibre cathodes were generally unsuccessful due to the "noise" generated by the fibre and silicon cathodes [8] prepared by etching techniques were not resistant to ion bombardment. Japanese workers [9,10] have claimed that a single fabricated point of titanium carbide works satisfactorily at pressures of 10^{-6} torr which is more readily obtained than the ultra-high vacuum required for tungsten components.

1.

Materials with properties similar to those of titanium carbide appear therefore to have potential both as single point emitters and as broad sources for use in devices that operate at higher power. An attractive method of producing multi-needle arrays of fine points is by the directional solidification of suitable eutectic alloys which is a technique that has been extensively investigated in recent years to produce materials for use in high temperature gas turbines. Such materials, especially the refractory metal carbides have been studied at Fulmer to produce composites of high strength and good corrosion resistance, the structures of which are clearly of interest in the fabrication of cold cathode needle arrays.

The Fulmer work to date to fabricate needle arrays in conducting materials which would appear to be suitable to cold cathode applications together with the results of tests on suitable samples, is described in the present report. Initially, a survey of the literature was made [11] to identify refractory compounds with suitable physical properties that could be prepared by directional solidification. The properties of the needle and matrix materials considered as essential for good cathode performance were as follows:-

Needles   a)   A melting point above $2000^{\circ}C$.

         b)   A low vapour pressure.

         c)   High strength to give adequate stiffness.

         d)   A low sputter yield to resist ion damage.

         e)   Electrically conducting but not necessarily metallic.

         f)   Chemically inert to allow selective etching of matrix.

         g)   A low work function.

Matrix   i)   A melting point above $800^{\circ}C$.

        ii)   A low vapour pressure at around $500^{\circ}C$.

     iii)   Suitable for selective etching.

From the data obtained in the literature survey, a selection of materials was made for fabrication trials and apparatus was specially designed to investigate the operating life-times and field electron emission characteristics of suitable samples. Cold cathodes consisting of both single needles and multi-arrays of needles were included.

2.   THEORETICAL BASIS FOR CHOICE OF MATERIALS

2.1 Literature Survey

The literature survey[11] was aimed at identifying systems with a eutectic reaction between a refractory component and a conducting metal. In addition it was necessary to assess the likelihood of a given system being suitable for fabrication of needle arrays by plane front unidirectional solidification at practicable temperature gradients and solidification rates to give a rod-like morphology. Other characteristics were noted such as the physical properties of the refractory compound and its field emission behaviour if known.

The search was restricted to alloys containing one or more of the non-metallic elements carbon, boron or nitrogen and to the transition metals from Groups IV, VA and VIA together with rhenium from Group VIIA. These metals are known to form carbides and nitrides of high melting point and many systems have been reported in which these refractory compounds form eutectics with metals suitable for cathode materials. In addition, many examples were found in which unidirectional solidification has yielded rod-like formations of carbides; studies have also been made of one boride system but apparently none involving nitrides. Of the ternary systems involving boron, carbon or nitrogen with the refractory metals, numerous

data have been reported indicating eutectic equilibria suited to unidirectional solidification.

Physical property data on carbides, borides and nitrides are recorded in Tables 1, 2 and 3 respectively, details of eutectic equilibria in binary systems in Tables 4 and 5 and in ternary systems in Tables 6, 7 and 8. The results of unidirectional solidification experiments on ternary and multicomponent systems are summarized in Tables 10 and 11 respectively.[12 - 61]

2.2 Discussion of Data

Materials for cold cathode applications must have a long operating lifetime. Tungsten and tantalum carbide can be operated successfully as field emitters in high vacuum largely because of their very low metal vapour pressures even at elevated temperatures. The operating temperatures at the tips of needle arrays are uncertain so a deliberately pessimistic temperature of $3000^{\circ}K$ was assumed to make an assessment of the expected performance of candidate materials under the most severe working conditions. (It is expected however, that in practice the operating temperature may be much lower than this and even as low as $900^{\circ}K$).

For a refractory compound, the equilibrium constant representing its degree of dissociation into its constituents in vacuo at $3000^{\circ}K$ is a very relevant parameter. The equations involved are:

$$MC \text{ (condensed)} \rightleftharpoons M\text{(gaseous)} + C \text{ (condensed)}$$

$$MN \text{ (condensed)} \rightleftharpoons M\text{(gaseous)} + N \text{ (gaseous)}$$

$$MB_2 \text{ (condensed)} \rightleftharpoons M\text{(gaseous)} + 2B \text{ (condensed)}$$
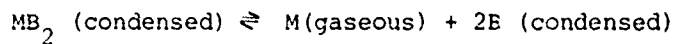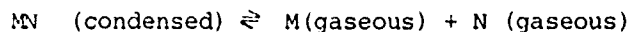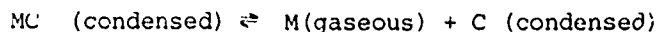
Storms[17] has reviewed the reactions for carbides and quotes the reaction pressure for the metallic element at $3000^{\circ}K$ as follows:

Carbide	Reaction Pressure of metal at $3000^{\circ}K$, torr
TaC	1.3×10^{-6}
NbC	7.6×10^{-4}
ZrC	4.0×10^{-4}

4.

HfC	1.4×10^{-3}
TiC	2.1×10^{-1}
VC	1.0

On the basis of the above figures, TaC has the lowest reaction pressure at 3000°K and should therefore be the most stable of the six carbides listed. As no comparable data for the borides and nitrides was found in the literature, calculations were made from available thermodynamic data with the following results:

Compound	Reaction Pressure of metal at 3000°K, torr
TiB_2	1.4×10^{-2}
TiC	2.1×10^{-1}
TiN	2.5×10^{-1}
ZrB_2	1.3×10^{-5}
ZrC	2.4×10^{-4}
ZrN	6.3×10^{-3}

From these calculations it appears that the borides are more stable than the carbides and the nitrides are the least stable of the compounds. It will be observed also that the compounds of zirconium are markedly more stable than those of titanium. No corresponding figures are available for WC, but rapid evaporation is reported [17] at 2400°C and above although very little metal evaporates below 2700°C. The molybdenum carbides are known to be unstable and chromium carbides have relatively low melting points. Thus the compounds of the Group VI A metals do not appear to have as suitable characteristics as those of the other refractory metals.

If the six best carbides are selected on the melting point criterion, their suitability is in a similar order to that given by the metal reaction pressures, i.e.

$$HfC > TaC > NbC > ZrC > TiC > Nb_2C$$
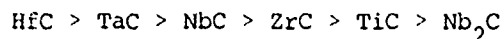
On the same basis, the orders for the borides and nitrides are:

$$HfB_2 > TaB_2 > ZrB_2 > NbB_2 > TiB_2 > VB_2 \text{ and}$$

$$HfN > TaN \gtrsim TiN \gtrsim ZrN > VN \gtrsim NbN$$
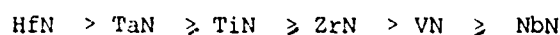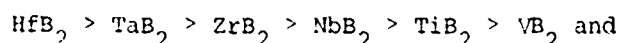
Comparison of the three types of compound indicates that the carbides have the highest melting point and the nitrides the lowest. Few other physical property data are known but generally the borides have the lowest electrical resistivities and the nitrides the highest.

From the available information on stability, nitrides appear to be least favourable for cold cathode application. There may also be problems with unidirectional solidification of nitrides in that a high pressure atmosphere of nitrogen may be required to prevent their decomposition. It is suggested that the most promising candidates are the carbides and borides of tantalum, hafnium and niobium together with zirconium carbide.

The choice of matrix metal would appear to be wider but most of the refractory compounds considered give eutectic equilibria with Ni, Cr and Co. These three metals also have cubic symmetry which would favour the desired rod-like morphology of the eutectic. Examination of Tables 1 to 2 shows that the linear expansion coefficients for all the refractory compounds are around 10×10^{-6} $\deg^{-1}$ or less. Of the metallic elements, those with coefficients of the same order include Cr, W, Ti and Mo but the expansions of Ni and Co are both higher. All the metals considered [62] have very low vapour pressures at $500°C$ ($<10^{-9}$ torr).

On the basis of all the above considerations, the list of most suitable systems for experimental work is

Nb_2C with niobium

NbC with cobalt, chromium or nickel or their alloys.

TaC with cobalt, chromium or nickel or their alloys.

If it is found that the following three systems show suitable eutectic equilibria, they too would appear to be worthy of investigation.

HfC with nickel

HfB_2 with chromium

TaB_2 with chromium

6.

2.3 Lanthanum Hexaboride, LaB_6

In the original FRI literature survey, LaB_6 was not included, but
in view of the exceptional promise already shown by the compound as
a cathode material, the state of knowledge or its characteristics
was reviewed in the Interim Scientific Report 1 May 1978 - 30 April 1979
and included in this report as Appendix I. Lanthanum hexaboride has a
melting point in excess of $2500^{\circ}C$,[63], good chemical stability, a low
electrical resistivity and a low work function[64]. As an electron
emitter, LaB_6 surpasses tungsten in respect of brightness, operating
lifetime and stability to ionic bombardment. It has a cubic structure
containing covalently bonded B_6 octahedra and the lanthanum provides
nearly free electrons which accounts for the good electrical con-
ductivity and exceptional thermionic behaviour. Although there is
little information on the nature of the phase equilibria in ternary
La-B-X systems, some evidence is available[65,66], to suggest that
LaB_6 and aluminium form a eutectic equilibrium, thereby creating
a possible means of growing a fibre structure by directional solid-
ification.

If we express the reaction pressure of lanthanum as follows:

$$LaB_6 \rightleftharpoons La \text{ (gaseous)} + 6B \text{ (solid)}$$

the thermionic data [67,68] gave values $\log_{10}$(reaction pressure) in
atmospheres of -20.6 at $1000^{\circ}K$ and -5.9 at $2000^{\circ}K$. It will be
noted that these pressures are somewhat higher than those of refractory
carbides and nitrides at corresponding temperatures.

Various values of the work function have been reported which range
from about 2.07 to 3.4 eV and depend on the purity of the sample,
surface condition[69], and crystallographic orientation[70], of the
face measured.

However the most favoured values are in the lower part of this
range so that the work function compares favourably with those of the
carbides.

Vikhrev et al [71] found that composites containing 10% by weight of rhenium, molybdenum or tantalum had virtually the same thermionic properties in the temperature range 1150 to 1600°C.

In view of these outstanding characteristics of LaB_6, a limited programme to investigate the production of crystals suitable for single fibre emitters, was considered worthwhile.

3. MATERIALS USED FOR FULMER EXPERIMENTAL WORK

3.1 Fabrication

The ideal configuration of a field emission cathode is an array or area of equispaced points of uniform height above a surface and having a uniform tip radius. This ensures that an applied field across each of the points will be uniform and hence electron current can be extracted from each point. Unfortunately, with a directionally solidified eutectic structure, ideal uniformity is never achieved and there are variations both in the diameter of the fibres and in the spacings between them. However the large number of fibres present ensures that some of them experience a sufficiently high field to cause electron emission. This high field results from either a very small tip radius or a large separation between the fibres (or a combination of the two). Deterioration of one fibre by ion bombardment causing emission to cease and accompanied by a change in its physical shape, results in an increased field being generated on an adjacent fibre.

The principal of fabrication of the emitter is to etch back the matrix supporting the fibres and then remove material from the fibres to produce pointed ends using a second etching solution. Usually the face of the ingot is first finely polished and then the ingot is spark-machined to form the required shape and size. In the case of single fibres, the difficulties experienced in handling them has been overcome by electroless nickel plating to produce a coating of about 100μm thick. The internal stress in the nickel coat may be sufficiently high to break up the

8.

coating so that it is preferable to coat a small bundle of fibres
together and then finish coat to the required thickness after
separation. Cathode samples consisting of a specific number of
fibres were prepared by taking a suitable segment and removing
the outer pins by spark-machining until the required number were
obtained.

The directionally solidified ingots were obtained from various
laboratories but were all fabricated into the required geometry
for testing at Fulmer. The earlier emitters were prepared from
NbC fibres (10% by weight) in a Ni-Cr matrix containing 18 wt.% Cr
and TaC fibres (16% by weight) in a Ni-10% Cr matrix. A nickel
alloy designated A77-205 with 31.8 wt.% Ta and 5.5 wt.% Al was
also used. This ingot consisted of γ/γ' fibres (1μm diameter) in an α-matrix
and electron micro-probe analysis gave the following results for
the composition of the fibres and matrix.

	Fibres	Matrix
Nickel, wt.%	27.9	70.1
Molybdenum, wt.%	65.7	20.8
Tantalum, wt.%	2.0	2.8
Aluminium, wt.%	4.5	6.2

Other carbide fibre systems tested consisted of 12 wt.% VC in
cobalt, 17.7 wt.% TaC in a matrix of Ni-10 wt.% Cr, (designated
Cotac CF83) and single fibres of NbC. A limited programme was
also initiated to examine the feasibility of preparing LaB_6 compound
in an aluminium matrix, containing respectively 3, 6 and 12 wt.% LaB_6.
The starting materials were lanthanum of purity better than 99.7%,
boron of purity >99.8% and aluminium of >99.99% purity.

In the electrochemical etching process to form the needle array,
the matrix is quickly removed compared with the stable carbide fibres
and the resultant increase in field on the fibre tips produces
preferential etching at the tip. The failure to produce the fine
sharpening of the NbC fibres was due to the very high stability

9.

of the compound. The etching reagents used for the carbide arrays were as follows:

a) For TaC, 5% by volume of sulphuric acid in methanol.

b) For VC, an aqueous solution containing 29.3 vol.% hydrochloric acid, 7.3 vol.% nitric acid and 7.3 vol.% acetic acid.

c) For NbC, the matrix was best removed in an etchant consisting of 72 vol.% orthophosphoric acid, 18 vol.% butanol and 10 vol.% water. Some sharpening of the fibre points could be produced subsequently by using an aqueous solution of 2g. picric acid and 25g. sodium hydroxide in 100 ml. water.

3.2 Configurational Characteristics of Samples

The cold cathode specimens were all examined in the scanning electron microscope both before and after testing. The first specimen of TaC material was machined to a right circular cylinder 1mm diameter prior to etching of the matrix during which a cone shaped nose developed as in Figure 1. Figure 2 shows typical fibre needles and the variations in their shape and spacing. To produce high density emission from a broad area cathode, an ingot of TaC was segmented using a high speed carborundum wheel to form a structure consisting of ~1mm pins spaced 0.6mm. apart as in Figure 3. Initially, the sample consisted of 32 pins but the number was subsequently reduced to 20 and later to 9. Single TaC fibres were also produced by prolonged etching of the eutectic. From the resultant bundle of fibres, individual fibres were manipulated under an optical microscope on to small steel slabs where they were attached using conducting silver paste. The fibres had a maximum length of 2mm and a typical example is shown in Figure 4.

In contrast to the needle shaped TaC fibres, the NbC fibres did not exhibit sharp needle points, and the dome-like geometry was maintained throughout the etching process as in Figure 5. No procedure was found which resulted in fine points at the fibre tips but some fibres became more rounded in cross-section than others. Two samples were tested,

10.

one consisting of small fibres as in Figure 6 and the other of large fibres as in Figures 7 and 8. As the large fibre material was not very uniform, only limited testing of this sample was made. The structure of the A77-205 material was quite different from that of the carbide samples and is shown in Figures 9 and 10, from which the irregular nature of the γ/γ' fibres is observed.

The VC ingot available was smaller than that of the TaC sample so that a cathode consisting of nine pins only was machined from it as shown in Figure 11. Etching of this material gave reasonably acicular fibre needles as in Figure 12. This cathode was subsequently spark-machined to give four pins but the fibres were more blunted than those previously produced as in Figure 13. In the case of a single block of this material (1mm x 1mm) shown in Figure 14, the fibres were even more blunted in the central area as in Figure 15. After reducing to about 300 x 400µm size, the fibres were generally more acicular as in Figures 16 and 17. To investigate the effect of high current density emission, the "chisel" shaped cathode shown in Figure 18 was constructed in which the shape of the fibres was somewhat variable depending on their position in the cathode as in Figures 19 and 20.

3.3 Preparation of LaB_6

Plates of LaB_6 were grown by heating lanthanum and boron in the correct proportions in aluminium at 1500°C for several hours and cooling to room temperature at a controlled rate. The crystals were subsequently removed from the aluminium matrix by acid dissolution of the latter and the ingot containing a nominal 12 wt.% LaB_6 gave a reasonable yield of plates of the type shown in Figure 21. The morphology of these crystals suggests that a suitable cathode configuration might be produced by directional solidification of the ingot.

4. TESTING PROCEDURES

Evaluation of the cathodes was initially undertaken in a chamber evacuated to around 10^{-6} torr but at a later stage of the work

a UHV system was employed. The first stainless
steel chamber is shown in Figure 22 and the cathode assembly con-
struction in Figure 23. The chamber was pumped using a polyphenol
ether-based oil diffusion system and an electron bombardment
filament was operated prior to the cathode test to increase the
temperature of the cathode to 500°C and complete its outgassing.
The specimen support arm could be moved vertically from outside
the chamber so that the anode/cathode separation could be varied
if required. Normally, unless otherwise stated, the separation
was maintained at 1.0mm. A Brandenberg high voltage DC power
supply of 10kV, 10mA with 0.05% ripple and full output was used
for the tests and the diode current was measured using a Keithley
Electrometer connected to the copper anode.

To complete tests under better vacuum conditions which provide
more stable emission and greatly reduce the likelihood of ion
damage, the ion pump system sketched in Figure 24 was constructed.
The pressure obtainable in this apparatus is better than 10^{-10}
torr with a normal operating pressure of around 10^{-9} torr. The
high vacuum part of the system including the ion pump was first
baked at 250°C followed by heating the cathode to about 500°C by
electron bombardment. The construction of the cathode test
assembly used in this system is shown in Figure 25 and enabled
a more accurate alignment than hitherto but did not allow for the
interelectrode spacing to be changed during testing. Before
installation the molybdenum anode was fired under hydrogen at 1200°C
to reduce any surface oxide and hence prevent outgassing of the anode
during the start of the emission test.

Electron Energy Spectra: A high resolution spectrometer
was used at Aston University to study the energy spread of electrons
emitted from the multi-array specimen of TaC tips. The apparatus
has been described in detail by Allen and Latham [73] and consists
essentially of a 180°C hemispherical deflection spectrometer with
a design resolution of about 30 MeV operating under UHV conditions

12.

of around 5×10^{-11} torr. To analyse the emission from broad area specimens, a manipulator stage is incorporated to allow the specimen cathode to be scanned in front of a probe hole of a polished planar anode while maintaining a parallel, pre-set interelectrode gap. By applying a sufficiently high voltage between the specimen and anode, i.e. such that a pre-breakdown electron current of about 1µA flows between them, and scanning the specimen in a raster pattern, it is possible to locate the individual emission centres on the electron optical axis.

The voltage-current characteristics and electron energy spectrum of the emission centre were measured and the position of the fermi level of the substrate cathode was identified. In situ specimen cleaning was carried out by first outgassing the cathode and anode by electron bombardment followed by argon ion bombardment using a spherical source gun inclinded at 30° to the electron optic axis. The anode and cathode were usually outgassed at a dull red heat and the ion bombardment was typically at 4kV and from 30 to 50µA for about ten minutes.

Current-Voltage Relationships: Cathodes were compared using plots of Fowler-Nordheim functions of $\log_{10} (I_{/V}2)$ against $1_{/V}$ where V is the applied voltage. The emission characteristics J, are given by the Fowler-Nordheim equation [74]:

$$J = \frac{1.54 \times 10^{-6} \, F^2}{\phi t(y)} \; \exp \left(\frac{-6.83 \times 10^7 \, \phi^{3/2} \, v/v}{F} \right) A \; cm^{-2}$$

where ϕ is the work function of the cathode material in eV, t(y) and v(y) are tabulated functions [75] of $y = 3.79 \times 10^{-4} \, F^{1/2}/\phi$ and F is the field strength in v/cm which for a multifibre structure is given by [76]

$$F = \left(\frac{V}{R} \right) \left[\frac{1 + (4\pi R^2/a^2)}{1 + (4\pi(L-R)R/a^2)} \right]$$

13.

where R is the tip radius of the fibres,

a the distance between fibres and,

L the anode to cathode separation.

As $R \ll a \gg L$

we have $F \simeq V/R \Big/ \left(1 + \dfrac{4\pi LR}{a^2} \right).$

The slope of the Fowler-Nordheim equation is therefore

$$\frac{d(\log_{10} J/F^2)}{d(I/F)} = 2.98 \times 10^7 \ \phi^{3/2} \ s(y),$$

where $s(y)$ is a tabulated function of y[75]. As the applied field is directly proportional to the applied electron voltage V assuming the geometry and work function of the cathode does not change during testing, a plot of $\log_{10} 1/V^2$ against $1/V$ will produce a straight line provided that field emission is the dominant charge carrier and that space charge does not occur.

The above field strength equation applies strictly to a configuration in which the radius of the tip is equal to the radius of the fibre and does not therefore hold for the acicular-shaped tips generally produced in the Fulmer work. For this type of fibre, it has been found that the following relationship applies.

$$F \simeq \frac{V}{3R} \left(\frac{1}{1 + \dfrac{12\pi RL}{a^2}} \right)$$

Correlation between the experimental results and the theory has been attempted, but for this calculation to be accurate the geometrical factors, work function and the number of emitting sites need to be known. At the present time, it is not known how many sites emit and though most of the geometrical factors can be measured the tip radius can only be estimated. Also the work function of the fibres is dependent upon the orientation of the fibres in the matrix and published data for particular orientation of metal compound fibres is sparse. For these reasons no accurate correlation between the experimental results and the theory was obtained.

14.

5. EXPERIMENTAL RESULTS

5.1 Tantalum Carbide

Due to the cone-shaped end of the first sample of TaC to be tested,
it was difficult to estimate the overall emitting area of the
cathode. However, the F-N plots at two anode to cathode separations
of 1 and 2.2mm respectively are shown in Figure 26. Marked
deviations from linearity were obtained at both separations and it
appears probable that space charge effects developed at about $^1/V$ equal
to 4.0×10^{-4} (2.5Kv). Marked deterioration of the fibres occurred
as shown in Figure 27, suggesting that the doming of the ends was due
to melting.

If the emitting area of the cathode was limited to this damaged region
the maximum current obtained of 8×10^{-4}A at 10Kv corresponded to a
current density of $31Acm^{-2}$.

The second ingot of TaC to be tested provided a broad area cathode
with a multipin array. Originally this consisted of 32 $1mm^2$ pins
but these were subsequently reduced in steps to 20, 9 and 1 respectively.
Currents of up to 4mA were obtained from the 32 pin cathode corresponding
to an emission density of 1.25×10^{-2} Acm^{-2}. The F-N plots in the
four conditions are shown in Figure 28, after correction for cathode
area. The best emission characteristics (current density obtained
at a particular voltage) were from the 20 pin cathode assembly which
is surprising as the 1 pin cathode was expected to produce the best
emission characteristics. The most likely explanation of this discrepancy
is that emission occurred from untypical areas of the 20 pin cathode
containing taller fibres resulting in a much greater field. No
damage was observed to the fibres in any of the configurations tested
and the appearance of a typical area of the central pin of the 20
pin cathode is illustrated in Figure 29.

The voltage stabilities at constant current were monitored for the
cathodes consisting of 32, 20 and 9 pins and are recorded In Figures 30,
31 and 32 respectively. In each case, the voltage variations were
only minor illustrating that all three cathodes had good stability
characteristics.

Several tests were made on single fibres of TaC but in each case
the run was unsuccessful due to destruction of the fibre. Since
the fibres were only 1μm in diameter, it is probable that their
relatively high electrical resistivity and lack of mechanical support
contributed to the failure.

5.2 Niobium Carbide

The square-ended fibres in the NbC cathode sample operated
satisfactorily and gave the F-N plot in Figure 33 obtained for an
anode/cathode separation of 1.0mm. No significant damage of the
cathode was observed after 50 hours operation, the only areas of
damage being in small regions where arcs had occurred and removed
the fibres. The maximum emission current obtained was 3.56×10^{-4}A
corresponding to a current density of 1.3×10^{-2}A cm^{-2}.

A niobium carbide sample consisting of small fibres was used to
investigate the effect of prolonged running of a cathode under
relatively poor vacuum of about 1×10^{-6} torr. The cathode was
operated for 1,000 hours and to reduce the occurrence of arcing,
the applied potential was limited to 7kV. However, during the life
tests, a number of minor arcs did occur of the type shown in
Figure 34, but the greater part of the cathode remained undamaged.
A significant increase in the extracted current occurred during
the test as shown by the F-N plots in Figure 35 representing the
conditions before and after operation for 1,000 hours. After com-
pletion of this endurance test, the cathode was replaced in the
chamber and F-N plots were obtained at four different pressures.
The results plotted in Figure 36 clearly show that the emission
increased with decreased pressure in the chamber.

Larger fibre NbC cathode was also operated to provide a comparison
of its performance and that of the small fibres. As the field F
is given by

$$\frac{V}{3R} \left(\frac{1}{1+\dfrac{12\pi RL}{a^2}} \right)$$

Since L is a constant for all the tests, providing the tip radius
R remains the same, the field applied to the tips should increase

16.

as the tip separation a increases resulting in a higher current. The F-N plot produced by the larger fibres indicated that an improvement in emission was obtained but as the sample was not very uniform, the test was terminated after a short time. No damage was observed on examination of the fibres after testing.

A single fibre NbC cathode was run for several hours at emission levels between 1 and 5μA and a F-N plot taken during the run is shown in Figure 37. The straight line obtained demonstrates that field emission was the dominant current carrier. Examination of the fibre at this stage showed that some erosion of the fibre had occurred as in Figure 38 but as this did not change the emission characteristics, it is concluded that the damage was caused by a single small arc at the onset of the test. A further test for 50 hours at 5μA gave no further erosion and the same emission characteristics were maintained.

These tests on the single NbC fibre demonstrated that a very fine source can be run under stable conditions. Further, as no significant sharpening of the fibre was found possible by electrolytic treatment, there is a distinct probability that a significant improvement would be obtained when other materials are used which can be fabricated with sharp pointed fibres.

5.3 A77-205 Alloy

The cylindrical specimen of A77-205 alloy was operated for a total of 50 hours at various emission currents up to the onset of arcing. The general structure after test is illustrated in Figure 39 and that in the area where arcing occurred in Figure 40. However, no apparent overall deterioration in the performance of the cathode resulted from this arcing. The F-N plots for anode to cathode separation of 0.5 and 1.0mm are shown in Figure 41. The maximum current obtained was 5.0×10^{-3}A which corresponds to a current density of 6.8×10^{-3} Acm^{-2} at an extraction voltage of 5kV.

5.4 Vanadium Carbide

The tests on the VC cathode with 9, 4 and 1 pins respectively showed that the stability and emission characteristics of the

single pin system were superior to either of the multipin cathodes
as is illustrated by the F-N plots in Figure 42. Very slight
damage occurred during testing of the 9 pin cathode but this was
randomly distributed across the cathode surface and the stability
remained good throughout as shown by the plot in Figure 43.
No damage was detected after testing the 4 and 1 pin cathode.
In view of the improvement in emission characteristics resulting
from reducing the number of pins from 9 to 1, it was considered
probable that a further improvement would accrue from reducing
the cross-section of the single pin cathode from 1mm square to
300 x 400µm. This in fact proved to be the case as observed in
Figure 42, in which the results have been plotted in the form
$\log_{10}(I \text{ cm}^{-2}/V^2)$ against $^1/V$ to obtain a set of results independent
of cathode size. The highest current density obtained from the
300 x 400µm cathode was 40mA cm^{-2} at an extraction voltage of 1.1kV.
Slight blunting of the points occurred in one area of the reduced
cathode as shown in Figure 44.

A VC cathode of area 1.6 x 10^{-4} cm^2 was used to evaluate the effects
of prolonged running of this particular material. The life test
was run for 1,000 hours at a pressure of 5 x 10^{-7} torr. An average
emission current of 80 x 10^{-6} A(0.5 Acm^{-2}) was maintained throughout
the life test with a maximum current of 930 x 10^{-6} A (5.8 Acm^{-2})
being obtained. No significant damage occurred during the test,
but a small number of fibres had shown signs of melting when examined
at the end of the 1,000 hours.

The chisel shaped cathode was used to investigate the stability
of VC to high density emission of up to 1 amp cm^{-2}. It would
be expected that any damage due to the high density ion bombardment
of the cathode surface would occur along the apex due to the greatly
enhanced field. A life test of 175 hours was completed on the
cathode at 100µA but currents greater than 200µA were readily
obtained without the occurrence of arcing. Examination showed
that melting of the fibres was confined to an area along the apex

18.

20µm wide as in Figure 45. This indicated that only a very small area of the cathode was emitting at a high current density but the fibre melting had only a minimal effect on the emission characteristics of the cathode as the deterioration observed was only slight. Figure 46 shows a plot of the stability over a two hour period. A F-N plot of the emission characteristics is given in Figure 47 but as the emission area cannot be measured accurately, this result cannot be directly related to those on the other VC samples although the emission density is almost certainly considerably higher.

5.5 Cotac CF83

Compared with the previous samples of TaC tested, (the results of which are given in Section 5.1), the Cotac CF83 material had a more uniform structure and a larger fibre separation of about 9µm compared with 3µm of earlier samples. Initially the fibres as prepared were comparatively blunt as shown in Figure 48 but it was decided to test them in this form to provide a comparison with their performance and that of a similar cathode after further etching treatment. A typical stability plot is shown in Figure 49 and the F - N plot obtained together with that from the original 1 mm^2 TaC cathode in Figure 50. Due to the differences in the test conditions for the two samples, however, it is not possible to draw any precise conclusion from this comparison but there does not appear to be a marked difference between them. Examination of the cathode after testing showed that no damage had occurred to the cathode due to either ion bombardment or arcing.

By improving the electrolytic etching technique, the TaC fibres were produced in a pronounced acicular form as in Figure 51. Two cathodes were produced in this form and were tested in both the UHV and oil pumped systems. The results indicated that the cathode ran in the improved vacuum at a pressure of around 5×10^{-9} torr gave a significantly more stable emission than that operated in the original oil pumped system at around 7×10^{-7} torr as shown in Figure 52. Both cathodes produced improved levels of emission at corresponding

19.

voltages compared with the blunt CF83 fibres and the original
TaC cathodes (see Figure 50). The difference in emission levels
obtained from the two sharply pointed fibre cathodes is possibly
due to lack of emission from fibres in the oil pumped system as
the near parallel F-N plots indicate that the work function and
the field factor for the two cathodes are very similar.

Both cathodes were run for 400 hours to establish if ion damage
would occur to either. Emission levels up to 1.2 mA (0.3 Amp cm^{-2})
were obtained from the ion pumped cathode with an average emission
level during both tests of 200µA (0.05 Amp cm^{-2}). Subsequent
examination of the cathodes showed only very minor damage to
individual fibres and no evidence of ion bombardment damage was
found on either cathode, the fibre tip radius remaining constant
as in Figure 53.

In addition to the emission tests, a limited examination was made
of the re-start characteristics of the Cotac cathode to find if
instant emission occurred after a short storage period. These tests
were made by turning off the power supply to the cathode manually
after dwell time varying between a few seconds up to a period of
one hour. At a current level of 500µA, a total of 100 restarts
were made without any deterioration or change in the cathode's
performance being observed.

5.6 Energy Spectra

The sample of tantalum carbide which had previously given the
F-N plots recorded in Figure 26, was used to study the electron
energy spectral characteristics. The out-gassed TaC specimen
was set to give an anode/cathode gap of 0.5mm and a voltage of
about 3.5 kV was applied. It was found that there were only three
distinct emission sites on the surface in spite of the multi-point
structure of the specimen. For one of these sites, the electron
energy spectrum is shown in Figure 54A which has a broad half-width
of about 0.44 eV, a shallow high-energy shape and is displaced in
energy by over one volt below the fermi level. This spectral shift

20.

is conventionally regarded as the energy difference between the fermi level in the bulk of the specimen (the position of which can be found by prior calibration) and the energy value corresponding to a point 3/4 of the way up the high energy slope of the spectrum. For a free-electron metal, Young and Kyatt[77] have shown that these two points will coincide so that the degree of spectral shift gives a measure of the deviation of the emission source from free-electron behaviour. The magnitude of this shift is frequently dependent on the emission conditions and can be presented as either a function of the applied field of total emission current as in Figure 55.

The characteristics of the second emission site was essentially similar but the third site exhibited a markedly different behaviour. The spectrum is shown in Figure 54B and has an exceptionally narrow half width of 0.26 eV. Further, the smaller spectral shift was found to be independent of both field and emission currents.

A corresponding voltage/current characteristic of the two types of emission site are revealed by the F-N plots in Figure 56. Since these are linear , it appears that both sites follow a metallic emission law in spite of the non-metallic characteristics of the emission spectra. The differences in slope of the F-N plots may be due to a difference in the local field enhancement factors.

Subsequent to these initial measurements, the specimen surface was bombarded with argon ions using a 40μA, 4kV beam. On retesting, several new emission sites appeared, many of which were too close to the edge of the specimen to focus the emission into the spectrometer. Any that could be focussed, however, had similar emission characteristics to those of the third original site, i.e. a narrow half-width corresponding to that of Figure 54B and a spectral shift which was independent of both field and emission currents.

6. DISCUSSION

6.1 Choice of Compounds

Thermodynamic criteria of stability can provide, at best, only a partial guide to the response of the refractory needles to temperature/pressure conditions. They serve to pinpoint those compounds most likely to succeed but cannot forecast sputtering response while the

21.

influence of physical properties such as work function, can only
be gauged empirically by experiment. Sputter-induced degradation
is certain to have an adverse effect upon all needle materials,
but no systematic data are available. For elements, the sputter yield
under ion bombardment is related to the heat of sublimation and
therefore to the vapour pressure. The inference is that elements
suitable for needles have low vapour pressures and, by the same
token, compounds with low decomposition (i.e. reaction) pressures
should be prime candidates. The short list of compounds given
earlier represent a group of materials designed to test our working
assumptions and is not a final short list of proven compounds.

The tests made on the carbide emitters have been restricted to
those available from development programmes made for gas turbine
applications. The lack of tests using boride emitters was caused
by the unavailability of suitable alloys. The alloy preparation
of LaB_6 grown in an aluminium matrix demonstrates that this compound,
with a particularly low work function, may lend itself to
directional solidification techniques, and hence prove to have a
very high emission density when fabricated into a cold cathode.

6.2 Emission tests on Cathodes

The tests performed on the refractory carbide emitters have shown
the expected improved performance compared with tungsten, silicon
and molybdenum field emitters. These results are summarised in
Figure 57 where the Fowler Nordheim plots have been corrected for
cathode area. It should be noted, however, that the tests performed
by other workers[78] on tungsten and silicon have been made at
smaller anode to cathode separations and have experienced a higher
electric field across the emitter tips. The tests at Fulmer have
all been made at a cathode to anode separation of 1mm; the values
obtained for TaC and VC demonstrating the highest emission for
the field applied. The lower values for NbC are possibly caused by
the failure to point the NbC fibres to the same sharpness as the
TaC and VC. As mentioned previously, the tests performed on NbC were
made earlier in the programme and hence an improvement in experimental

22.

techniques could also contribute to the improved performance of the TaC and VC. The tests made on the A77-205 alloy where the emitting fibres are mainly molybdenum also demonstrated a poor performance. This was primarily due to the irregular distribution of the fibres in the composite and is consistent with the original predictions that even the most refractory metals are likely to compare with refractory compounds such as carbides.

The life tests performed on the refractory carbide cathodes, have also shown that life times in excess of 1,000 hours can be achieved. Table 12 summarises the life tests to date and also includes comparative test data for tests made at SRI and GIT. Direct comparison between all of the SRI and GIT data cannot be made since thin film extraction electrodes are used to extract the beam and hence high energy ions are absent. Also, the test conditioned(DC pulsed and AC tests) are different. However, the GIT test made with a diode at a 0.5mm anode - cathode separation compares favourably with the results from the present work. There is every likelihood therefore that if the present carbide materials are applied to the thin film extraction techniques then similar results would be found with the added advantage of better ion erosion resistance.

6.3 Energy Spread

Spectral shifts are frequently observed in studies in which laboratory fabricated semi-conducting emission sources are used. The most common explanation of the shift assumes that it is a property of the emission process and is probably associated with tunnelling of electrons into the vacuum from localised surface states. The peaks with narrow half-widths obtained on the TaC samples are consistent with their being derived from sharp semi-conducting emitters which are relatively free from surface contamination. This is confirmed by the fact that argon ion etching created further emitters with narrow peaks. The variable shift spectra obtained from the sample in its original condition may have arisen from a microregime which was typical of the cathode surface such as a contaminating dust particle since such features are known to give strong field emission.

The non-uniform emission obtained indicating that only a few needles
emit at any one time probably resulted from the non-uniformity
of the sample since needles of different diameters and tip radii
were present.

6.4 Applications

The precise and most immediate application for cold cathodes in
practical devices cannot be accurately predicted until electron
optics studies have been made. However, from the work performed to date
it is apparent that the current densities and lifetimes found
for the refractory carbides are sufficient for cathode ray tubes
where only low total currents are required. Also, for applications
where robustness and instant turn-on are a prime requirement, such
as ECM's (electronic counter measures) and expendable TWT's
(travelling wave tubes), the cold cathode has many advantages.
These tubes must be rugged enough to withstand vibrational specifications
used in the aerospace industry, be able to restart after months of
storage without pre-conditioning and have a low power consumption[79].
The indications are that the refractory carbides field emitters will
fulfil this requirement.

7. CONCLUSIONS

The work reported here has demonstrated that the field emission process
operates for directionally solidified eutectics confirming earlier
work on materials such as tungsten and others of lower melting point.
The particular advantage in using the range of materials short-listed
from this study is that under demanding service conditions they should
provide a long life-time for practical devices used in current electronic
tube technology. Lifetimes in excess of 1,000 hours are obtained and
current densities above 1A cm^{-2}.

The previous impetus on the development of directionally solidified
eutectics has concentrated upon high strength and corrosion resistance
properties suitable for turbine blade applications. The use of these
materials as cold cathodes would benefit from a similar development
programme on boride eutectics and with particular emphasis on lanthanum
hexaboride.

24.

8. ACKNOWLEDGEMENTS

REFERENCES

1. F.M. Charbonnier et al., Proc. IEEE, 1963 July 991-1004.

2. K.T. Considine and M.M. Balsinger, Research/Development, 1976 April, 38-44.

3. J. Shelton, "Field Effect Electron Emission", Army Missile Command, Redstone Arsenal, AD 738 529, August 1971.

4. G.A. Wardly, J. Vac. Sci. Techn. 1973, 10 (6), 975-978.

5. R.K. Feeney, A.T. Chapman and B.A. Keener, J. Appl. Phys., 1975, 46(4) 1841-43.

6. F.S. Baker et al., Nature, 1972, 239, Sept., 8, 96-97.

7. E. Braun et al., Vacuum, 1975, 25, (9/10), 425-426.

8. R.N. Thomas, R.A. Wickstrom, D.K. Schroder and A.C. Nathanson, "Fabrication and some applications of large area silicon field emission arrays", Solid State Electronics, vol. 17, 155-163 (1974).

9. Y. Kumashiro et al. J. Less-Common Metals, 1973, 32 21-37.

10. K. Senzaki and Y. Kumashiro, Proc. 6th Int.Vac. Congress 1974. in: Jap. J. Appl. Phys. Suppl. 2, Pt.1, 1974, 289-292.

11. V.G. Rivlin and D. Stewart, FRI Report R744/1, 31st October, 1977. Field Emission Cold Cathodes AFOSR-77-3292, Interim Scientific Report 1 May 1977 - 31 Oct. 1977.

12. M.A. Filyand and E.I. Semenova, Handbook of The Rare Elements, Vol.2 (Transl. M.E. A'.ferieff), London, MacDonald, pp 12 - 15, Tables 388 - 392.

13. L.E. Toth, Transition Metal Carbides and Nitrides, New York and London, Academic Press, 1971.

14. H.J. Goldschmidt, Interstitial Alloys, London. Butterworths, 1967.

15. G.V. Samsonov, Refractory Carbides, (Transl. N.B. Vaughan), New York and London, Consultants Bureau, 1974.

16. V.S. Fomenko, Handbook of Thermionic Properties (G.V. Samsonov, Ed.) Transl. and Published - Plenum Press Data Division, New York, 1966.

17. E.K. Storms, The Refractory Carbides, New York and London, Academic Press, 1967.

18. C.J. Smithells and E.A. Brandes, (Eds.) Metals Reference Book, 5th Edition, London and Boston, Butterworths, 1976.

19. G.V. Samsonov (Ed.) Boron, Its Compounds and Alloys, Book 2, Kiev, Akad. Nauk Ukr. SSR, 1960, see especially pp 394 - 436. (USAEC Transl. AEC-tr-5032, Book 2).

20. E. Rudy, Ternary Phase Equilibria in Transition Metal - Boron-Carbon-Silicon Systems. Part V. Compendium of Phase Diagram Data. Technical Report AFML-TR-65-2 May 1969. AD 68984. (Includes data for binary systems).

21. A.M. Zakharov, I.I. Novikov and V.S. Pol'kin, Tsvetnaya Met., 1971, (6), 126 - 129.

22. P.R. Sahm, M. Lorenz, W. Hugi and V. Frühauf, Met. Trans., 1972 3, (4), 1022 - 1025.

23. J.P. Guha and D. Kolar, J. Less-Common Metals, 1972, 29, (1), 33 - 40.

24. S.S. Ordan'yan et al., Neorg. Mat., 1966, 2 (2), 299-302.

25. E.M. Savitskii and A.M. Zakharov, Doklady Akad. Nauk SSSR, 1967, 177 (6), 1397-1399.

26. V.N. Eremenko and R.Ta Velikanova Vysokotemperatury Neorg. Soed., Kiev, Nauka Dumka, 1965, 265 - 273.

27. S.S. Ordan'yan et al., Nauka Issled. v. obl. Khimii Silikatovi Oksilov, M - L 1965, 220 - 228.

28. E.M, Savitskii and A.M. Zakharov Izv.AN SSR Metally. 1970, (6), 204 - 207.

29. G.M. Leidermann and V.A. Nikolaeva, Izv. AN SSSR, Neorg. Mat., 1973, 9 (10), 1721 - 1723.

30. V.N. Eremenko and Ye.I. Tolmacheva. Porosh, Met., 1961, (2), 21 - 29.

31. W.C. Bellamy and E.E. Hucke, J. Metals, 1970, 22, (8), 43 - 50.

32. S.S. Ordan'yan, N.V. Kosterova and A.I. Avgustnik, Izv. AN SSSR, Neorg. Mat., 1969, 5 (2), 389 - 390.

33. Yu. N. Vilk, I.N. Danisina and Yu. A. Omel'chenko, Izv. AN SSSR, Neorg. Mat., 1973, 9 (1), 145 - 148.

34. N.V. Cherkashina et al., Izv. AN SSSR, Neorg. Khim, 1960, 5, (9), 2025 - 2031.

35. A.M. Zakharov, I.I. Novikov, V.S. Pol'kin and F.A. Gimel'farb Izv. AN SSSR, Metally, 1973, (4) 236 - 239.

36. S.S. Ordan'yan, R.Ya. Serbezova and T.A. Lebedeva, Izv. AN SSSR, Neorg. Mat., 1972 8, (11), 2037 - 2038.

37. Ya. V. Levinskii et al., Porosh., Met., 1965, (11), 66 - 69.

38. G.A. Yasinskayo and M.C. Groisberg, Porosh. Met., 1963, (6), 36 - 38.

39. A.K. Shurin and D.M. Barabash, Metallofiz. Resp. Mezhved, sb., 1973, 45, 84 - 87.

40. N.V. Ageev (General Editor), Diagramnay Sostoyaniya Metallicheskikh Sistem, 1960 - 1973.

41. K.I. Portnoi and V.M. Romashov, Sov. Powder Metall. Met. Ceram., 1972, 11, (5), 378 - 384.

42. W. Kurz and P.R. Sahm, Gerichtet Erstarrte Eutektische Werkstoffe, Berlin Springer-Verlag, 1975 (see especially Appendix, pp 305 - 335).

43A M.N. Crocker, R.S. Fidler and R.W. Smith, Proc. Roy. Soc., 1973, 335, 15 - 37.

43B E.R. Thompson amd F.D. Lemkey in: Metallic Matrix Components, (K.G. Kreidler, Ed.) 1974, 4, 3, 101 - 157.

44. A.F. Giamei, E.H. Kraft and F.D. Lemkey in: New Trends in Materials Processing, ASM 1976, Proc. of Sumposium in Detroit 1974.

45. L.M. Hogan, R.W. Kraft, and F.D. Lemkey in: Advances in Materials Research (H. Herman, Ed.,) 1971, 5, 83 - 216.

46. F.W. Crossman and A.S. Yue, Met. Trans. 1971, $\underline{2}$. 1545-1555.

47. J. Westbrook, J. Metals, 1957, 9/10, 1277.

48. S.A. David and H.D. Brody. Proc. 1975 Int. Conf. on Composite Materials, I. Met., Soc., AIME, N.Y. 806 - 819.

49. M.H. Lewis and J.M. O'Sullivan, Conf. on In-Situ Composites, 1973, $\underline{1}$, 169 - 179 (NMAB 308-1).

50. E.R. Thompson and F.D. Lemkey, Met. Trans., 1970, $\underline{1}$, 2799-2806.

51. M. McLean et al., Preprints, Sheffield Int. Conf. on Solidification and Casting, 18 - 21 July 1977, For Al-C-Cr-Ni see: E. Bullock, M. McLean and D.E. Miles, Acta Metallurgica, 1977, $\underline{25}$, 333 - 344.

52. E.R. Thompson and F.D. Lemkey in: Composite Materials, (L.J. Broutman and R.H. Krock, Eds.) $\underline{4}$, Metallic Matrix Composites (K.G. Kreider, Ed). New York Academic Press, 1974., Ch.3 pp 101 - 157.

53. J.L. Walter and H.E. Cline, on In-Situ Composites, 1973, $\underline{1}$, 61 - 74 (NMAB-308-I).

54A A.J. Van Den Boomgard and A.M.J.G. Van Run, Proc. Conf. In-Situ Composites, NMAB-308, 1973, $\underline{2}$, 1961.

54B B.J. Van Den Boomgard and L.A. Wolff, J. Cryst. Growth, 1972, $\underline{15}$, 11 - 19

55. E.M. Breinan et al., Proc. Conf. In-Situ Composites, NMAB-308, 1973, $\underline{2}$, 201.

56. P.R. Sahm and N. Lorenz, J. Mat. Sc. 1972, $\underline{7}$, 793.

57. F.M. Denlevey and J.F. Wallace, Met. Trans., 1974, $\underline{5}$, 1351 - 1356.

58. Y.G. Kim, Abstract in J. Metals, 1975, $\underline{27}$. A43.

59. H. Bibring, M. Rabinovitch and G. Seibel, Comptes Rendus Acad. Sci. Paris, 1969, 268C, 1666 - 1669.

60. H.E. Bates et al., J. Mat. Sci., 1969, $\underline{4}$, 25.

61. M.F. Henry, Proc. Conf. In-Situ Composites, NMAB-308, 1973, $\underline{2}$, 173.

62. An. N. Nesmayanov, "Vapour Pressure of the Elements" (translator and Editor, J.I. Carasso) Infosearch Limited (London 1963).

63. G.V. Samsonov, Ju. B. Paderno and V.S. Fomenko, Poroshk, Metall., 1963, (6), 449 - 454.

64. A.A, Kosyacktov, A.N. Stepanchuk and V. Ya Shlyuko, "A comparison of the properties of cast and sintered LaB_6 (casting using comparable electrodes)", Poroshk, Metal, 1974, $\underline{13}$, (3), 74 - 76.

65. T. Aita, U. Kawable, Y. Honda, "Single Crystal Growth of LaB_6 in molten aluminium" Jap. J. Appl. Phys. 1974, $\underline{13}$, (2), 541.

66. M. Futamoto,T. Aita amd V. Kawable, "Crystallographic Properties of LaB_6 formed in molten aluminium", Jap. J. Appl. Physics, 1975, 14, (9), 1263 - 1266.

67. T. Barry and T.G. Short, 1977, Private Communication.

68. V.V. Fesenko, A.S. Bolgar and S.P. Gordienki, Rev. Hantes Temper. Refract. 1966, 3, 261 - 271.

69. M. Aono, T. Tanaka, E. Bannai and S. Kawai, "Structure and initial oxidation of the LaB_6 (ool) surface". Applied Phys. Letters, 1974, 31, 323^6- 325.

70. C. Oshina, E. Bannai, T. Tanka and S. Kawai, "Thermionic work function of LaB_6 single crystals and their surfaces", J. Appl. Phys. 1977, 48 (9), 3925 - 3927).

71. Yu. I. Vikhrev, G.V. L'vov, V.P. Savchenko and F.A. Fekhvetdinov, "An investigation of compoiste thermionic emitters based on LaB_6", sv. Leningrad Elektrotekh Inst., 1971, 104, 132 - 136.

72. D. Stewart, N.K. Allen, P.D. Wilson and R.V. Latham, "Energy Spectra of electrons field emitters from a broad area composite cathode of tantalum carbide." To be published Jnl. Materials Science.

73. N.K. Allen, R.V. Latham, J. Phys. D: Appl. Phys., 11, 1978, L55 to 57.

74. R.H. Fowler and L. Nordheim, Proc. Roy.Soc., 1928 A, 119, 173 - 181.

75. F.H. Good Jr. and E.W. Muller, "Field Emission" in handbuch de Physik edited by S. Flugge (Springe-Verlag, Berlin, 1956), Vo. 21, pp 181 - 191.

76. J.D. Levine, Analysis and Optimization of A Field-Emitter Array, R.C.A. Review, Vol. 32, March 1971.

77. R.D. Young, C.E. Kuyatt, Rev. Sci. Instr. 39, 1968, 14 - 18.

78. R.K. Feeney et al., "Investigation of field emission electron guns for gas lasers", Final Report, 12th Oct - 31 May 1975, DAA Hol-4-C-0029, Georgia Inst. of Technology.

79. G.A. Haas, Recent Thermionic Emission Studies at NRL. Conference on Vacuum Devices, 25 - 27 March 1980. University of Cambridge (to be published in Vacuum).

BIBLIOGRAPHY

The following list of papers and reports has been produced as
a result of work completed under grant number AFOSR-77-3292.

1. V.G. Rivlin and D. Stewart, Field Emission Cold Cathode Devices
    based on Eutectic Systems. A literature search, Interim
    Scientific Report, 1 May 1977 - 31 October 1977, AFOSR-77-3292.

2. D. Stewart, P.D. Wilson and V.G. Rivlin, Field Emission Cold
    Cathode Devices Based on Eutectic Systems, Interim Scientific
    Report, 1 November 1977 - 30 April 1978, AFOSR-77-3292.

3. D. Stewart, P.D. Wilson and V.G. Rivlin, Conference on 'in-situ'
    composites, CICS III, November 28 - December 1 1978, Sheraton -
    Boston. Metals Research Society.

4. D. Stewart, P.D. Wilson and V.G. Rivlin, Field Emission Cold
    Cathode Devices Based on Eutectic Systems, Interim Scientific
    Report, 1 May 1978 - 20 April 1979, AFOSR-77-3292.

5. D. Stewart, N.K. Allen, P.D. Wilson and V.R.Lantham, "Energy
    Spectra of electrons field emitted from a broad area composite
    cathode of tantalum carbide", to be published in "Journal of
    Materials Science".

6. D. Stewart and P.D. Wilson, "Recent Developments in Broad Area
    Field Emission Cold Cathodes", Vacuum Devices Conference, 25 - 27
    March, Cavendish Laboratory, Cambridge, U.K. to be published in
    "Vacuum".

TABLE 1. SELECTED PHYSICAL PROPERTIES OF REFRACTORY CARBIDES

cpd.	Melting Point, °C	Resistivity		ϕ eV		Thermal cond., 10^3 cal. $cm^{-1}s^{-1}deg^{-1}$	Linear Coeff. Exp., $\alpha \times 10^6 \; deg^{-1}$ (0-1200°C)
		ρ μ ohm.cm	Temp. Coeff. x 10^3	TH	FE		
TiC	3150 [12] 3067 [17]	52.5 [12]	1.16 [12]	2.35 [12]	2.72 [16]	58 [12]	7.74 [12]
ZrC	3530 [12] 3420 [17]	50 [12]	0.95 [12]	3.8 [12]	-	49 [12]	6.73 [12]
HfC	3890 [12] 3950 [17]	45 [12]	1.42 [12]	2.03 [12]	-	15 [12]	6.06 [12]
V_2C	2165 [17]	-	..	-	-	-	-
VC	2830 [12] 2700 [17]	65 [12]	-	3.85 [16]	-	59	7.2
Nb_2C	3080 [17]	-	-	-	-	-	-
NbC	3760 [12] 3600 [17]	51.1 [12]	0.86 [12]	2.24 [12]	-	34 [12]	6.5 [12]
Ta_2C	3330 [17]	-	-	-	-	-	-
TaC	3880 [12]	42.1 [12]	1.07 [12]	3.14 [12]	-	53 [12]	8.29 [12]
Mo_2C*	2570 [12] 2580 [17]	71.0 [12]	0 [12]	3.85 [16]	-	16 [12]	6.8/9.3 [12]
MoC^+	2580 [17]	19? [14]	-	-	-	-	-
W_2C	2776 [17]	80 [14]	-	-	2.6 - 4.42 [16]	-	-
WC	2870 [12] 2776 [17]	19.2 [12]	0.495 [12]	3.6 [16]	-	70 [12]	3.84/3.90 [12]

* Subject to decomposition reactions at temperatures below m.p. [13, 18].

+ Stable only at high temperatures.

In Tables 1, 2 and 3

    TH $\equiv$ Thermal

    FE $\equiv$ Field Emission

    ϕ = Work Function

TABLE 2. SELECTED PHYSICAL PROPERTIES OF REFRACTORY BORIDES

| cpd. | Melting Point, °C | Resistivity | | Ø eV | | Thermal cond., 10^3 cal. $cm^{-1}s^{-1}deg^{-1}$ | Linear Coeff. Exp., $\alpha \times 10^6\ deg^{-1}$ (0-1200°C) |
		ρ, μohm, cm	Temp. Coeff. x 10^3	TH	FE		
TiB	(decomposes) 1900 [14]	40 [14]	-	-	-	-	-
TiB$_2$	2980 [12]	14.4 [12]	2.78 [12]	3.88 [12]	-	58 [12]	6.5/5.1 [12]
ZrB$_2$	3040 [12] >3200 [18]	16.6 [12]	1.76 [12]	3.67 [12]	-	58 [12]	6.63 [12]
HfB$_2$	3250 [12] ~3350 [12]	8.8 [12]	3.6 [12]	3.85 [16]	-	-	5.8
V$_3$B$_2$	~2300 [18] 2070 [19] 1900 [14]	35-40 [14]	-	-	-	-	-
VB$_2$	2400 [12] 2425 [18]	19 [12]	3.16 [12]	3.95 [12]	-	-	7.5
NbB	~2300 [18]	64.5 [14]	-	-	-	-	-
NbB$_2$	3000 [12]	34.0 [12]	1.39 [12]	3.65 [12]	-	40 [12]	7.9/8.3 [12]
TaB$_2$	3100 [12] ~3200 [14] 3030 [18]	37.4 [12]	1.48 [12]	2.89 [12]	-	26 [12]	5.12 [12]
Cr$_2$B	1850 decomposes? 1870 [18]	-	-	-	-	-	11.6/11.1 [19]
CrB$_2$	1900- 2200 [19]	20 [14]	-	3.36 [19]	-	-	-
Mo$_2$B	decomposes ~2000 [14] ~2270 [18]	40 [14]	-	-	-	-	-
Mo$_2$B$_5$	2100 [12] 2200 [18]	18 [12] 25 [14]	3.3 [12]	3.38 [12]	-	64 [12]	-
MoB$_2$	~2350 [18]	45 [14]	-	3.38 [16]	-	-	-
W$_2$B	2770 [14]	-	-	-	-	-	-
W$_2$B$_5$ (WB$_2$?)	~2330 [14] 2370 [18]	43.6 [12] 21 [19]	4.26 [12]	2.62 [12]	-	76 [12]	-

32.

TABLE 3. **SELECTED PHYSICAL PROPERTIES OF REFRACTORY NITRIDES**

cpd.	Melting Point, $^{\circ}C$	Resistivity		$\emptyset$ eV		Thermal cond., 10^3 cal. $cm^{-1}s^{-1}deg^{-1}$	Linear Coeff.Exp., $\alpha \times 10^6 deg^{-1}$ (0-1200°C)
		ρ μ ohm.cm	Temp. Coeff., x 10^3	TH	FE		
TiN	3205 [12] 2950 [18]	25 [12]	2.48 [12]	2.92 [12] 3.75 [16]	–	48 [12]	9.35 [12]
ZrN	2980 [12]	21.1 [12]	2.92 [12]	2.92 [12] 3.90 [16]	–	40 [12]	10.1 [12]
HfN	3300 [12] 3310 [14]	33 [14] for HfN0.86	–	–	–	–	–
VN	2360 [12]	85.0 [12]	0.7 [12]	3.56 [16]		42 [12]	8.35 [12]
NbN	2300 [12] 2o50 [14]	60.0 [12]	–	3.92 [16]		8 [12]	10.1 [12]
TaN	3090 [12]	200 [12] 128 [14]	0.06 [12]	4.0 [16]		11 [12]	–

33.

TABLE 4. EUTECTIC EQUILIBRIA IN BINARY CARBON SYSTEMS

Binary Carbon Systems		Eutectic Temperature °C	Eutectic Composition at %C	COMPONENTS				Ref. No.
				Refractory Compound	m.p., °C	2nd Phase	m.p., °C	
TiC	1.	1645 ± 8	4.4 at %C	~TiC	3150	TiO.6 at %C	(1667?)	18
		3050	58	~Tic	3150	C	(1500)	
	2.	1650 ± 7	1.5 at %C	~Tic	3067 ± 25 at 44 at %C	Ti	(1667)	20
Zr-C	1.	1835 ± 20	3 ± 1.5 at %C	ZrC	3445 ± 20 at 44 ± 1 at %C	Zr	(1852)	20
	2.	2850 ± 50	65 at %C	ZrC	3420 at 46 at %C	C	(5000)	18
Hf-C	1.	2210 ± 50	9.5 at %C	HfC	3830 at 47 at %C	Hf	(2227)	18
		3050 ± 50	68 at %C	HfC	3830 at 47 at %C	C	(5000)	20
	2.	No Hf/HfC eutectic. HfC/C eutectic as follows:						
		3180 ± 30	68 ± 1.5 at %C	HfC	3928 at 48.5 + 0.3 at %C	C	(5000)	20
V-C	1.	1630	1.5 at %C	~V₂C	2165	V 6 at %C	(1888)	18
	2.	1650 ± 70	15 ± 1 at %C	~V₂C	2187 ± 10	V 5.5 ± 1 at %C	(1888)	20
		2625 ± 12	49.5 ± 0.5 at %C	~VC	2648 ± 12 at 43 ± 0.5 at %C	C	(5000)	
Nb-C	1.	2335	10.5 at %C	~Nb₂C	3080 at 48 at %C	Nb~7 at %C	(2468)	18
		3220 - 3300	60.5 at %C	~NbC	3080 at 48 at %C	C	(5000)	
	2.	2353 ± 10	10.5 ± 0.5 at %C	~Nb₂C	3035 ± 20	Nb 7 ± 1 at %C	(2468)	20
		3305 ± 20	60.1 at %C	~NbC	3613 ± 26 at 44 + at %C	C	(5000)	
Ta-C	1	2825	10.8 at %C	~Ta₂C	?	Ta~5 at %C	(2980)	18
		3375	61 at %C	~TaC	3825 at 48 at %C	C?		

TABLE 4. (Continued.)

Binary Carbon Systems		Eutectic Temperature °C	Eutectic Composition at %C	Refractory Compound	COMPONENTS			Ref. No.
					m.p., °C	2nd Phase	m.p., °C	
Ta-C (Continued)	2.	2843 ± 15	12 +0.5 at %C	~Ta₂C (NB. transformation near 2020°C)	3330 ± 30	Ta 7.5 ± 0.5 at %C	(2980)	20
		3445 ± 26	61 ± 0.6 at %C	~TaC	3985 ± 40 at 47 ± 0.5 at %C	C	(5000)	18
Mo-C	1.	2200	12.1 at %C	M~₂C	2400	Mo~7 at %C	(2615)	20
	2.	2200 ± 5	17	Mo₂C (NB α ⇌ β transformation at ~1430°C)	2522 at 34 at %C	Mo< 1.5 at %C	(2615)	
	3.	2180 ± 20	19 at %C	Mo₂C	2420	Mo ~1 at %C	(2615)	15,pp 143-155
W-C	1.	2475	17.9 at %C	~W₂C	2750	W 0.4 at %V	(3400)	18
	2.	2710 ± 12	22 at %C	~W₂C	2776 ± 12 at 31 at %C	W<1 at %C	(3400)	20
Re-C		2500	?	No carbide known.				

35.

TABLE 5.   EUTECTIC EQUILIBRIA IN BINARY BORON SYSTEMS

Binary Boron Systems	Eutectic Temperature °C	Eutectic Composition at %B	COMPONENTS				Ref. No.
			Refractory Compound	m.p. °C	2nd Phase	m.p. °C	
B-Cr	1620	14 at %B	Cr_2B	1870	Cr 2 at %B	(1857)	18
	2050	55	CrB	2100	Cr_3B_4	2070	
	1830	81	CrB_2	2200	B	(2300)	
B-Hf	1820	12 at %B	HfB_2	~3350	Hf~2 at %B	(2227)	18
	2070	98	HfB_2	~3350	B	(2300)	
B-Mo 1.	~2200	23 at %B	Mo_2B	~2270	Mo 1 at %B	(2615)	18
	~1950	83 at %B	Mo_2B_5	~2200	MoB_{12}	2100	
	~2040	~95	$MoB_{~12}$	~2100	B	(2300)	
2.	2190	21.5 at %B	Mo_2B	-	Mo 0.9 at %B	(2615)	21
B-Nb	1625	20 at %B	NbB	2300	Nb 2 at %B	(2467)	18
	1950	90	NbB_2	3000	B 2 at %Nb	(2300)	
B-Re	1830	42 at %B	Re_7B_3	2000	ReB_2	2400	18
	2050	92	ReB_2	2400	B	(2300)	
B-Ta	~2360	24 at %B	Ta_2B	~2380	Ta 2 at %B	(2980)	
	(NB. Eutectoid reaction of Ta_2B at 2040°C to give Ta + TaB, mp 3090°C)						
	~3000	63	Ta_3B_4	3030	TaB_2	3030	18
	~2070	97	TaB_2	3030	B 1.7 at %Ta	(2300)	
B-Ti	1540	15 at %B	TiB	>2600	Ti	(1667)	18
B-V	1575	15 at %B	V_3B_2	~2300	V 3 at %B	(1888)	18
	2025	44	V_3B_2	~2300	VB	2225	
	2200	52	VB	2225	V_3B_4	2225	18

TABLE 5. (Continued)

Binary Boron Systems	Eutectic Temperature °C	Eutectic Composition at %B	COMPONENTS				Ref. No.
			Refractory Compound	m.p., °C	2nd Phase	m.p., °C	
B-V (Contd.)	2000	90	VB_2	2425	B	(2300)	
B-W	~2650	24 at %B	W_2B	~2740	W	(3400)	18
	~2550	42	W_2B	~2740	WB	2800	
	~2270	85	W_2B_5	2370	WB_{12}	2440	
	2100	96	WB_{12}	2440	B	(2300)	
B-Zr	1680	14 at %B	ZrB_2	>3200	W 3 at %B	(1852)	18
	1975	96	ZrB_2	>3200	B 1 at %W	(2300)	

TABLE 6.   EUTECTIC EQUILIBRIA IN TERNARY CARBON SYSTEMS

Ternary Carbon Systems	Eutectic Temperature °C	Eutectic Composition	COMPONENTS				Ref. No.
			Refractory Compound	m.p. °C	2nd Phase	m.p. °C	
C-Co-Cr			$Cr_{7-x}Co_xC_3$		Co,Cr (=γ-Co)		22
C-Co-Nb	1225 ± 10	87 ± 0.5 wt.%Co	NbC 1.5 wt.%Co		Co 4.3 wt.%NbC		23
C-Cr-Nb	1110 ± 10	76 ± 0.5 wt.%Cr	Nb 3 wt. %Cr		Cr 0.9 wt.% NbC		23
C-Fe-Nb	1310 ± 10	90.5 ±0.5 wt%Nb	Nb 1.8 wt.%Fe		Fe 0.98 wt.%NbC		23
C-Hf-Mo	1. 2310	75 at %Mo	HfC (dissolves 8 at % Mo).	3900	Mo	(2615)	24
	2. 2350 ± 20		HfC		Mo 3.3 Wt.% HfC at 2100°C		25
C-Mo-Ti	1. 2175 ± 15	20 mole % TiC	TiC 38 at % Mo		Mo 4 mole % TiC	(2615)	26
	2. 2290 ± 20		TiC		Mo with 3 wt.% TiC	(2615)	25
	3. 2240 ± 15	37 ± 2 mole % $Ti_{0.52}C_{0.48}$	$Ti_{0.52}C_{0.48}$	3000°C (incongruent)	Mo 10 at %Ti	(2615)	20
C-Mo-Zr	1. 2250	70 at %Mo	ZrC 8 at %Mo		Mo	(2615)	27
	2. 2260 ± 20				Mo 3.5 wt.% ZrC		25, 28
C-Nb-Ni	1. 1330	9.6 wt.% NbC	NbC 2 wt.% Ni		Ni 7 wt.% NbC	(1455)	29
	2. 1115 ± 10	88.5 wt.% Ni			Ni 3.5 wt.% NbC		23
C-Nb-Re	2225 ± 15	70 at %Re	NbC 1.5 at %Re		Re 2-4 mole %NbC	(3180)	15 pp 165-171
(NB. volatilization of Re and C in Argon atmosphere and at 2100 - 2200°C).							
C-Ni-Ti	1280	9.3 (mole?)%TiC	TiC 0.7 - 0.8 (mole?) % Ni at 1280°C		Ni 6.2(mole?)%TiC	(1455)	30, 31
C-Ni-Zr	1270	11 wt.% ZrC	ZrC		Ni 2.7 wt.% ZrC	(1455)	29
C-Re-Ta	2420	70 at %Re	TaC 3-4%Re		Re	(3180)	32
C-Re-Zr		67 at %Re	ZrC		Re	(3180)	33

TABLE 7. EUTECTIC EQUILIBRIA IN TERNARY BORON SYSTEMS

Ternary Boron Systems	Eutectic Temperature °C	Eutectic Composition at %C	COMPONENTS — Refractory Compound	m.p., °C	2nd Phase	m.p., °C	Ref.No.
B-C-Zr	2390 ± 15	33 ± 2 mole %C	ZrB_2	3245 ± 18	C	(5000)	20
	2220 ± 20	65 ± 5 mole %B_4C	ZrB_2 1-2 mole B_4C	3245 ± 18	B_4C ~1 mole %ZrB_2	2450	
B-Cr-Ti	~1320	40 mole %Ti_2B	Ti_2B (may be identical with TiB)	(~2200?)	Cr	(1860)	34
B-Hf-W	2309 ± 18	94 mole %"WB_2"	"$WB_{\sim 2}$"(given as W_2B_5)	2365	HfB_2 23 mole % "$WB_{\sim 2}$"	3390	20
B-Mo-Zr 1.	2040 ± 20	>15 wt.%ZrB_2 (68.9 at %Mo.)	ZrB_2	(>3200)	Mo 0.6 wt.%ZrB_2	(2615)	35
2.	2060 ± 25	47.7 at %Mo	ZrB_2	(>3200)	Mo	(2615)	36
B-C-Hf	3140 ± 15	34 <2 mole %HfC	HfB_2 <2 mole %HfC	3380 ± 20	$Hf_{1.00}C_{0.90}$	3900	20
	2515 ± 10	38 ± 2 mole %C	HfB_2 - 2mole%C		C 10 mole %HfB_2	(5000)	
	2330 ± 25	78 mole %B_4C	HfB_2 <mole %B_4C		B_4C 1 mole %HfB_2	2450	
B-C-Nb	~2600	32 mole %C	NbB_2	3000	C	(5000)	37
B-C-Ta	~2600	32 mole %C	TaB_2	3030	C	(5000)	37
B-C-Ti	2507 ± 15	32 mole %C	TiB_2	3225 ± 20	C	(5000)	20
B-C-V	~2450	30 mole %C	VB_2	2425	C	(5000)	37
B-C-W	2330 ± 20	38 ±3mole %W_2C_2	W_2C~5 mole %WB	2776	WB 6 mole %W_2C	2665	20
	2360 ± 15	13 ± 1.5 at %C	WB 4 at %C	2665	C	(5000)	
	2275 ± 15	7 ± 1.5 at %C	W_2B_5 -3 at %C	2365	C	(5000)	
	2220 ± 20	24 ± 3 mole %B_4C	W_2B_5 ~3 mole %B_4C	2365	B_4C	2450	
B-Nb-Ti	~2130	10 mole %TiB_2	$NbTiB_2$	2840	Nb	(2467)	38
	~2690	95 mole %TiB_2	$NbTiB_2$	2840	TiB_2	–	
B-Ti-W	~2390	12 mole %TiB_2	$WTiB_2$	2690	W	(3400)	38
	~2560	88 mole %TiB_2	$WTiB_2$	2690	TiB 5 at %W	–	

TABLE 8. EUTECTIC EQUILIBRIA IN TERNARY NITROGEN SYSTEMS

Ternary Nitrogen Systems	Eutectic Temperature, °C	Eutectic Composition,	COMPONENTS				
			Refractory Compound	m.p., °C	2nd Phase	m.p., °C	Ref.No.
N-V-Ti	1870	6.0 mole % TiN	TiN		V	(1888)	39
N-V-Zr	1795	4.7 mole % ZrN	ZrN		V	(1888)	39

40.

TABLE 9. UNIDIRECTIONAL SOLIDIFICATION IN BINARY SYSTEMS

Binary Systems		COMPONENTS		Eutectic Temperature °C	Volume % Refractory Phase	Microstructures	Ref. No.
		Refractory Phase	Second Phase (matrix)				
B-Ti	1.	TiB	Ti	1670	10	Anomalous	42, p 310
	2.	TiB	Ti	-	(7.7 taking eutectic at 7.1 %B)	rod-like	46
C-Cr	1.	$Cr_{23}C_6$	Cr	1498	61	Cr Fibres	47
C-Mo		Mo_2C	Mo	2200	37	Lamellar	42, p 312
C-Nb	1.	Nb_2C	Nb	2335	31	Rectangular Fibres	42, p 312
	2.	Nb_2C	Nb			Rod-like or lamellar, depending on growth rate and C content.	48
C-Ta	T	Ta_2C	Ta	2800	39	Rod-like, rectangular fibres or Ta_2C plus lamellae.	42, p 312
C-V	1.	V_2C	V	1650	34	Lamellar	42, p 313
	2.	$VC_{0.87}$	C (graphite)	2625	-	Lamellar with graphite lamellae approx. to growth axis.	49

41.

TABLE 10. UNIDIRECTIONAL SOLIDIFICATION IN TERNARY SYSTEMS

Ternary Systems		COMPONENTS		Eutectic Temperature, °C	Volume % Refractory Phase	Microstructures	Ref. No.
		Refractory Phase	Second Phase (matrix)				
C-Co-Cr	1.	$(Cr,Co)_7C_3$	(Co,Cr)	1300	30	Rod-like [0001] texture.	50, 51
	2.	$(Cr,Co)_{23}C_6$	(Co,Cr)	1340 (range)	~40	Rod-like, anomalous	52
C-Co-Hf		HfC	Co	1365	15	Rod-like	42, p.322
C-Co-Nb		NbC	Co		12	Rod-like/lamellar	42, p.322
C-Co-Ta		TaC	Co	-	-	Cubic particles, [100] facet planes with trifoils and irregular whiskers, <111> fibre directions.	53
C-Co-Ti		TiC	Co	1360	16	Rod-like	42, p.323
C-Co-V		VC	Co		20	Rod-like	42, p.323
C-Fe-Ta		TaC	Fe	-		Cubic particles 100 facet planes with irregular trifoils and whiskers, <111> fibre directions.	53
C-Hf-Ni		HfC	Ni	1260	28/15	Rod-like	42, p.323
C-Nb-Ni		NbC	Ni	1328	11	Rod-like	42, p.323
C-Ni-Ta		TaC	Ni	-	-	Cubic particles [100] facet planes with irregular trifoils and whiskers, <111> fibre directions.	53
C-Ni-Ti		TiC	Ni	1307	5	Rod-like	42, p.323

TABLE 11. UNIDIRECTIONAL SOLIDIFICATION IN MULTICOMPONENT SYSTEMS (QUATERNARY AND HIGHER)

Multicomponent Systems	COMPONENTS		Eutectic Temperature, °C	Volume % Refractory Phase	Microstructures	Ref. No.
	Refractory Phase	Second Phase (matrix)				
Al-C-Co-Cr	$(Cr,Co)_7C_3$	(Co,Cr,Al)	1295	28	Rod-like	52
Al-C-Co-Cr-Ni	$(Cr,Co)_{23}C_6$	(Co,Cr,Ni,Al)	-	-	Rod-like, anomalous	52
Al-C-Co-Cr-Ni-Ta	TaC	(Ni,Co,Cr,Al)	-	9	Rod-like	52
Al-C-Cr-Ni	Cr_3C_2	$(Al,Ni)\gamma/\gamma$	-	-	Rod-like	51
Al-C-Cr-Fe-Y	Cr_7C_3	(Fe,Cr,Al,Y)	-	-	Rod-like	51
C-Co-Cr-Fe	$(Cr,Fe.Co)_7C_3$	(Fe,Co,Cr)	-	-	Rod-like	54A
C-Co-Cr-Nb	NbC	(Co,Cr)	1340	12	Rod-like	55
C-Co-Cr-Ni 1.	$(Cr,Co)_{23}C_6$	(Co,Ni,Cr)	-	-	Anomalous,rod-like	52
2.	$(Cr,Co,Ni)_7C_3$	(Co,Ni,Cr)	-	-	Rod-like	56
C-Co-Cr-Ni-Ta	TaC	(Co,Cr,Ni)	-	-	Rod-like	55, 57
C-Co-Hf-Ni-Zr	HfC/ZrC	(Co,Ni,Cr)	-	-	Rod-like and lamellar (NASA HAFCO-11Z)	58
C-Co-Cr-Ta	TaC	(Co,Cr)	1360	~9	Rod-like	52,59
C-Cr-Fe	$(Cr,Fe)_7C_3$	(Fe,Cr)	-	-	Rod-like	54B
C-Cr-Nb-Ni	NbC	(Ni,Cr)	~1320	11	Rod-like	55
C-Cr-Ni-Si	Cr_3C_2	(Ni,Cr,Si)	-	22	Rod-like	60
C-Cr-Ni-Ta	TaC	(Ni,Cr)	-	-	Rod-like	61

TABLE 12. SUMMARY OF RESULTS OBTAINED AT STANFORD WITH MOLYBDENUM CONES; GEORGIA WITH TUNGSTEN FIBRES AND AT FULMER USING REFRACTORY CARBIDE FIBRES

	Type	Material	Voltage	Maximum Current	Maximum Current Density $A\,cm^{-2}$	Number of Emitting tips cm^{-2}	LIFE TESTS				
							A	$A\,cm^{-2}$	Hours	Pressure mBar	
Stanford R.I.	Thin Film Electrode	Mo	300	100mA	30	6.4×10^5	2mA	3.2	7,000	5×10^{-10}	A.C. Test
Georgia Inst.Tech.	Thin Film Electrode	W	240	-	5	-	-	-	-	10^{-8}	Pulsed 0.1% Duty Cycle
Georgia Inst.Tech.	Diode 0.5mm separation of anode to cathode	W	8 – 10Kv	12.5mA	1	$10^6-5 \times 10^7$		0.1	2,000+	10^{-8}	
Fulmer R.I.	Diode 1.0mm separation of anode to cathode	VC NbC TaC	8 – 10Kv	1.0mA .36nA 5.0mA	5.8 1.3×10^{-2} 0.5	$2 \times 10^6-10^7$	80×10^{-6} 120×10^{-6} 200×10^{-6}	0.5 0.004 0.05	1,000+ 1,000+ 400	5×10^{-7}	D.C.
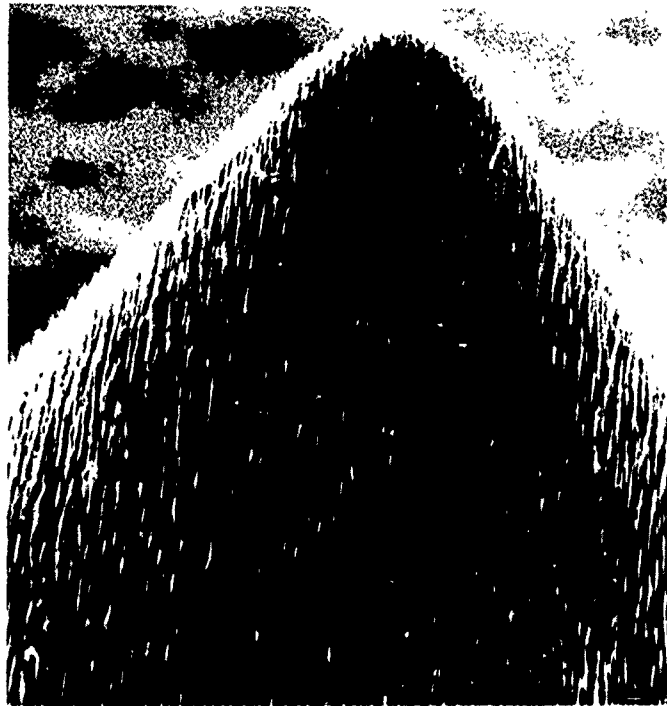
Figure 1.   TaC cathode before testing   x 500
C3911

Figure 2.   TaC cathode before testing   x 10K
C3913

45.

x 24
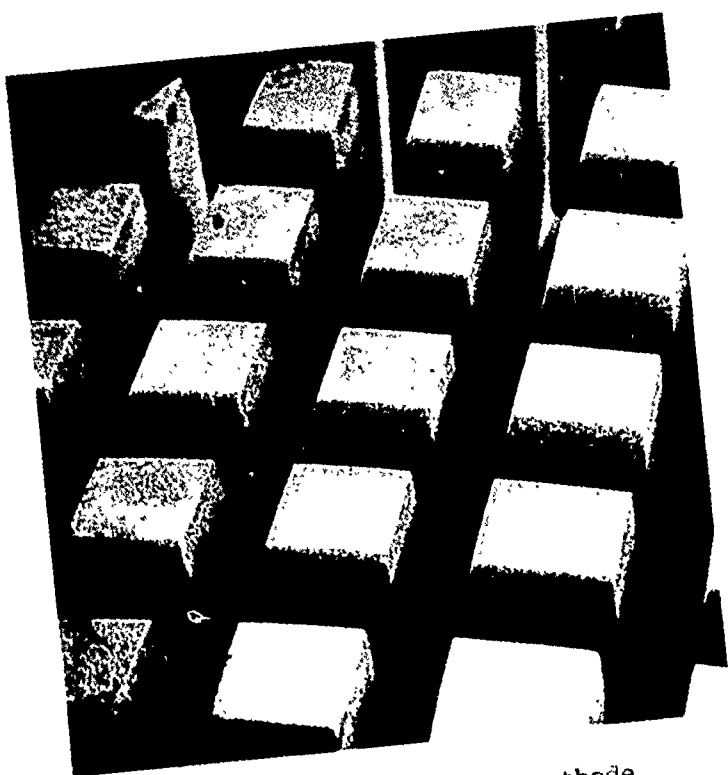
Figure 3. General View of 32-Pin TaC cathode before testing. Pin size is 1mm²

C6023

x 100
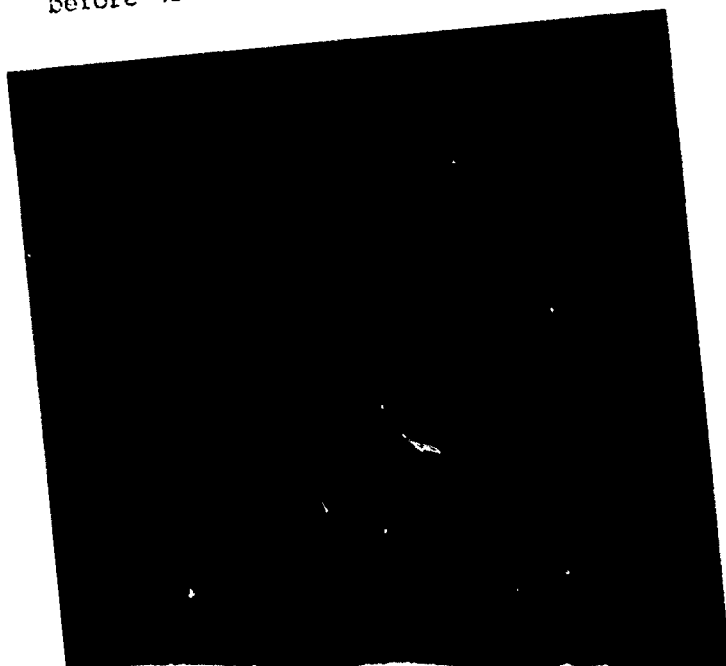
Figure 4. Single Fibre of TaC

C5542

46.
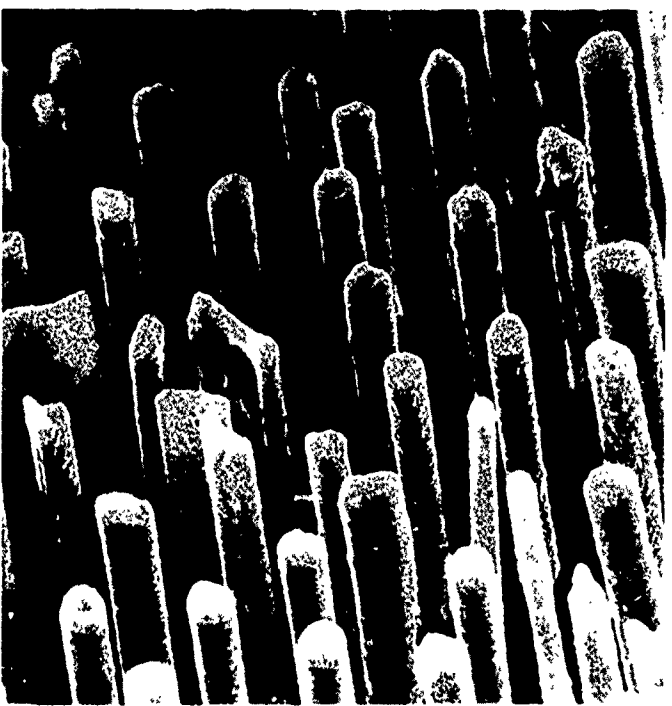
Figure 5.   Typical area of NbC cathode before   x 2.9K
C5577   1000 hour life test.
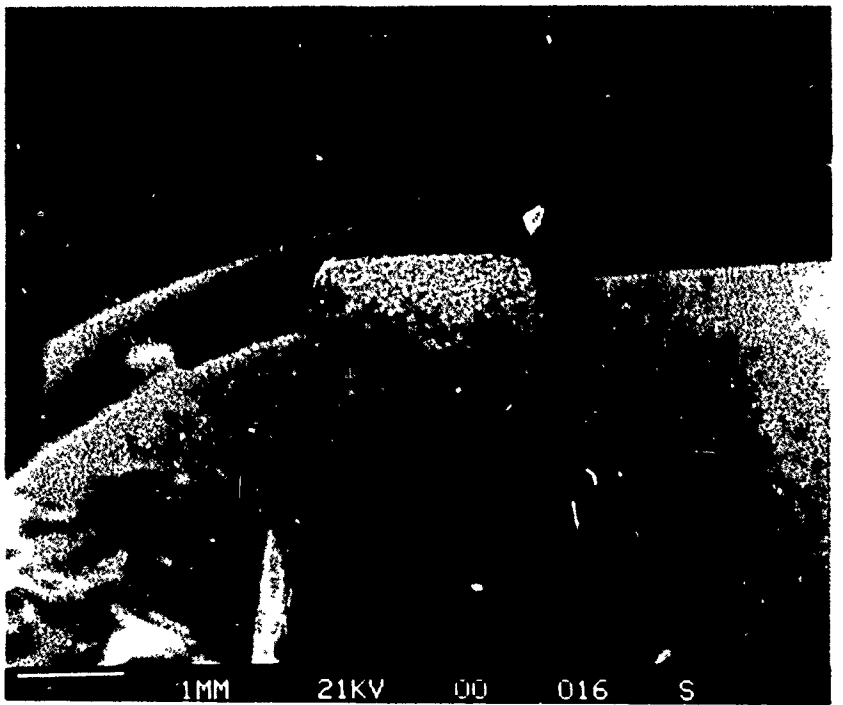
Figure 6.   General View of small fibre NbC   x 20
C6561   cathode before 1000 hour life test.

47.

Figure 7. General View of large fibre NbC cathode x 20
C6143 before testing.

Figure 8. Typical Area of large-fibre NbC cathode x 625
C6148 before testing.
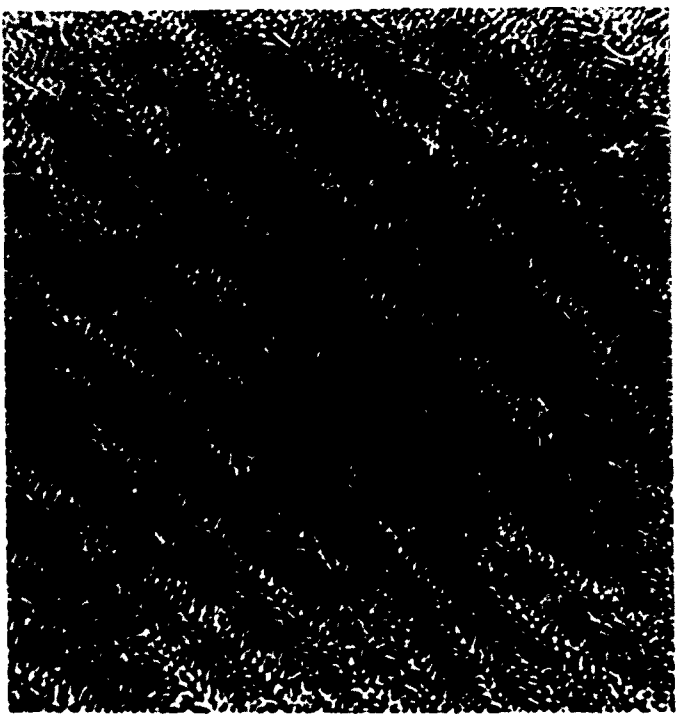
48.

Figure 9.   A-77-205 γ-γ'-α (Ni Mo Ta Al) before   x 900
C4500   testinq.

Figure 10. A-77-205 γ-γ'-α (Ni Mo Ta Al) before   x 10K
C4499   testing.

49.
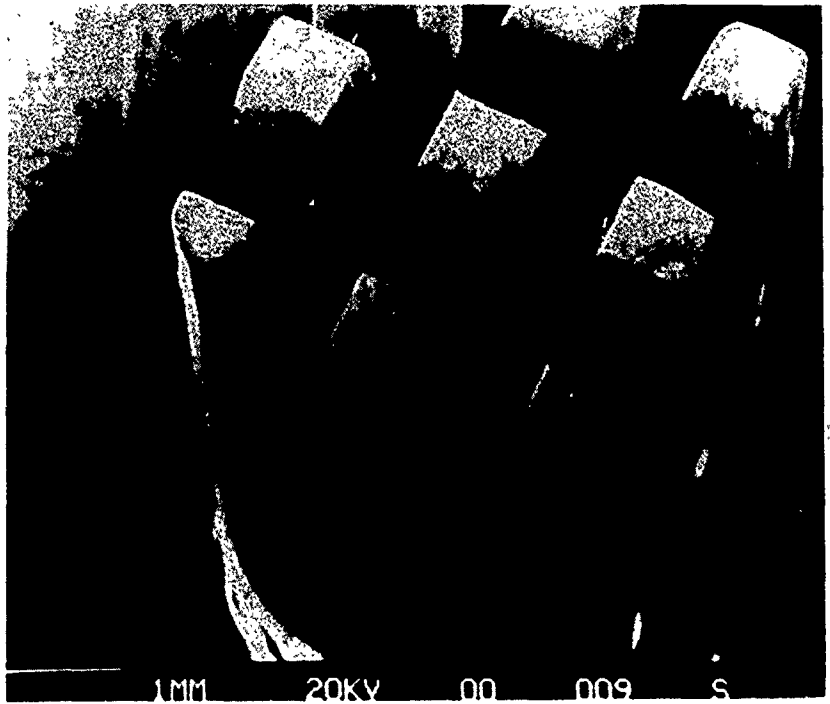
Figure 11. General View of 9-Pin VC cathode   x 20
C6288   before testing.
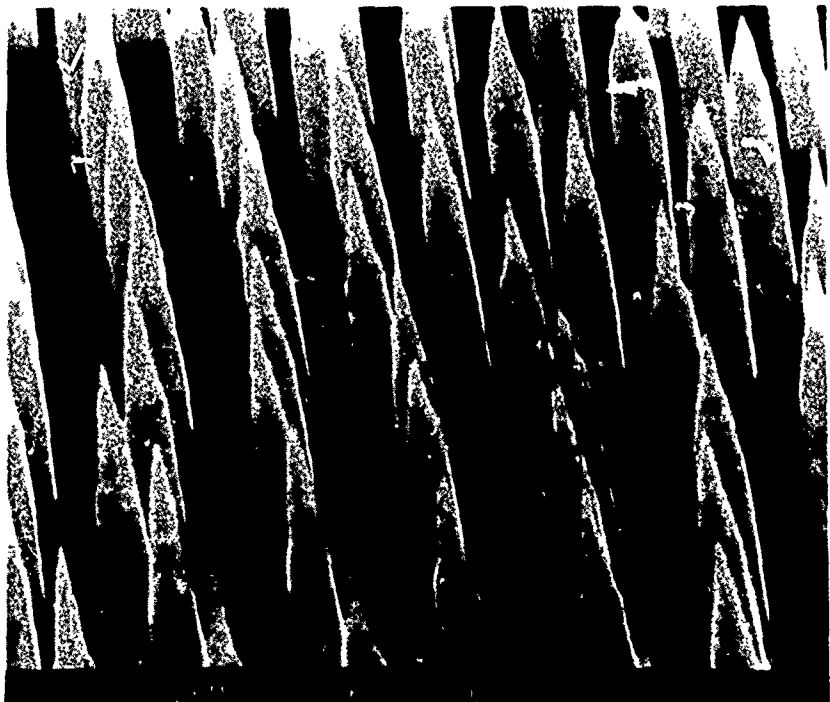
Figure 12. Central pin of 9-pin VC cathode   x 10X
C6346   before testing, typical area.

50.
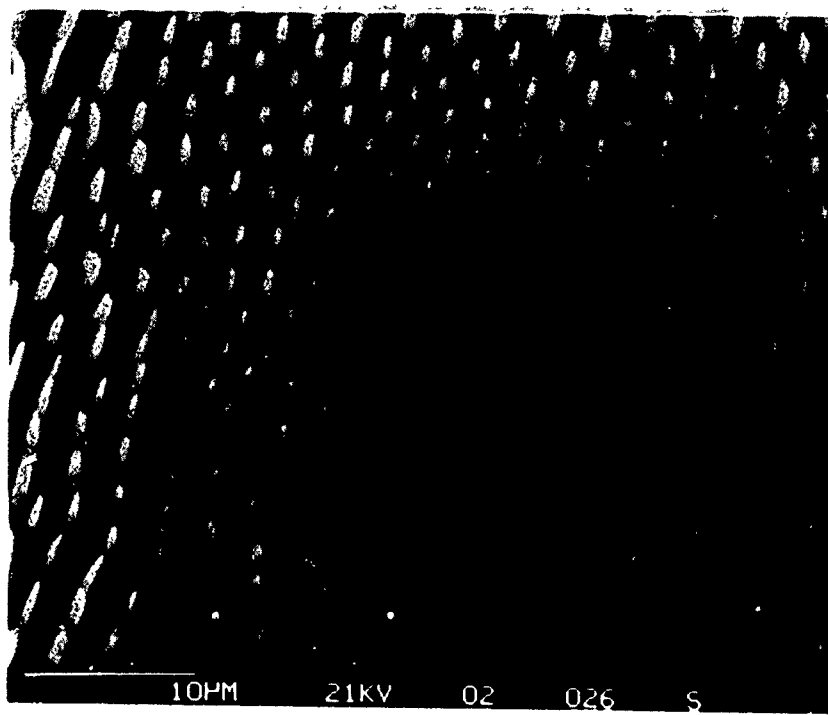
Figure 13. Good Area of 4-Pin VC Cathode   x 3K
C6514   before testing.
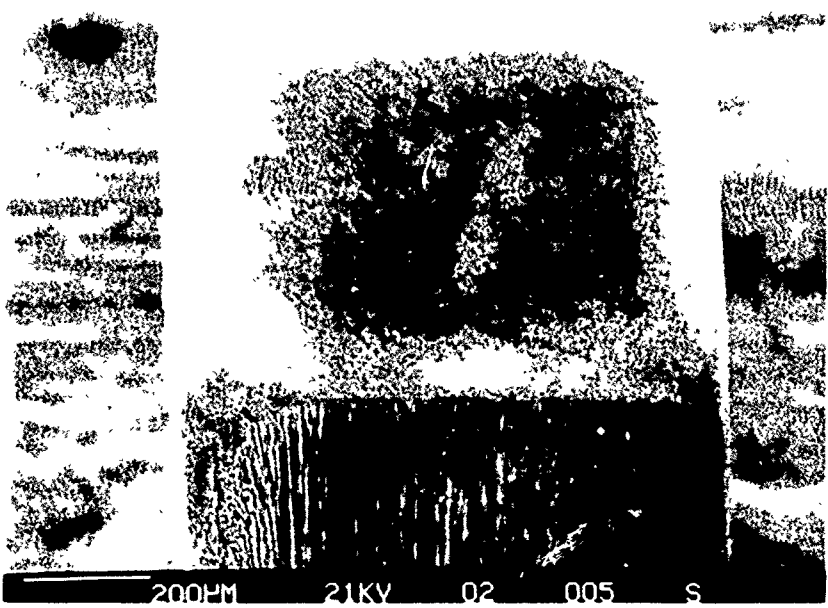
Figure 14. General View of 1 pin VC Cathode   x 100
C6494   before testing.

51.
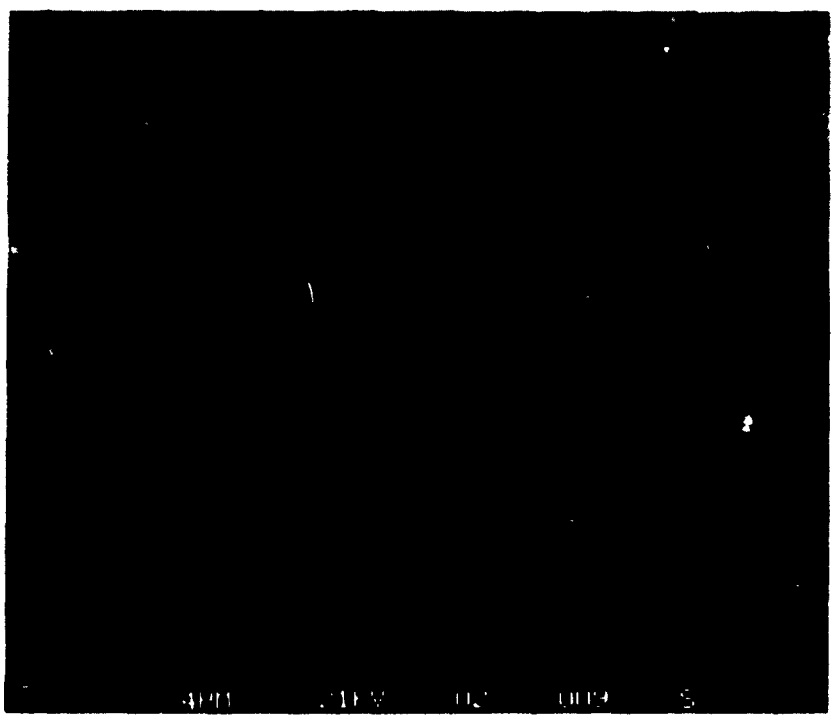
Figure 15.   Central area of 1 pin VC cathode   x 5K
C6498   before testing.
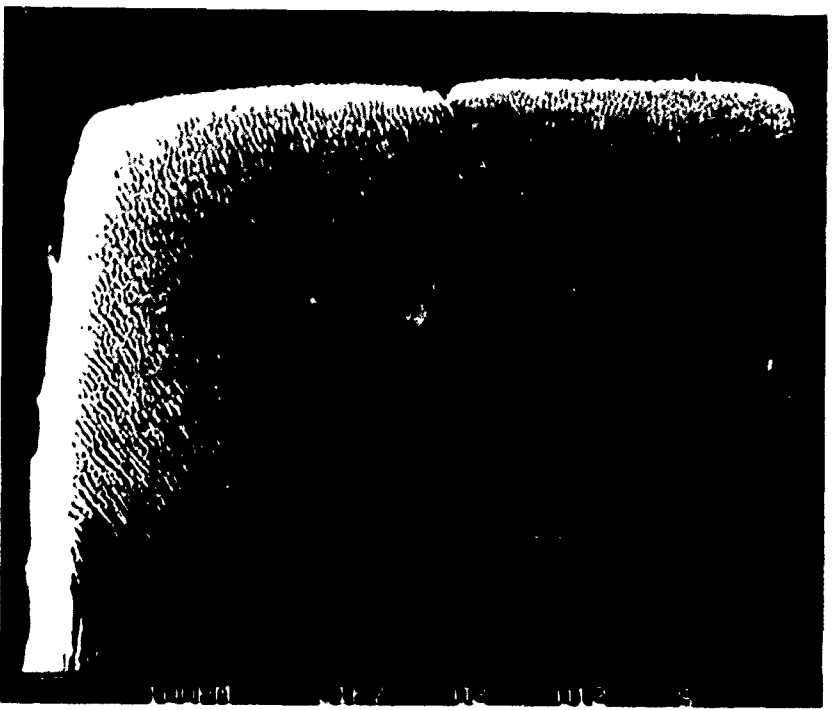
Figure 16.   General View of 300µ x 400µ VC cathode   x 200
C6475   before testing.

52.
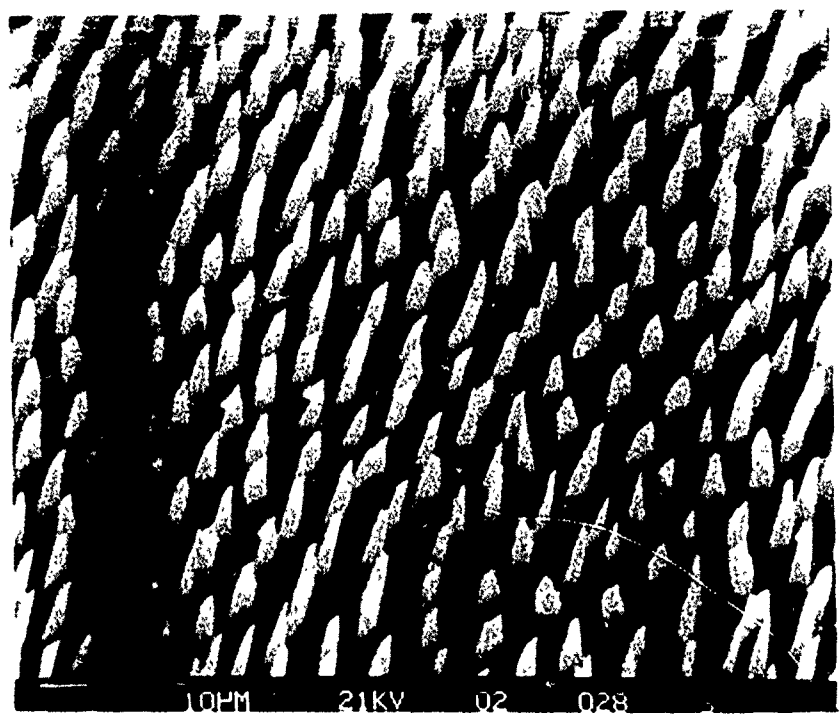
Figure 17. Typical Central area of 300μ x 400μ   x 2K
C6487   VC cathode before testing.
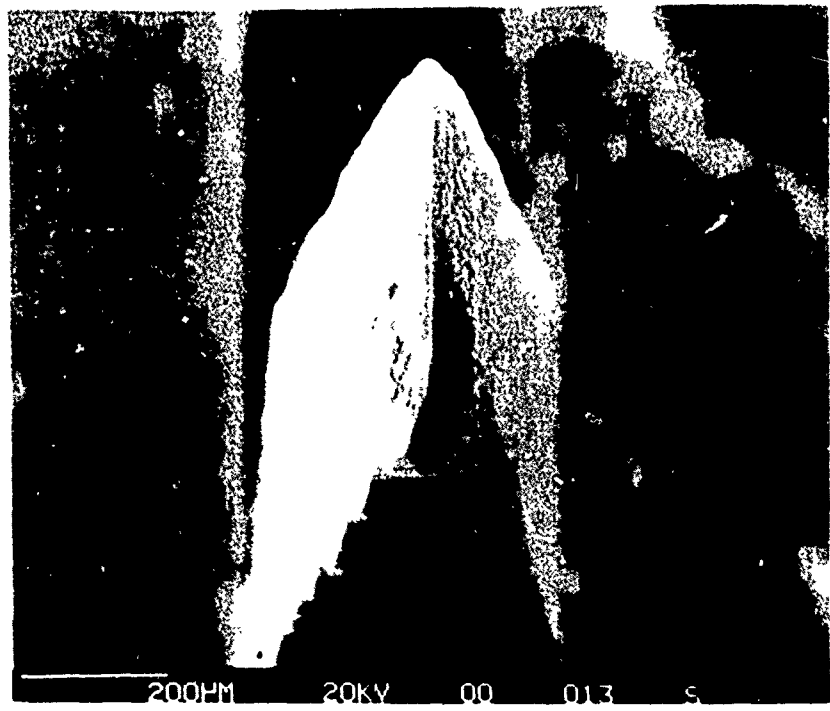
Figure 18. General View of "Chisel" shaped   x 150
C6389   VC cathode before testing.
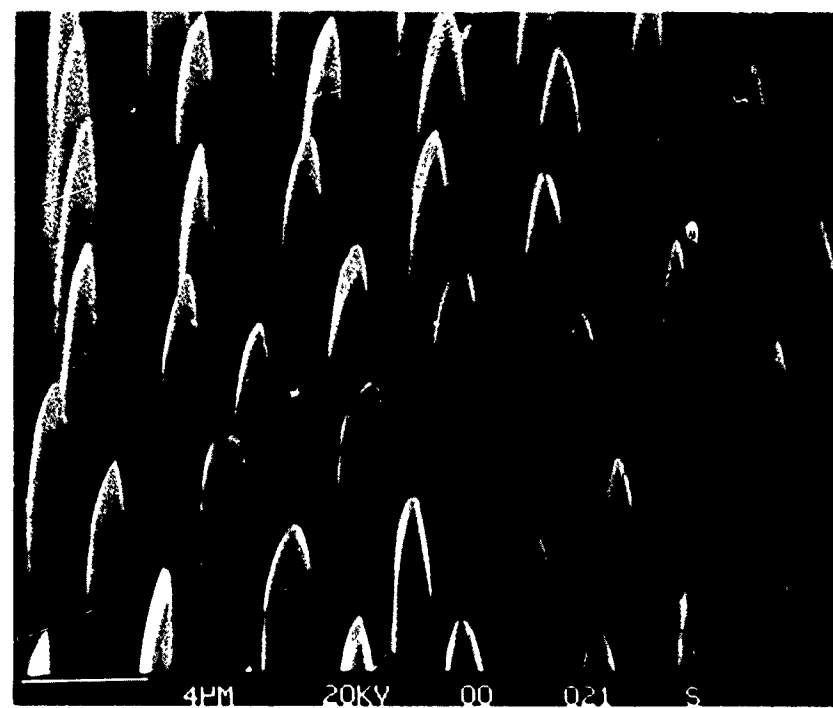
Figure 19. View along the top edge of "Chisel"   x 5K
C6397   shaped VC cathode before testing.
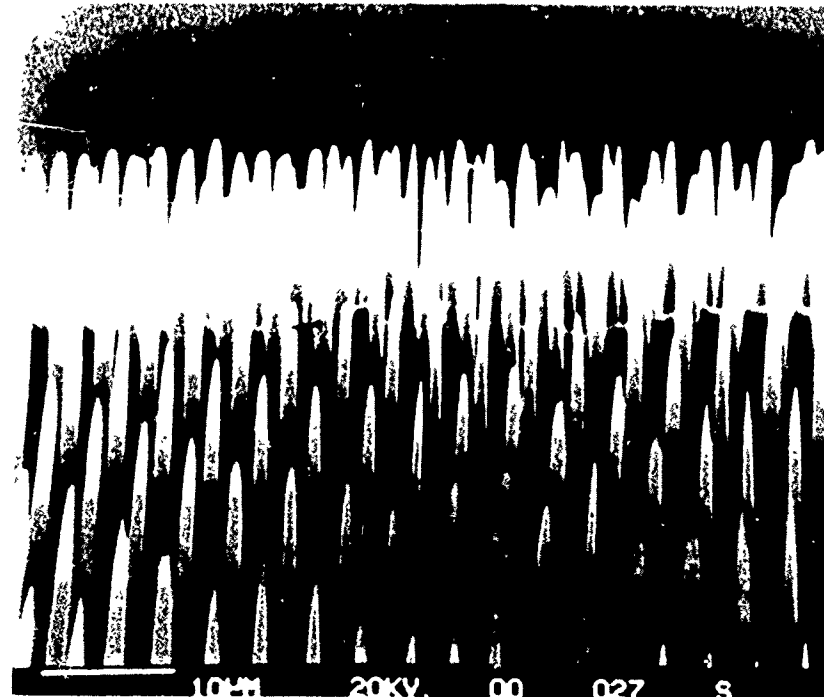
Figure 20. Side view of top edge of "Chisel"   x 2K
C6403   shaped VC cathode before testing.

54.

Figure 21. Separated plates of LaB$_6$
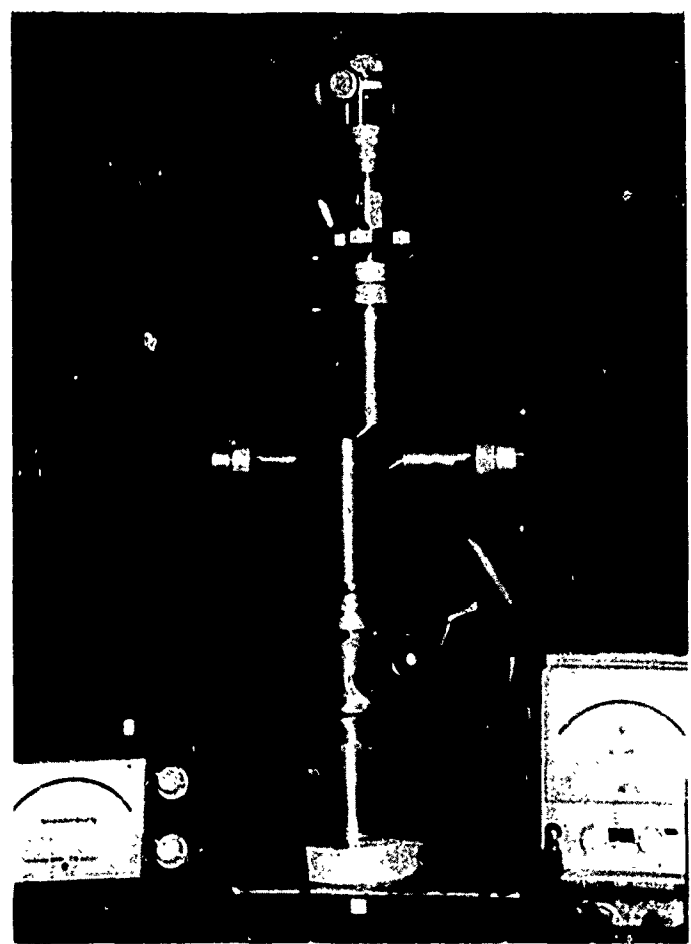
Figure 22. Stainless Steel Chamber used for
Evaluating Cathodes.
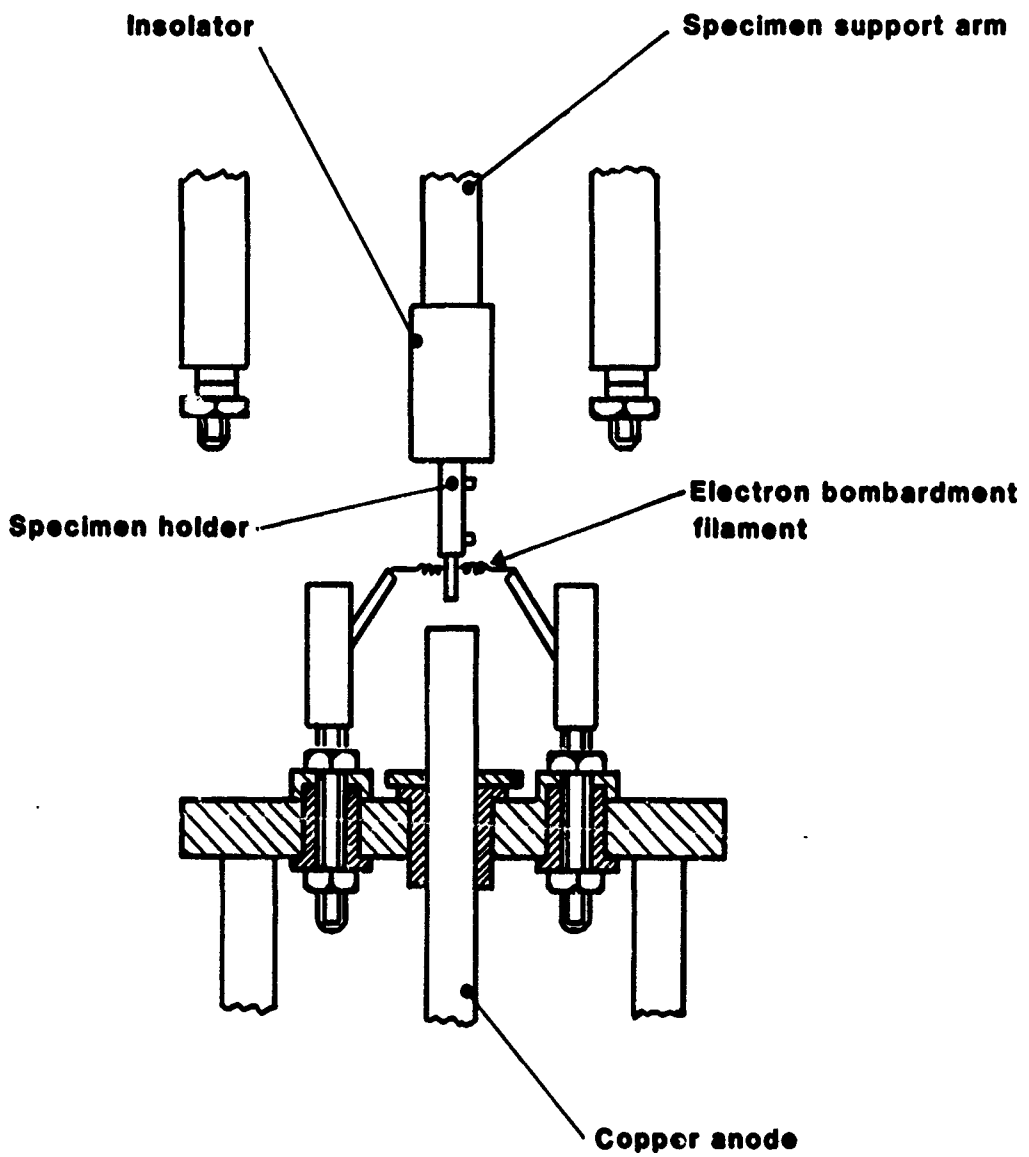
Figure 23. Cathode assembly in stainless steel vacuum chamber
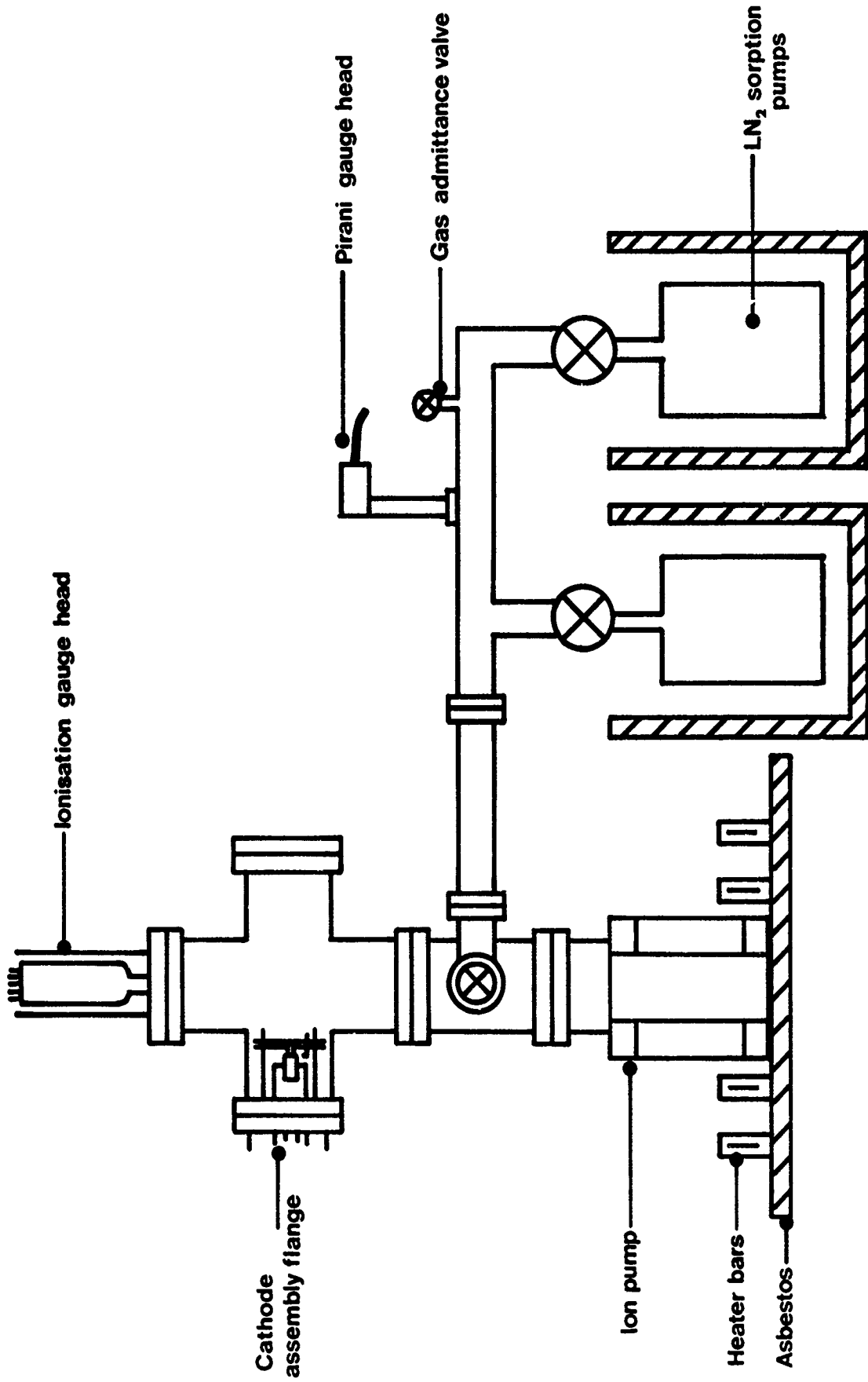
Figure 24. U.H.V. Pumping System
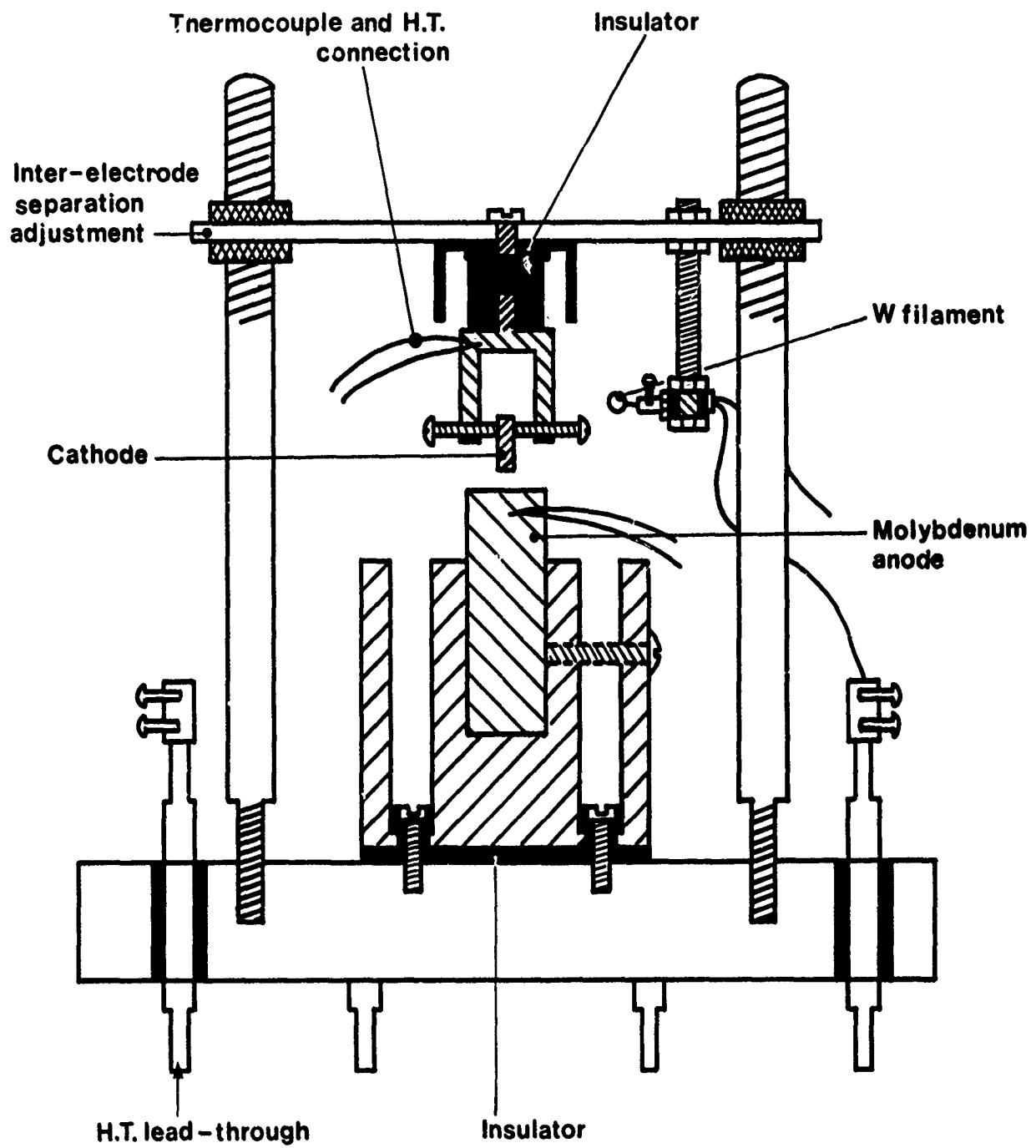
Figure 25. Field emission cold cathode assembly

Thermocouple and H.T. connection

Insulator

Inter-electrode separation adjustment

W filament

Cathode

Molybdenum anode

H.T. lead-through

Insulator
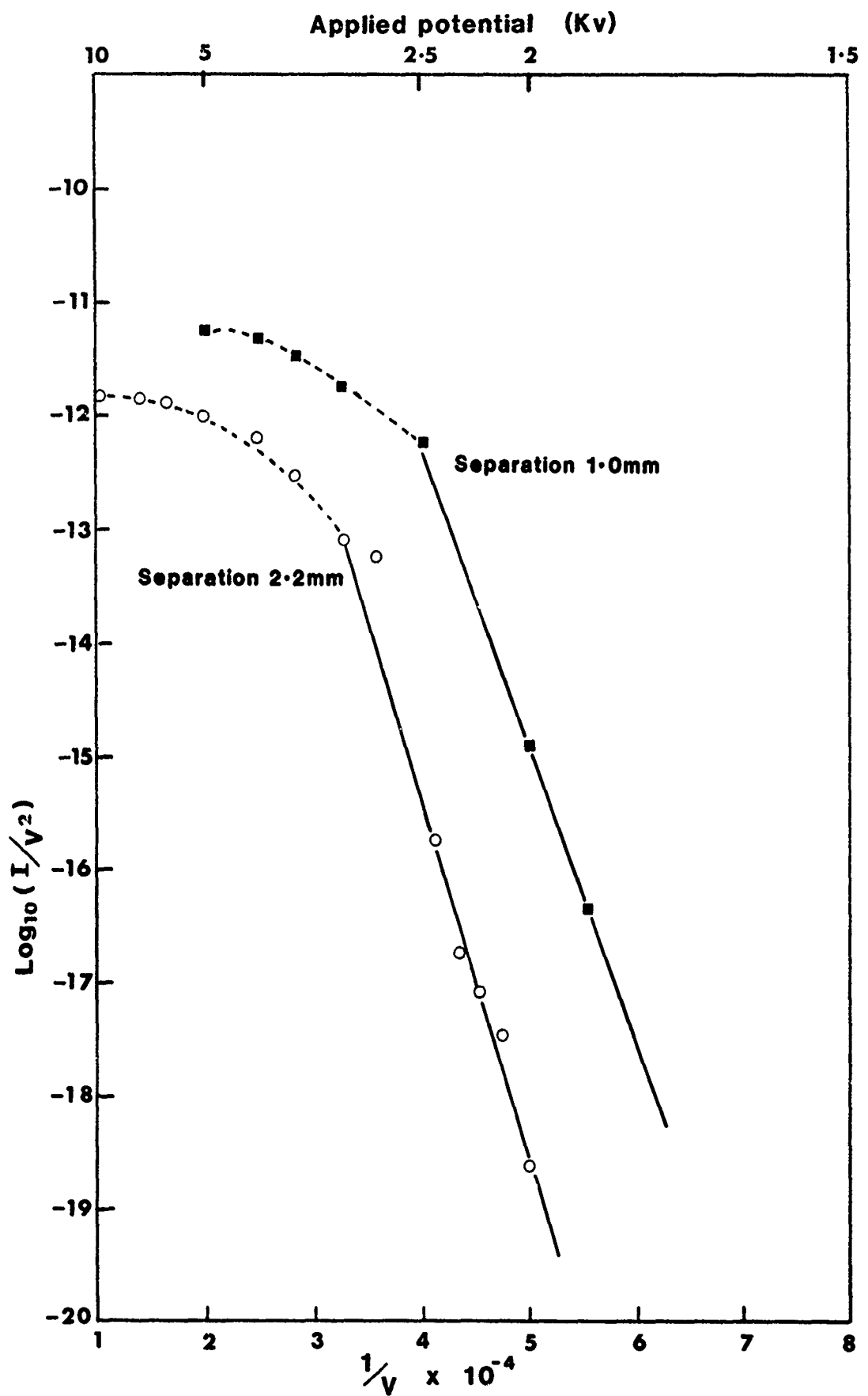
Figure 26. Fowler – Nordheim plots for TaC cathode at the anode to cathode separation shown
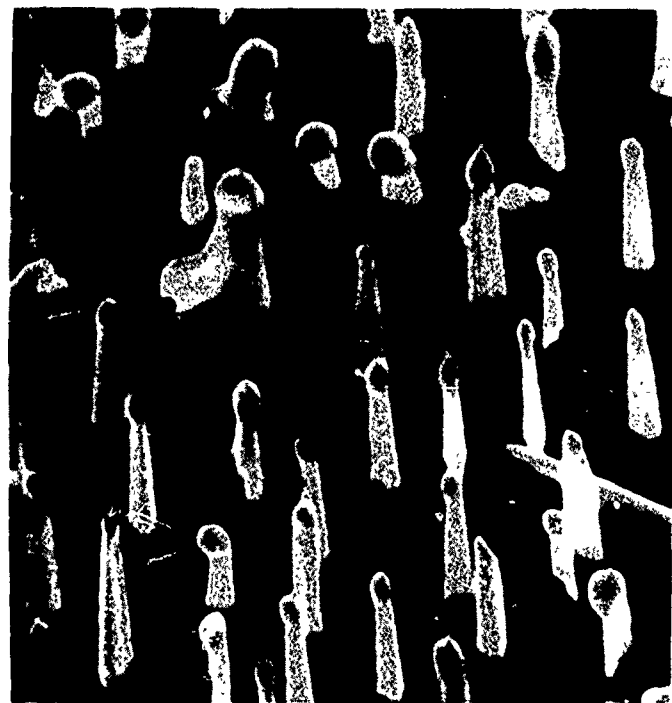
Figure 27. TaC after testing.
C3502

x 5.5K
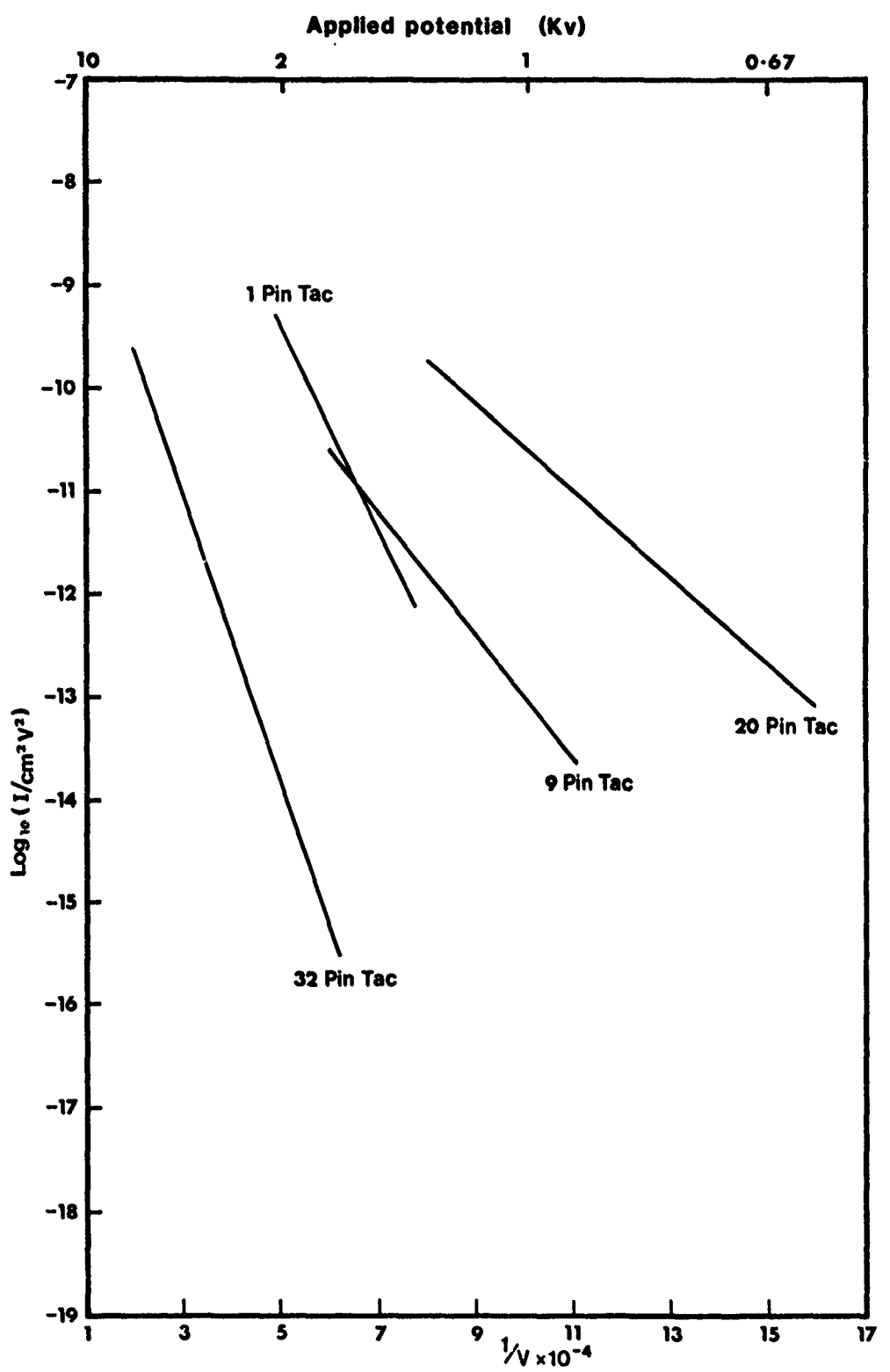
Figure 28.Comparison of Fowler–Nordheim plots for Tantalum Carbide cathodes
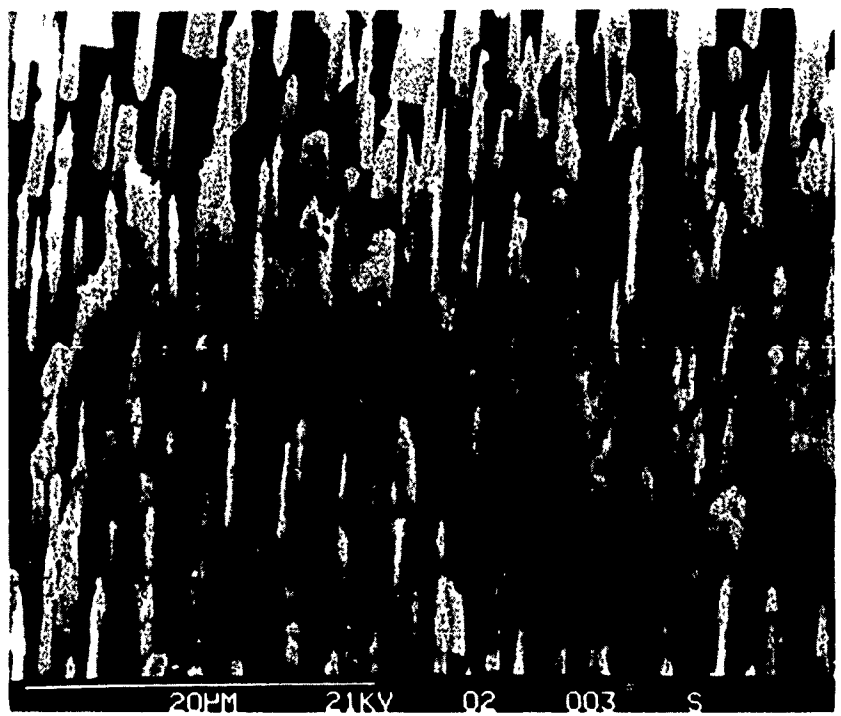
Figure 29.   Typical Area of Central pin of 20-pin   x 3K
C6492   TaC Cathode after testing.

R744/4

63.
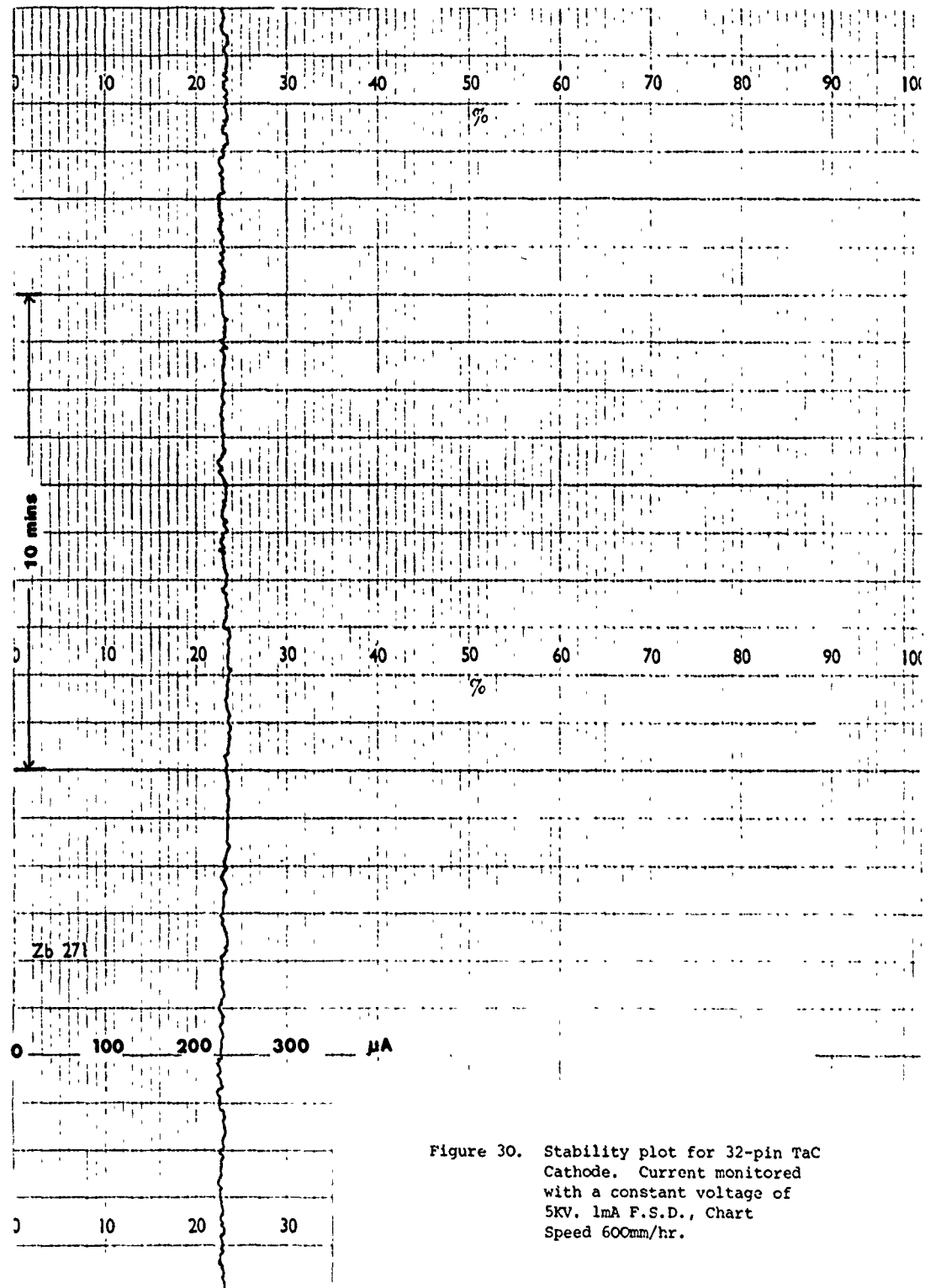
Figure 30.   Stability plot for 32-pin TaC Cathode.   Current monitored with a constant voltage of 5KV. lmA F.S.D., Chart Speed 600mm/hr.

64.
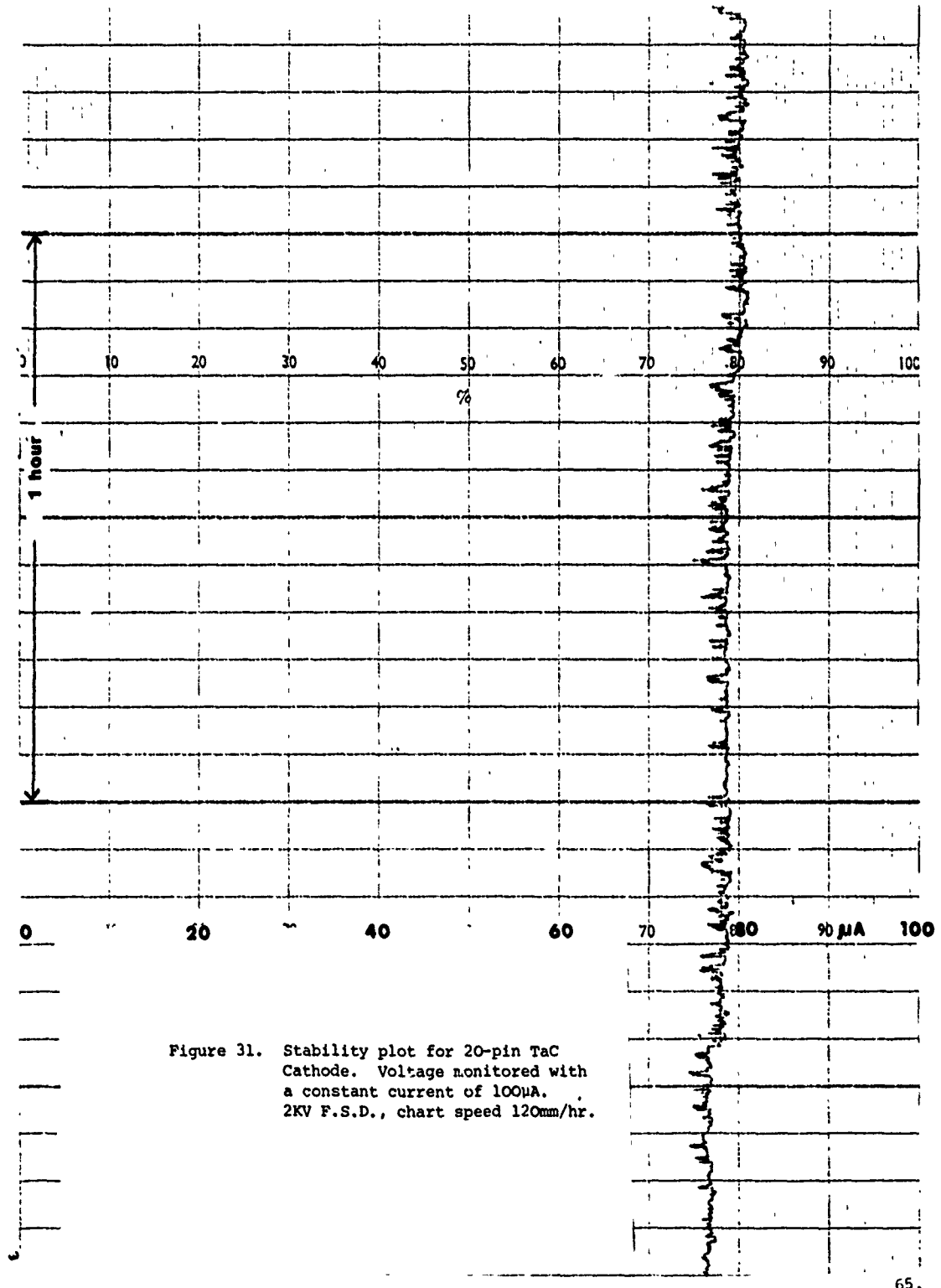
Figure 31.   Stability plot for 20-pin TaC
Cathode.   Voltage monitored with
a constant current of 100μA.
2KV F.S.D., chart speed 120mm/hr.

65.
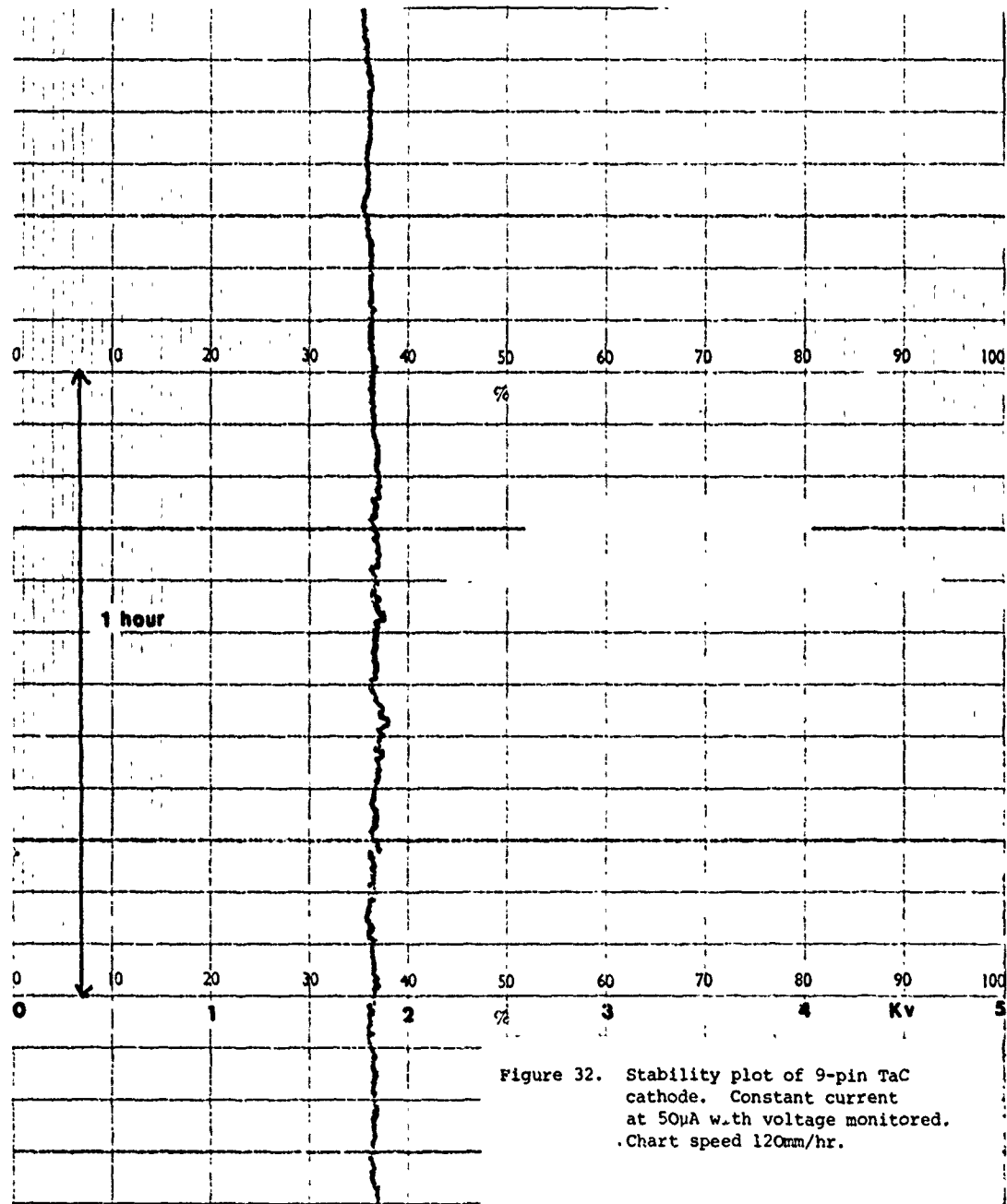
Figure 32. Stability plot of 9-pin TaC cathode. Constant current at 50μA w.th voltage monitored. .Chart speed 120mm/hr.

66.
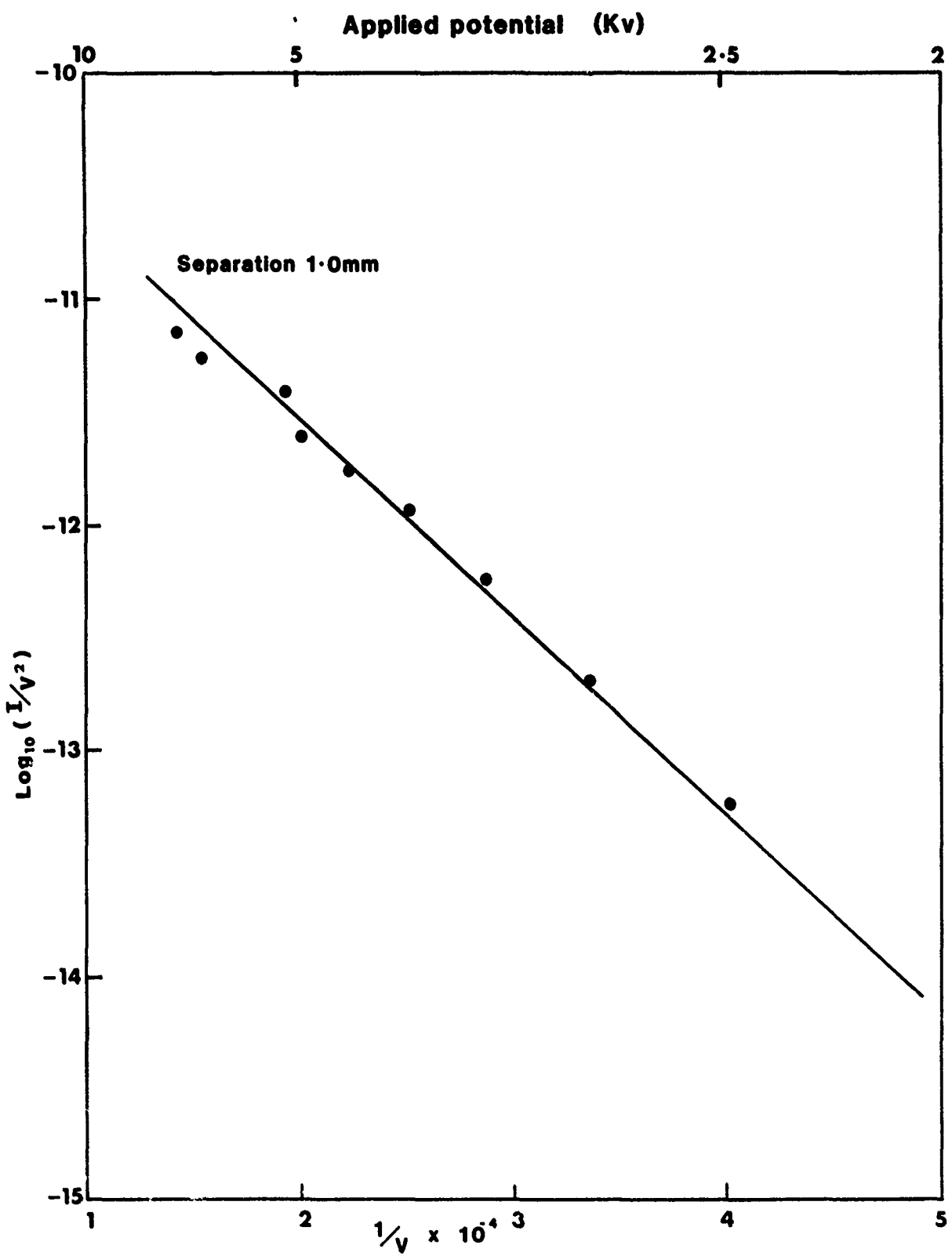
Figure 33. Fowler - Nordheim plot for NbC cathode at the anode to cathode separation shown
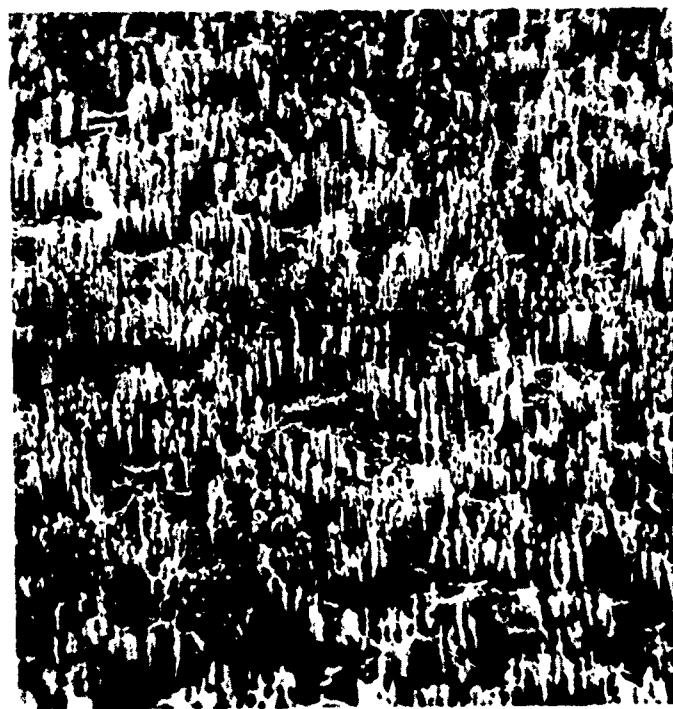
Figure 34.   NbC cathode after testing for 1000   x 260
C5859   hours showing destruction of fibres.

68.
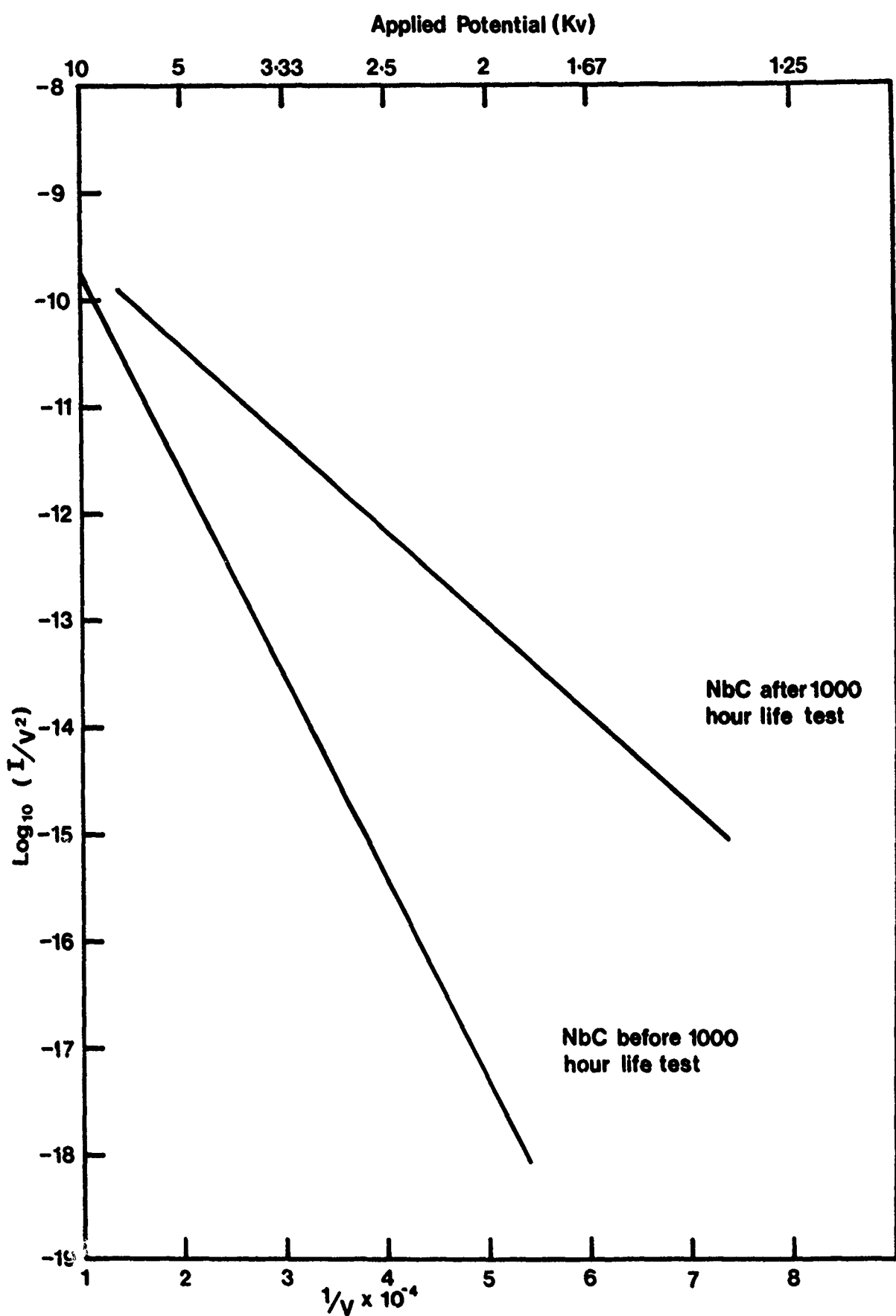
Figure 35. Fowler – Nordheim plots for small fibre NbC eutectic before and after 1000 hour life test

69.
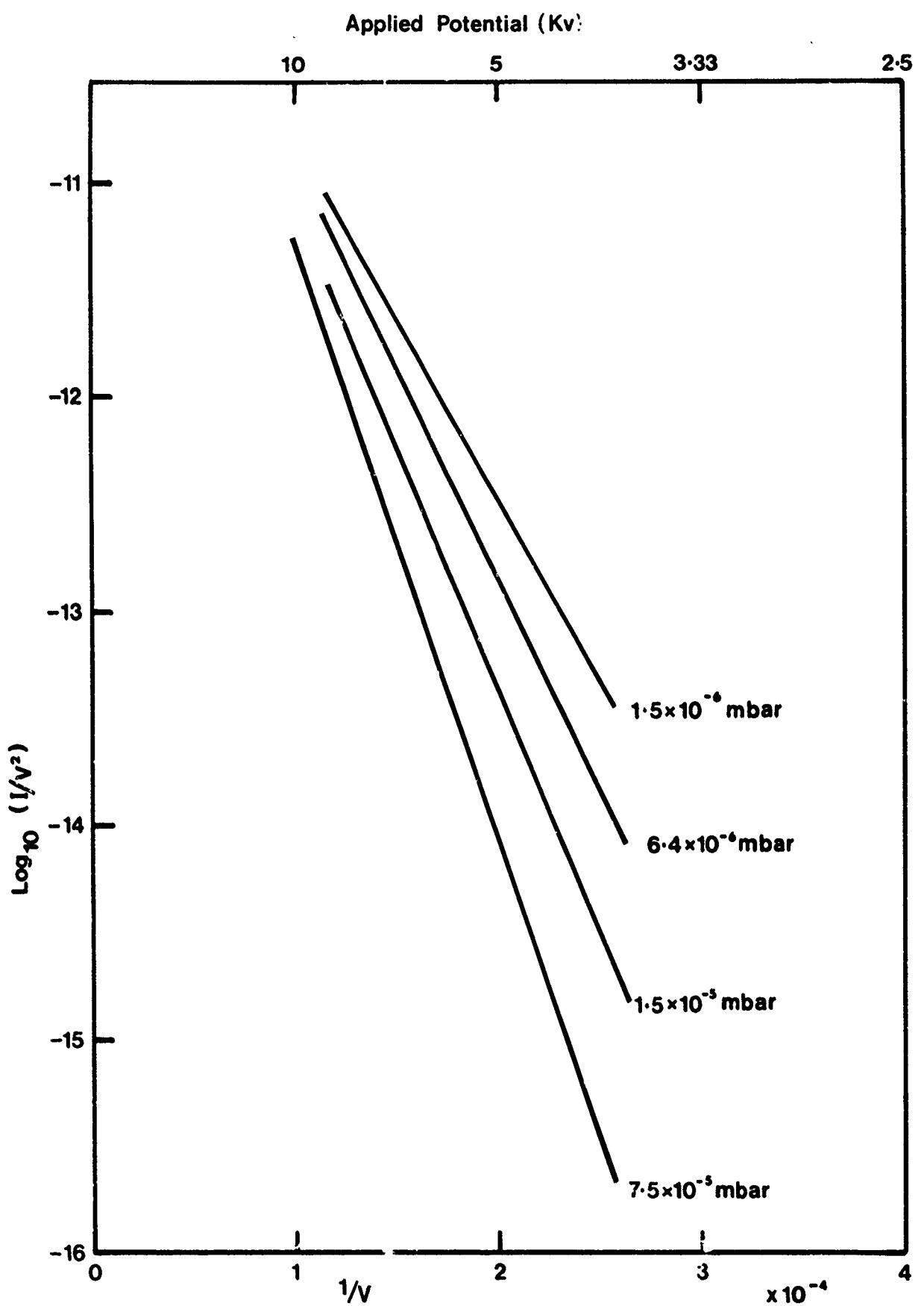
Figure 36. Fowler–Nordheim plots for NbC at the chamber pressures shown (after 1000 hour life test)
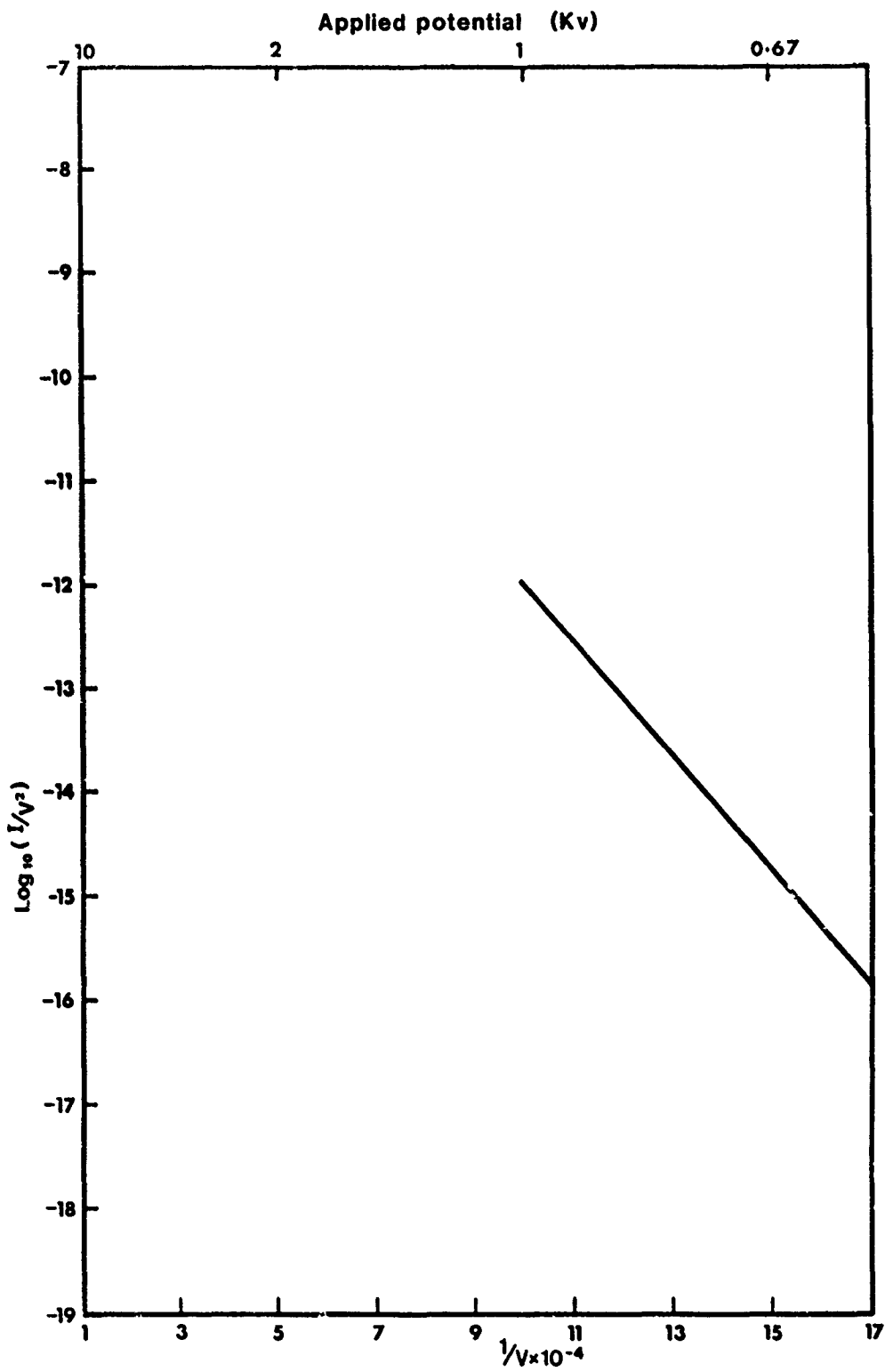
Figure 37. Fowler–Nordheim plot for single fibres of Niobium Carbide

71.

Figure 38. General View of Single Fibres   **x 1K**
C6639

72.
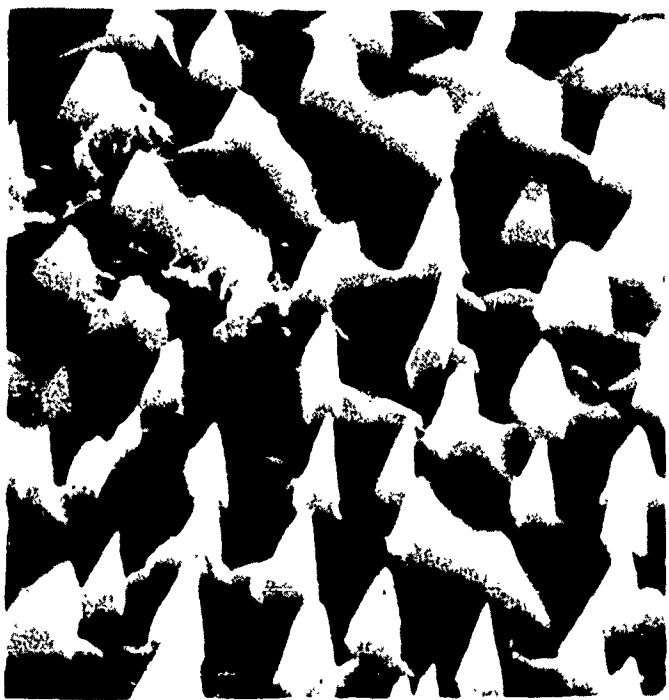
Figure 39. A-77-205 γ- γ'-α (Ni Mo Ta Al) after testing.
C4848   x 10K

Figure 40. A-77-205 γ-γ'- α (Ni Mo Ta Al) after   x 10K
C4847   testing showing area of arcing.

73.
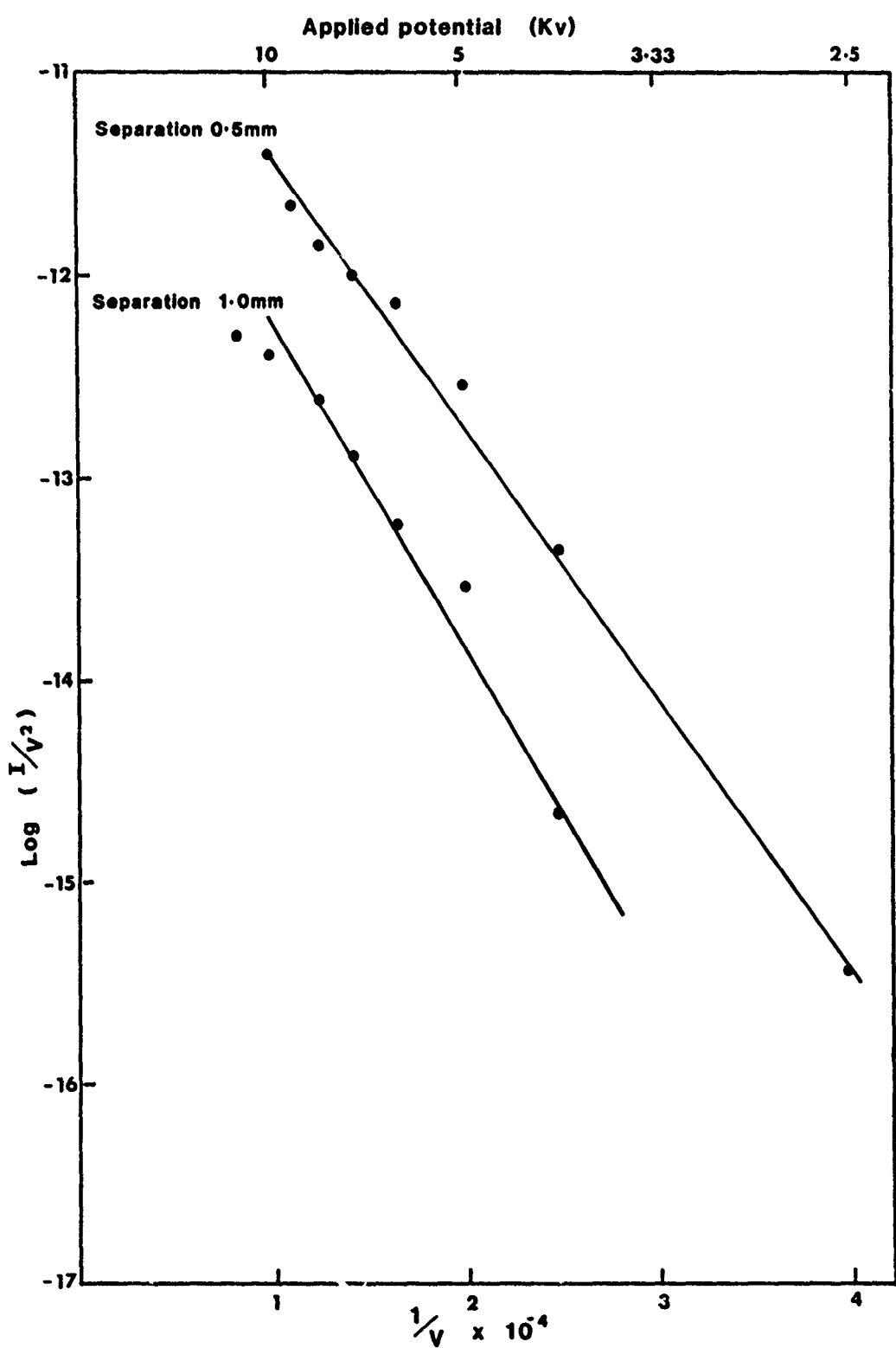
Figure 41. Fowler - Nordheim plots for material A77-205 cathode at the anode to cathode separation shown
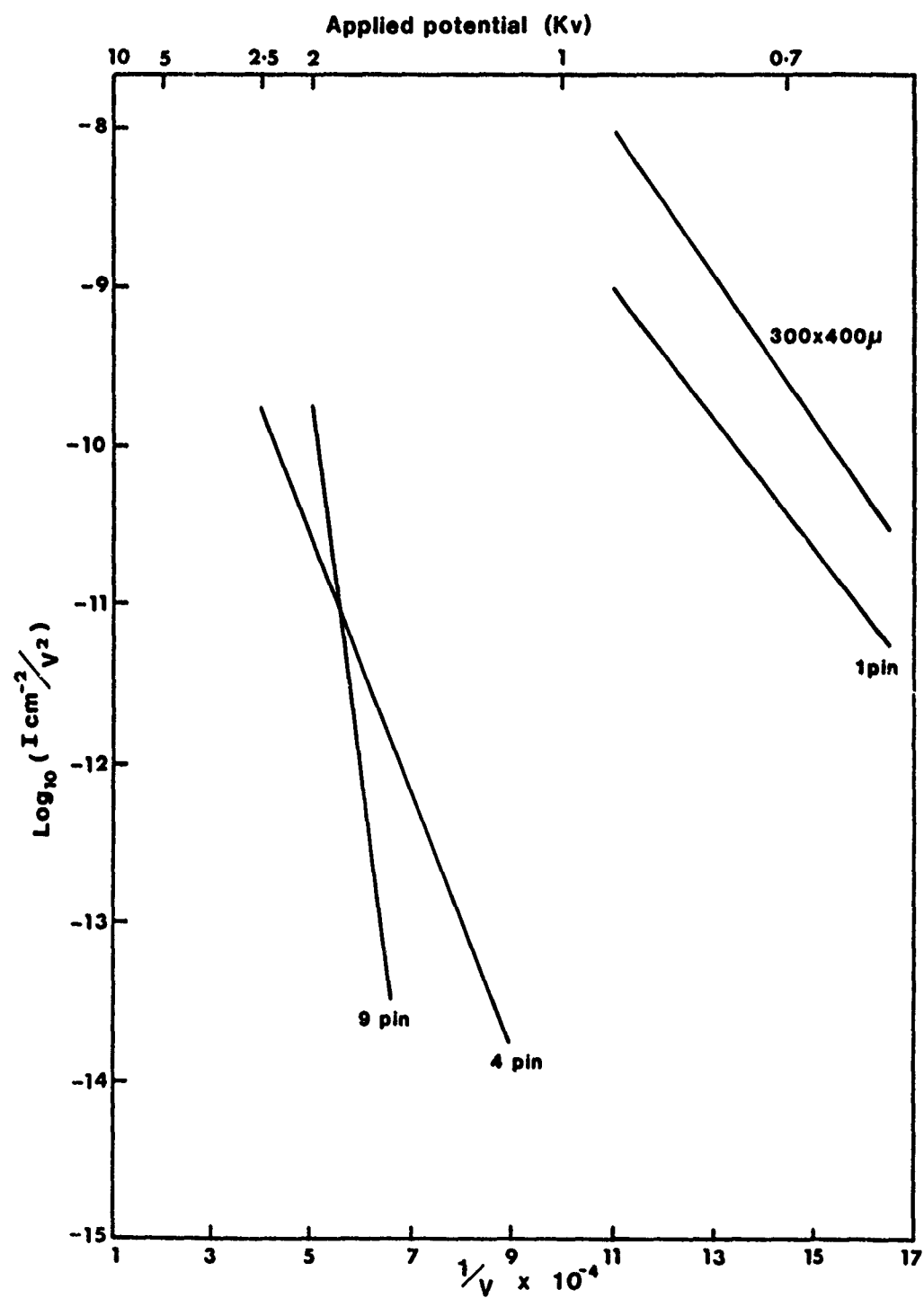
Figure 42. Fowler – Nordheim plots for Vanadium Carbide cathodes

75.

10 mins

%

%

0   100   200   300   400   μA   500
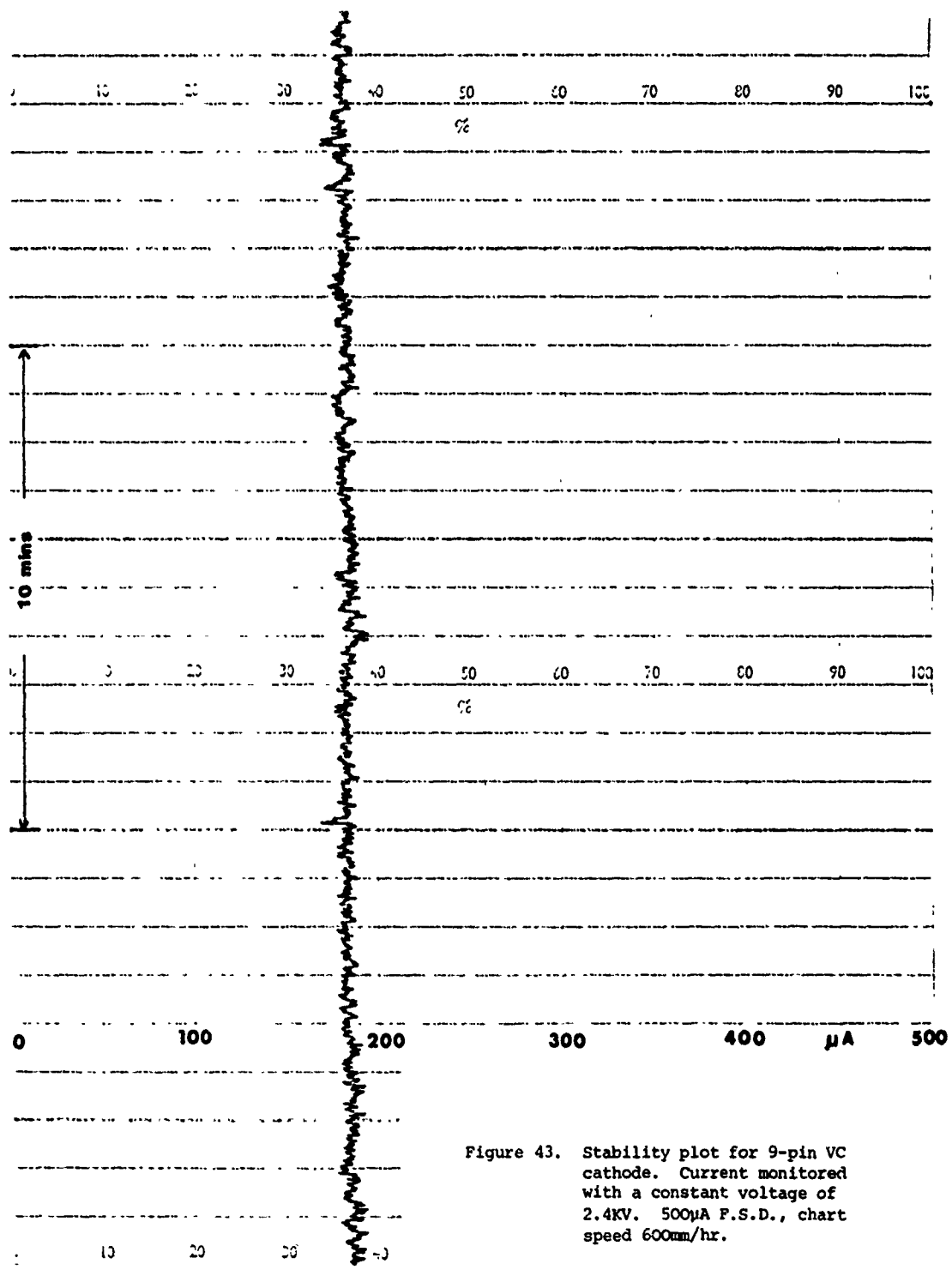
Figure 43. Stability plot for 9-pin VC cathode. Current monitored with a constant voltage of 2.4KV. 500μA F.S.D., chart speed 600mm/hr.

76.
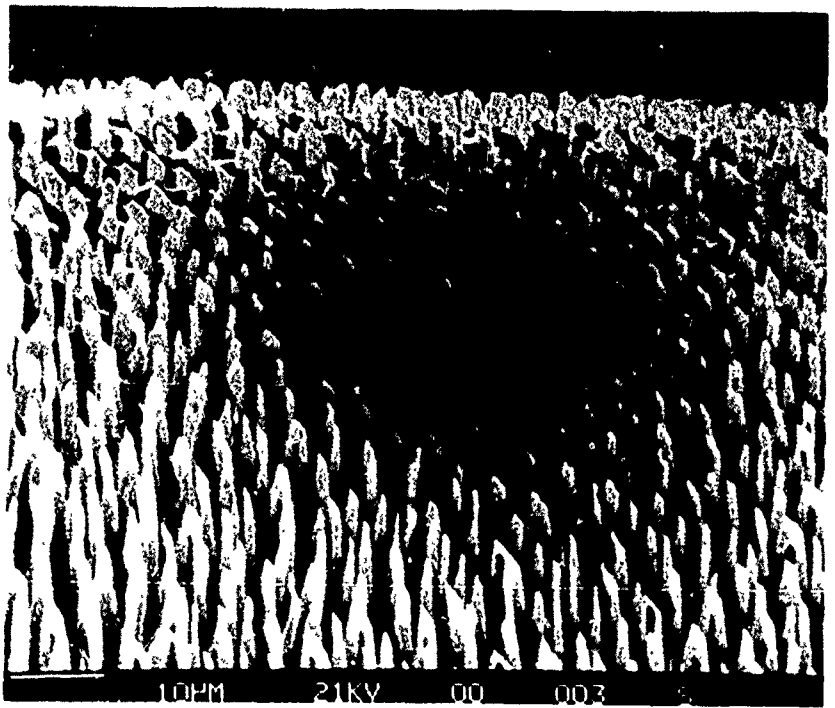
Figure 44.   Dark Area on 300μ x 400μ VC Cathode   x 2K
C6524   after testing.
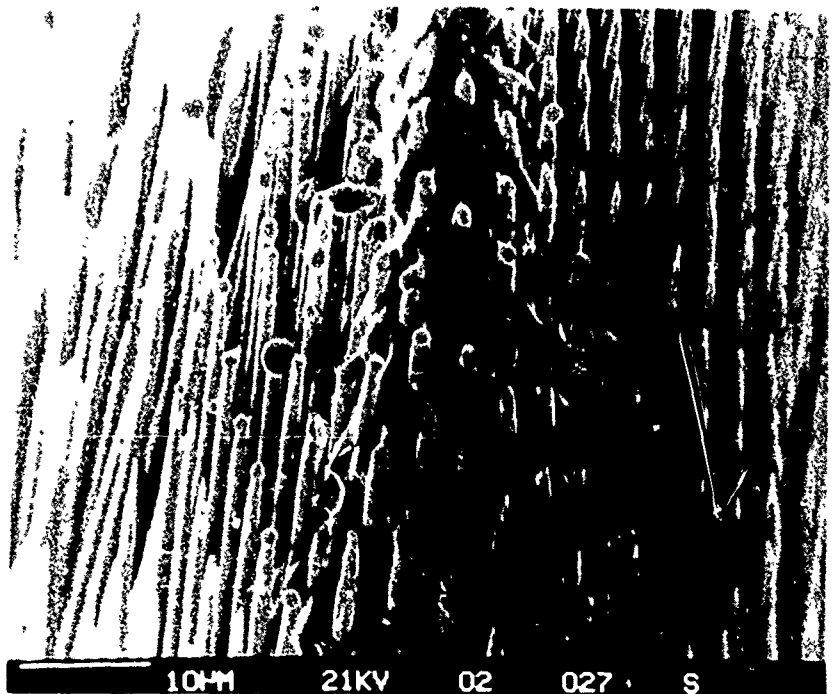
Figure 45.   End View of Corner B of "Chisel' shaped   x 2K
C6454   VC cathode after testing.

77.

173

| 10 | 20 | 30 | 40 | 50 | 60 | 70 | 80 | 90 | 100 |

%

1 hour

172

| 10 | 20 | 30 | 40 | 50 | 60 | 70 | 80 | 90 | 100 |

%

0   2   4   6   8   10 Kv
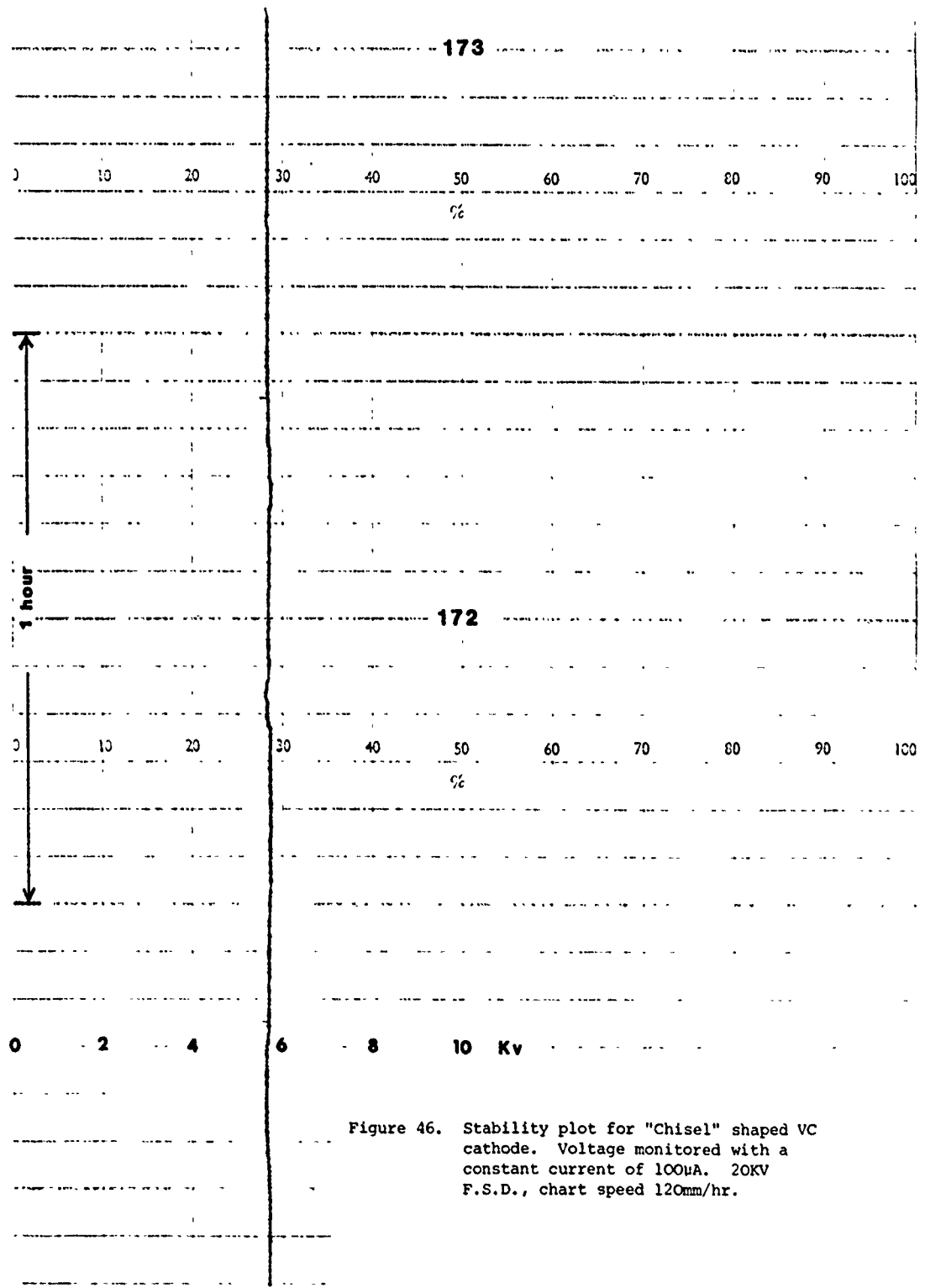
Figure 46.   Stability plot for "Chisel" shaped VC
cathode.   Voltage monitored with a
constant current of 100µA.   20KV
F.S.D., chart speed 120mm/hr.

78.
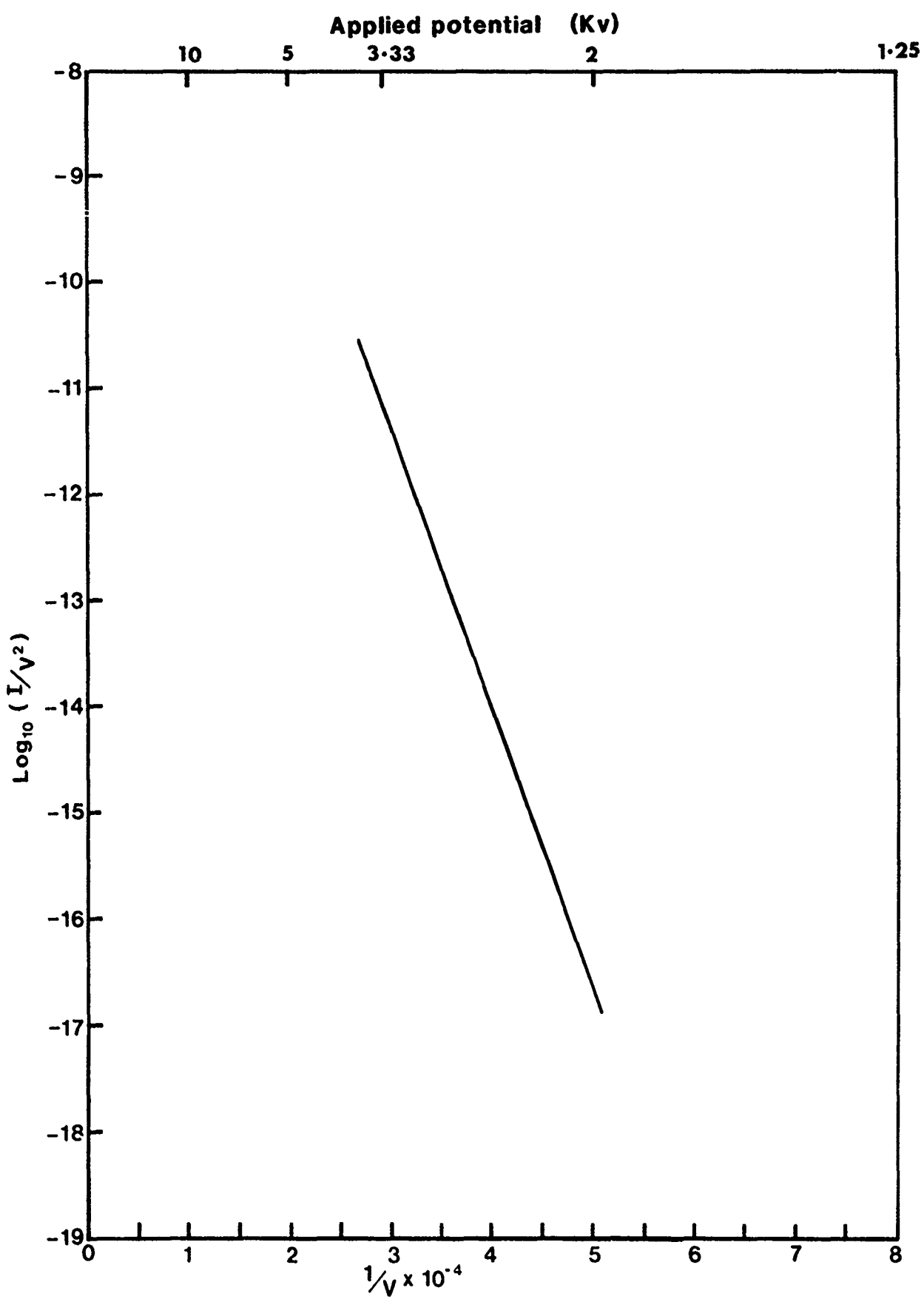
Figure 47. Fowler – Nordheim plot for "chisel" shaped Vanadium Carbide
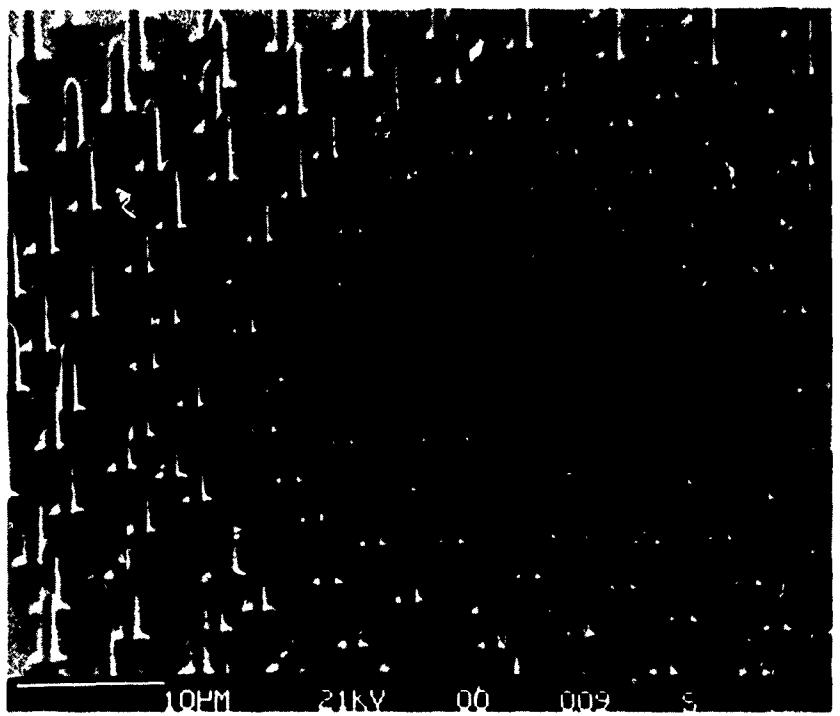
Figure 48. Typical Central Area of blunt   x 2I;
C6621   cotac cathode.

80.

Current

10   20 μA

Pressures
$\simeq 5 \times 10^{-9}$ Torr
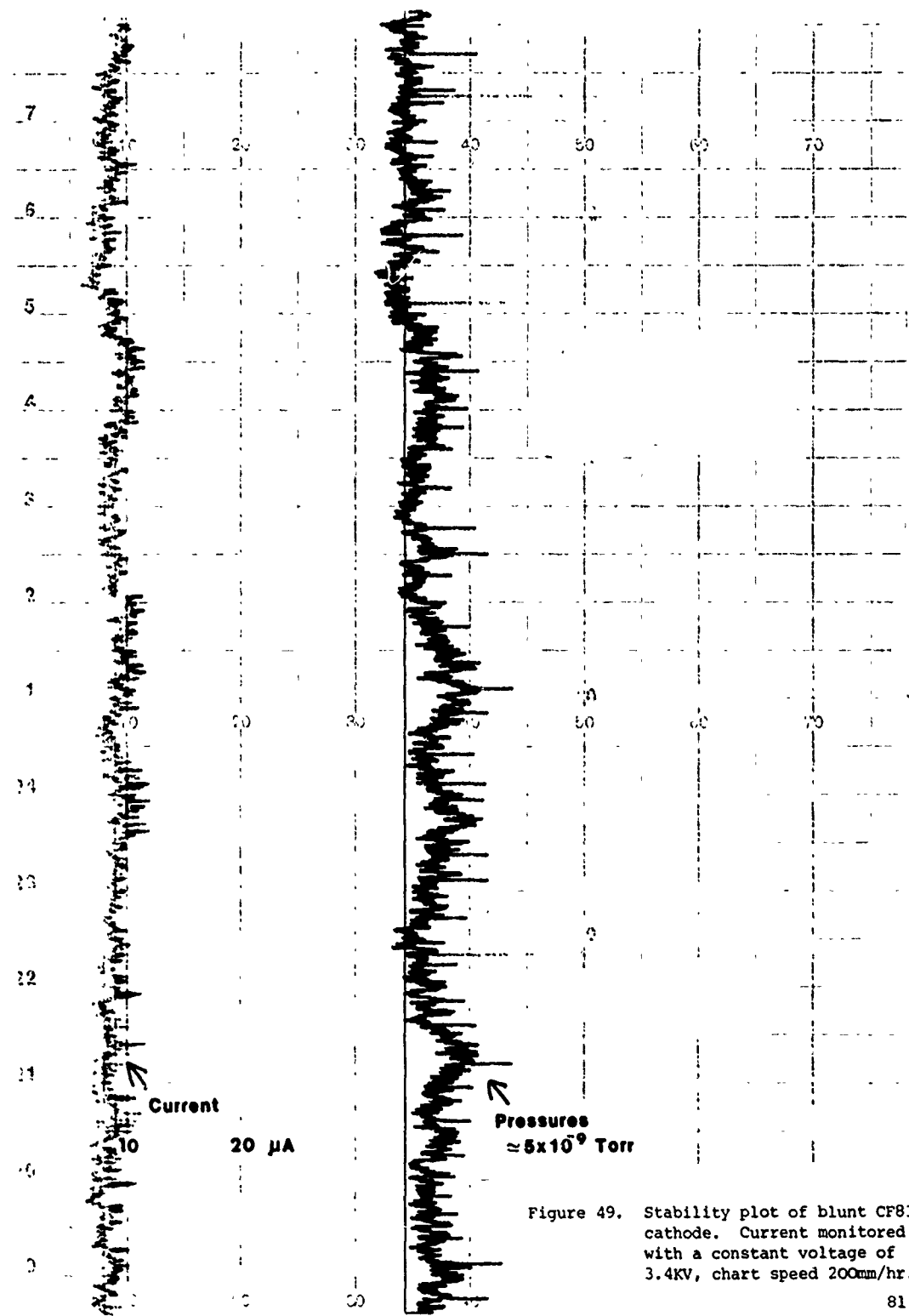
Figure 49. Stability plot of blunt CF83
cathode. Current monitored
with a constant voltage of
3.4KV, chart speed 200mm/hr.

81.
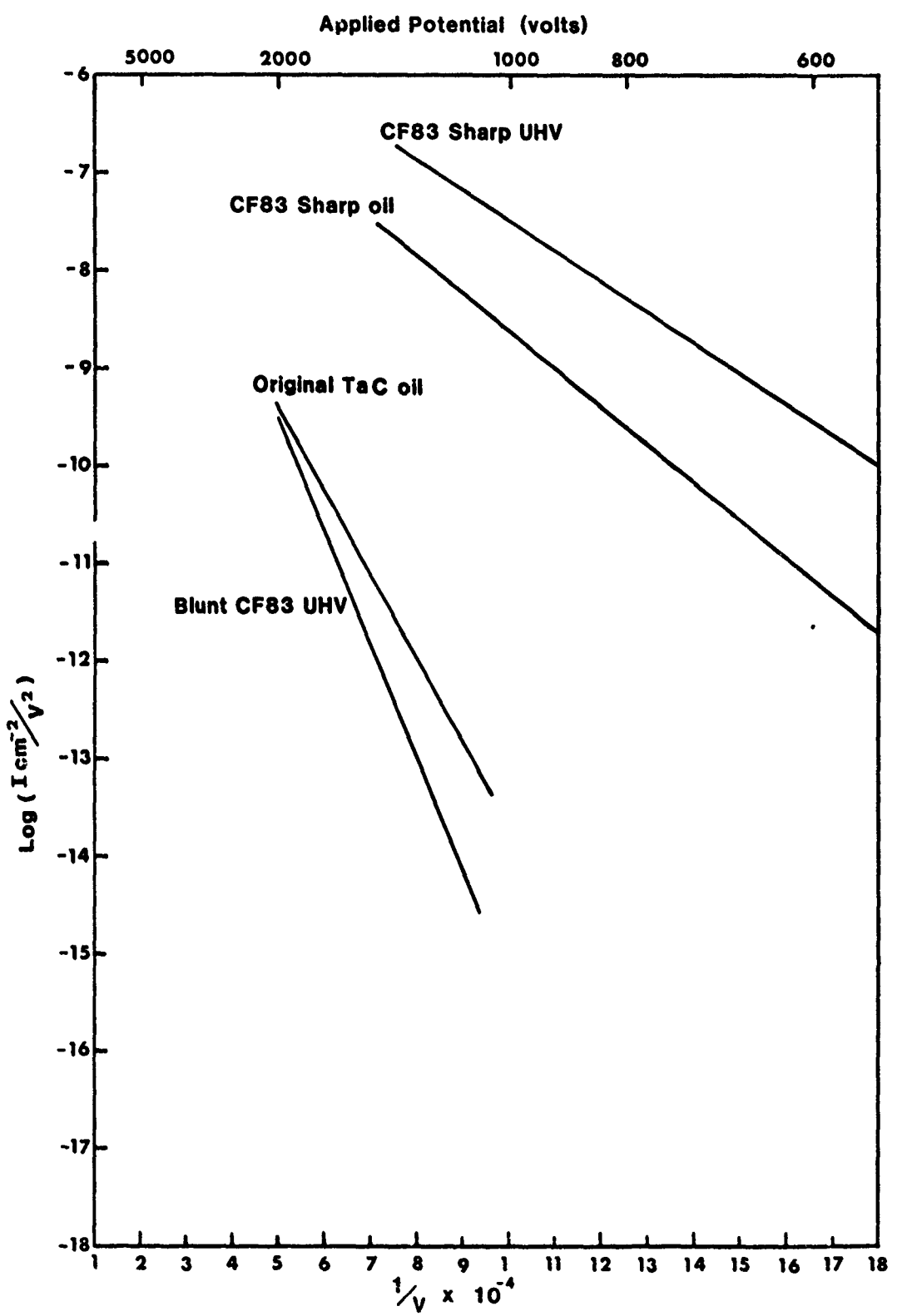
Figure 50. F-N Plots Comparing Sharp CF83 (oil and UHV), blunt CF83
and original TaC

82.
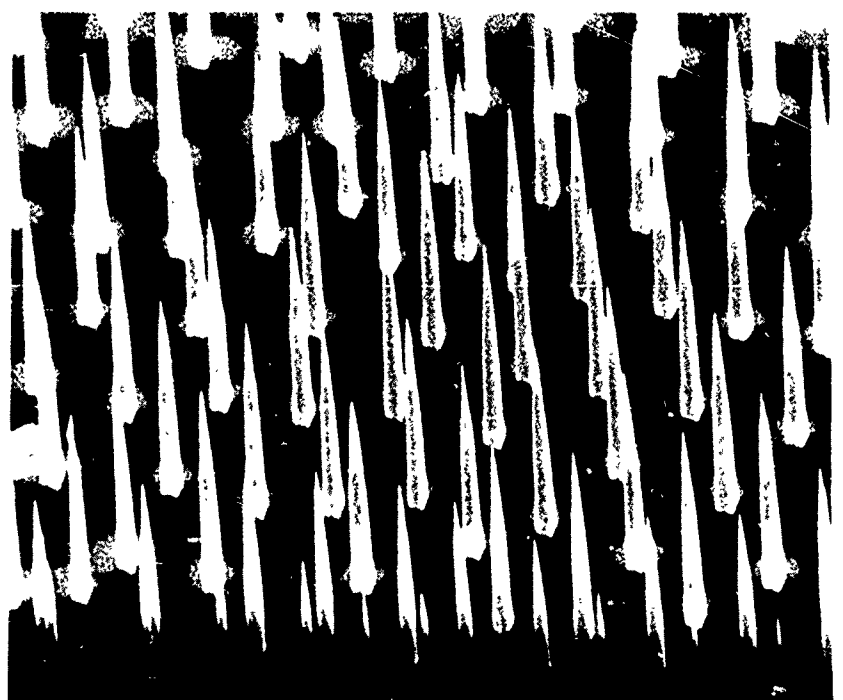
Figure 51. Typical Central Area of sharp   x 2K
C6913   cotac cathode.
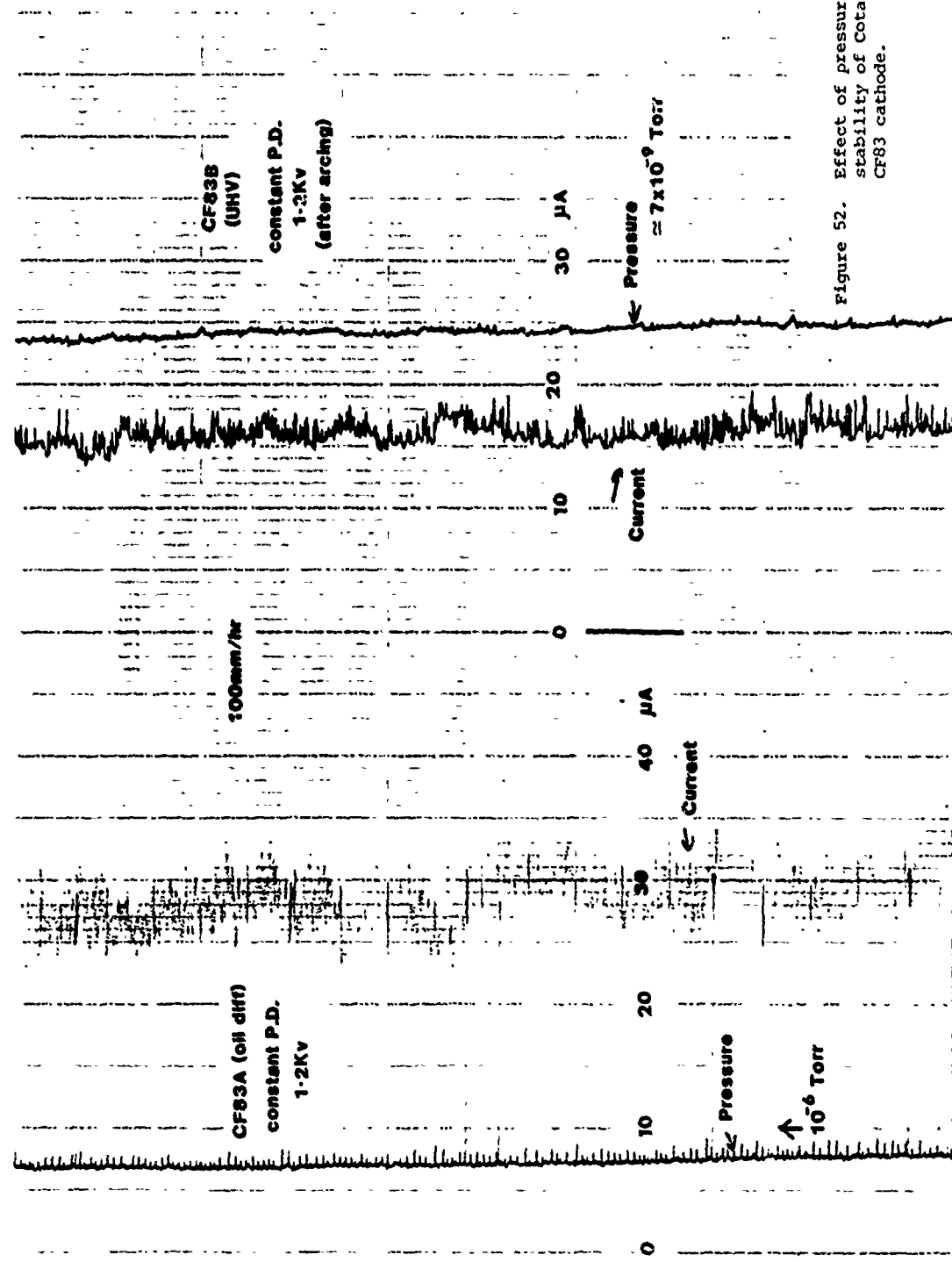
Figure 52. Effect of pressure on stability of Cotac CF83 cathode.

84.

Figure 53. Typical Central Area of sharp   x 5K
C6757   cotac cathode.

85.
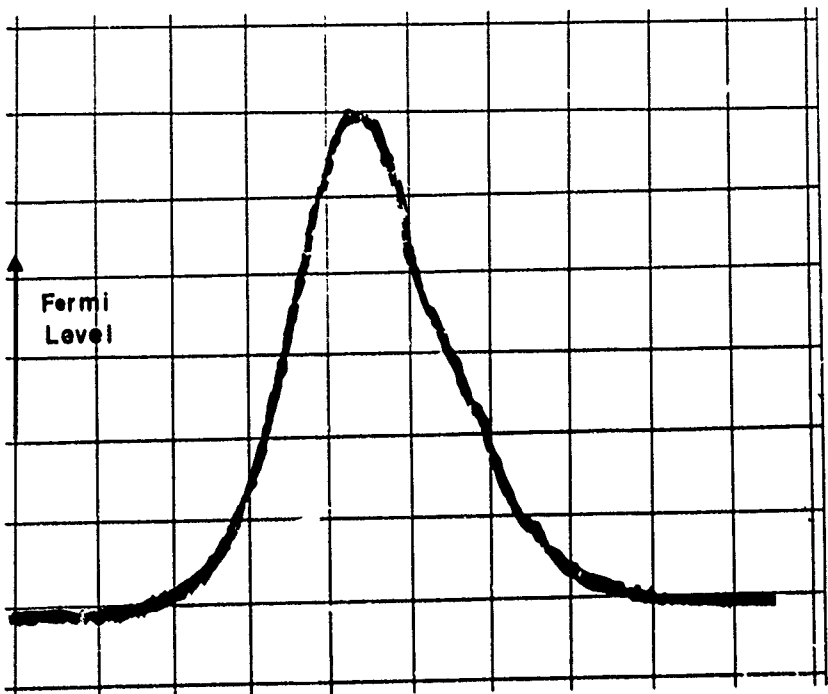
Figure 54A. Electron Energy Spectrum for 1st Site.
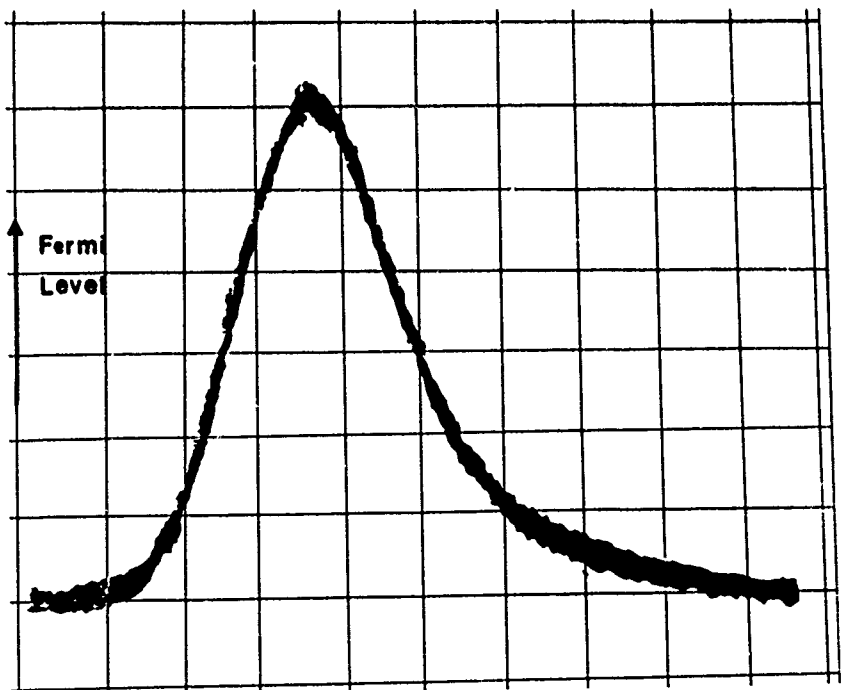
Figure 54B Electron Energy Spectrum for 3rd Site.

R744/4

86.
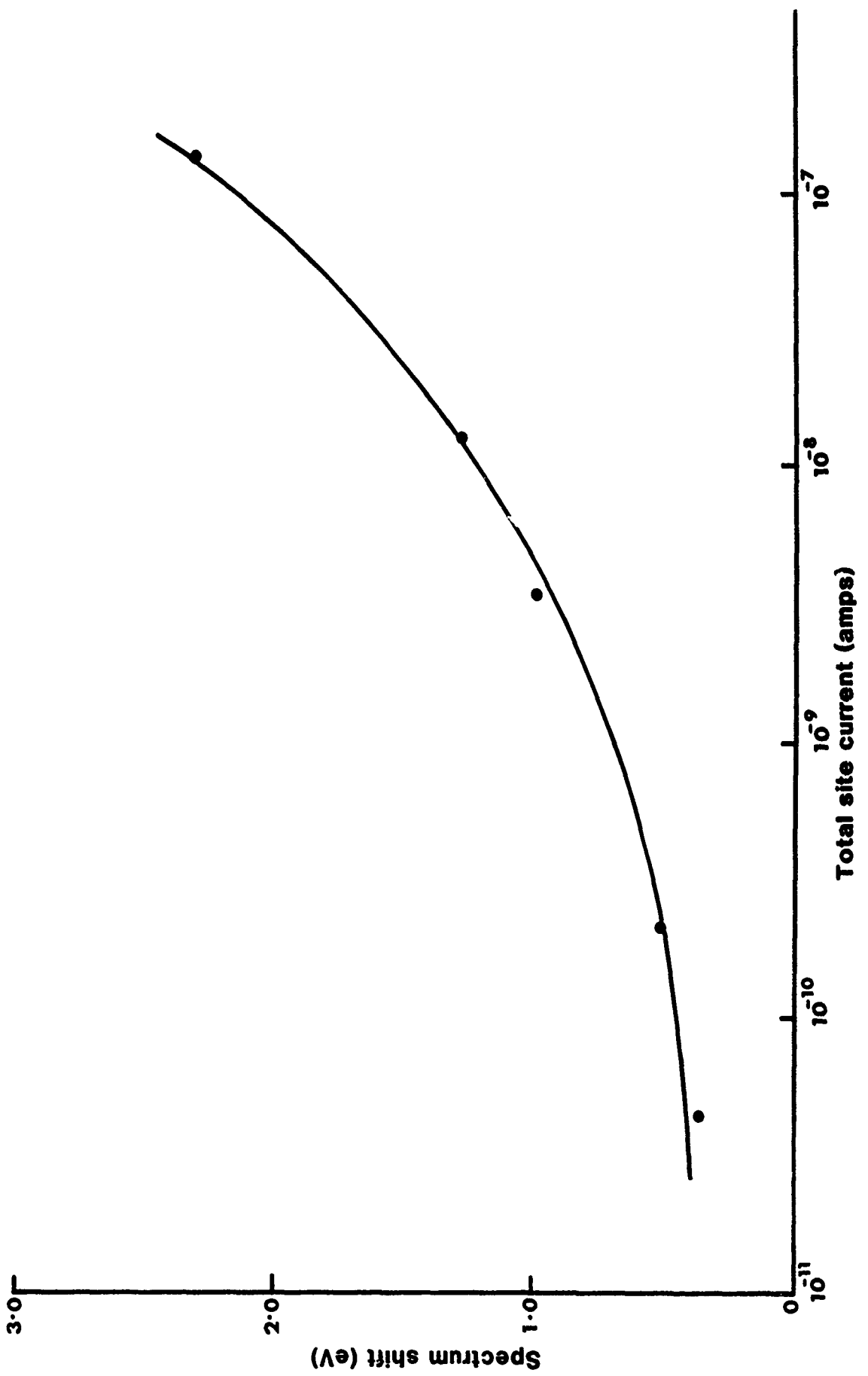
Figure 55. Variation of spectrum shift with site current
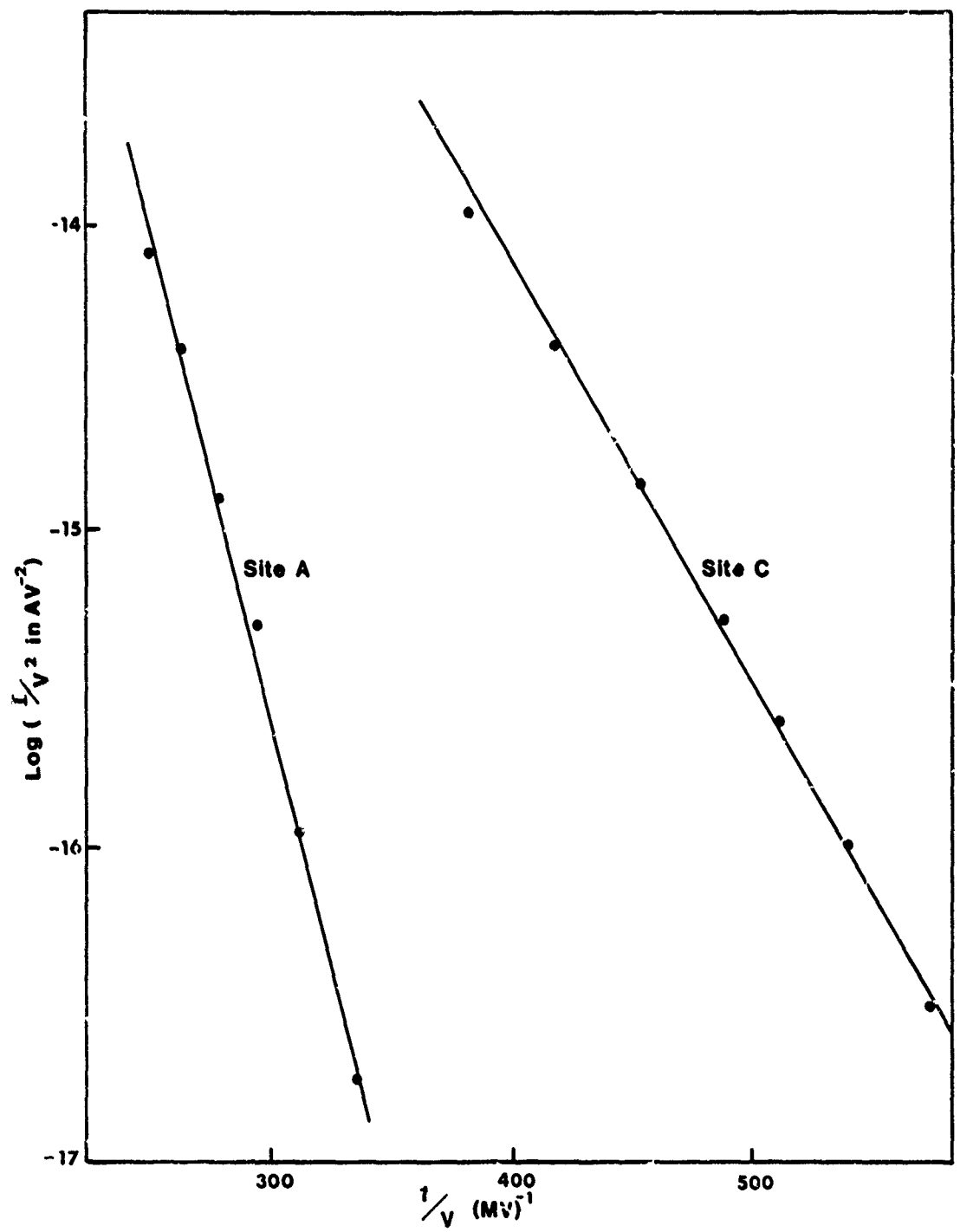
Figure 56.   F-N plots for two different TaC emission sites

88.
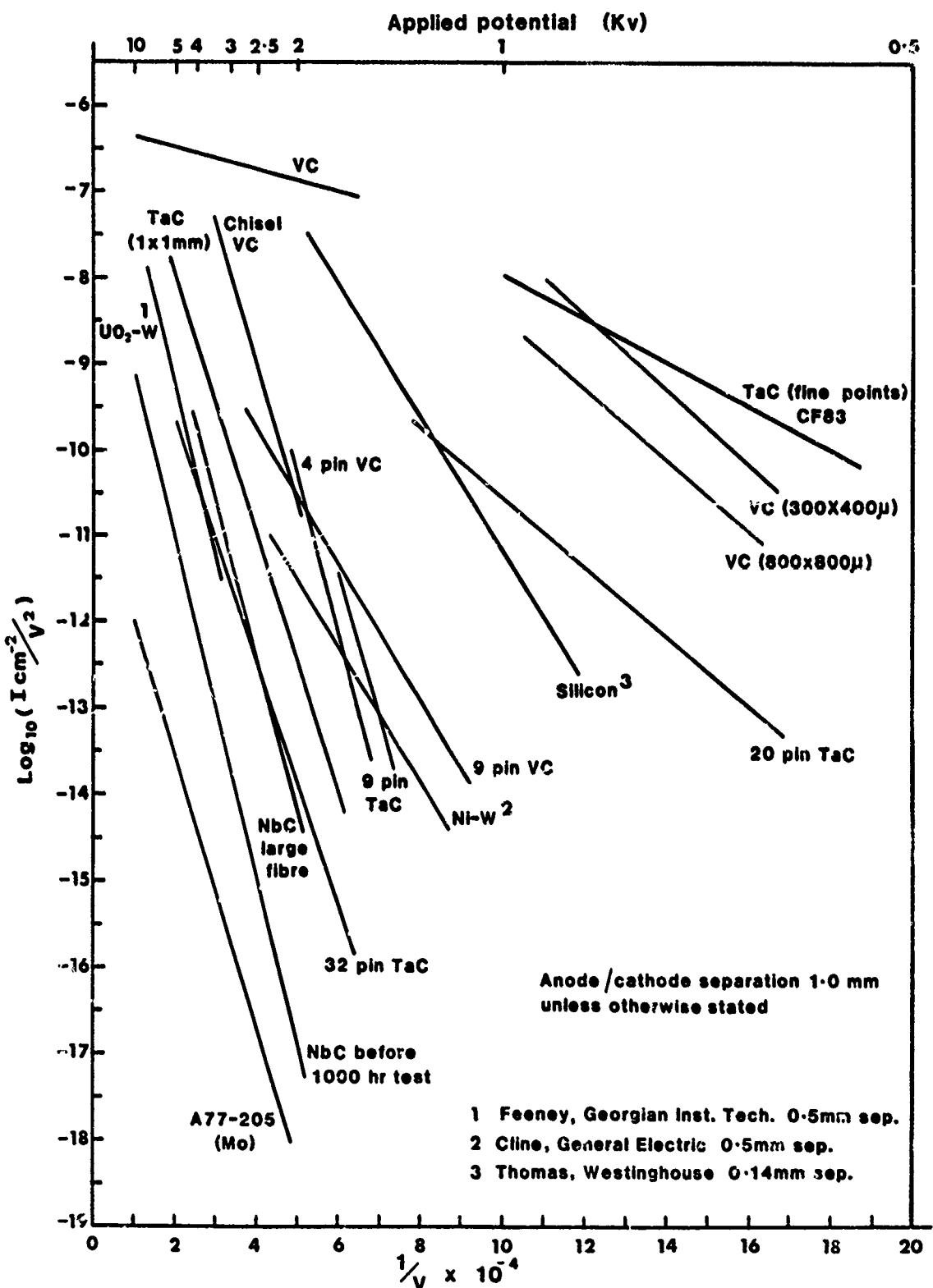
Figure 57. Set of F-N plots obtained at FRI and by Feeney et Al.

APPENDIX I

A SURVEY OF LANTHANUM HEXABORIDE (LaB$_6$)

The possibilities of the material as an electron emitter in the
thermal or in the field mode have been apparent since the immediate
postwar years(J.M. Lafferty[1],1951). Lanthanum hexaboride is a
refractory compound which combines a high melting point, chemical
stability and high hardness with a low electrical resistivity,
low work function and a Hall mobility compatible with that of
metals. As will be described in more detail below, the hexaboride
excels tungsten as an emitter in respect of brightness, operating
lifetime and stability to ionic bombardment.

The purpose of this enquiry is to establish the current state of
knowledge of this compound from the point of view of constitution,
structure, physical properties and to make a case for fabricating
lanthanum hexaboride needle arrays in a suitable matrix by directional
solidification.

1. BINARY SYSTEM

1.1 Phase Diagram of the La-B System

The phase diagram in Figure 1 is due in its essentials to Johnson
and Daane[2], 1961. The congruent melting point of LaB$_6$ is over
2500°C - 2530°C according to Samsonov, Paderno and Fomenko[3], 1963.
The only other compound, LaB$_4$, has a peritectic reaction at 1800°C
believed to be:

$$2LaB_4 \rightleftharpoons LaB_6 + (La + 2B)_{liquid}$$

The homogeneity range of lanthanum hexaboride lies between the
stoichiometric composition for LaB$_6$, 85.7 at %, and 88 at %B. This
range is attributed to a defect structure in which vacancies appear
on lanthanum sites in the crystal lattice.

1.2. Crystal Structure of Lanthanum Hexaboride, LaB_6

The compound belongs to the cubic, LaB_6, (hexaboride-type) structure, as illustrated in Figure 2. The lattice parameter has been shown to be very constant and unaffected by compositional variations:

Composition	Lattice Parameter, Å	Reference
LaB_6	4.156_6	Blum and Bertaut, 1954[4]
$La_{1.00}B_{6.00}$	4.1561	Johnson and Daane, 1961[2]
$La_{0.77}B_{6.00}$	4.1561	" " " "
LaB_6 and compositions close to stoichiometry	4.1566 ± 0.0006	Meerson et al., 1970[5]

The high melting point, high hardness and chemical stability are associated with the covalent (diamond-like) boron lattice of B_6 octahedra. The lanthanum appears to constitute a quasi-metallic phase within the B_6 framework and which provides nearly free electrons, thereby accounting for the good electrical conductivity and exceptional thermionic behaviour. It is interesting that although compositional variations within the homogeneity range of LaB_6 have no effect on lattice parameters, a colour change may be seen on moving from stoichiometric LaB_6 (pink-purple) to the lanthanum-deficient compound $La_{0.77}B_6$ (blue). The latter is still a metallic conductor but more akin to LaB_4. Similarly, Zhuravlev et al [6], 1973, note that colour changes are associated with a deficit of lanthanum which is not accompanied by a change of crystal symmetry.

2. TERNARY SYSTEMS

Information on the phase equilibria of La-B-X systems and in particular, of LaB_6 is not very extensive. Such information as has emerged from manual searches and computer searches via ESA (Recon) is noted below.

No liquidus data is available and all information refers to solid phases. It has been shown that the solubility of refractory metals (Hf, Ta, W and Zr) in solid LaB_6 is low, about 0.5 atomic %[7]. Solid

state reactions with carbides and borides of the refractory metals
are of double-composition type[8] e.g.

$$LaB_6 + NbC \rightarrow NbB_2 + LaB_6 + C$$
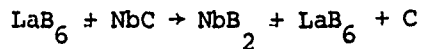
The hexaboride is said to dissolve the metals with increase in
hardness.

An investigation of the equilibria between LaB_6 and nickel gave
between 0.3 and 0.7 weight % nickel[9]. However, the La - B - Ni
system has six ternary borides which almost certainly exclude the
possibility of pseudo-binary eutectic equilibria, liquid $\rightleftharpoons LaB_6$ + Ni,
suitable for unidirectional solidification[10]. There are five
ternary compounds in the La - B - Co system[11] and for the same
reason this system is probably unsuitable. From an investigation
of isotherms at 800°C no ternary compounds were found in the La - B - Cr
system[12] which may therefore repay a quick survey of its liquidus
along the LaB_6 - Cr line. A similar study should be made of La - B - Al
because, as described later (Section 6) LaB_6 can be crystallised in a
very pure state from molten aluminium.

Finally it should be noted that at 800°C LaB_6 is in equilibrium with
a variety of ternary borides of molybdenum and tungsten, e.g. $(Mo, W)_{2-x}B_9$[13].

It is relevant to record here results by Vikhrev et al (14) for LaB_6
with 10 weight % of Mo, Ta or Re, which show that the thermionic
characteristics are virtually the same (Section 4). The phases present
after sintering in addition to LaB_6, are respectively MoB, TaB_2 and ReB_3.

3. PHYSICAL PROPERTIES: GENERAL

Properties such as density and electrical resistivity are known to
vary considerably with this type of specimen. A comparison of cast and
sintered material led to the following data for the fused state
(Kosyachkov et al[15], 1974).

Density: 4.68 g cm^{-3} (x-ray density 4.71).

Electrical Resistivity: 12.8 ± 0.4 μohm-cm

Work Function: 2.7 eV

In addition the cast material is 35 - 50% more stable to ion
bombardment than sintered material.

4. WORK FUNCTION: THERMIONIC AND FIELD EMISSION PROPERTIES

A range of values from 3.2 to 2.66 eV are quoted, chiefly from
Russian sources, by Fomenko[16], 1966. A standard, hot-pressed
high-density LaB_6 rod has been found (Ahmed and Broers[17], 1972)
by thermionic emission to have $\emptyset_{TH}$2.4 eV, Richardson constant, 40
amperes $cm^{-2}K^{-2}$. The current density reaches 100 Acm^{-2} at 1680°C
and a lifetime of over 200 h was recorded for 50 Acm^{-2} at 10^{-5} torr.
An initial build-up of emission (over one hour) during tests was
correlated with SEM observations which showed that surface evaporation
exposed sharp crystalline boundaries at a stage coinciding with full
emission. Contrary to earlier hypotheses (Lafferty[1], 1951) there
is no evidence of the low work function patches observed on some
dispenser cathodes - an important observation if tip radii of 10μm
or less are needed.

Swanson and Dickinson[18], 1976, measured the thermionic work function
of a LaB_6 single crystal at the (100) face, as follows:

$\emptyset_{TH}$,eV	Richardson Constant Amperes $cm^{-2}K^{-2}$	Zero-Field Current Density, Acm^{-2}	
		2000K	1500K
2.47 ± 0.06	14	33	0.16

Using a field emission retarding potential method for the same crystal
specimen at a thermally clean (100) face, they obtained a value for
$\emptyset_{FE}$ equal to 2.28 ± 0.03 eV. Auger spectra for the same surface
gave a B/La atomic ratio c: 2.3 - 2.6, about half that expected
theoretically from the molecular formula, and in accord with hypotheses
of La accumulation at the specimen surface (Lafferty, 1951)[1]. However,
flash desorption/mass spectrometry in the range 1700 - 2000K revealed
evaporation of B^+ and La^+ in near stoichiometric proportions (three to
six ions of B^+ for each one of La^+). From the nearly equal values of
desorption activation energies, 6.3 ± 0.3 for La and 6.8 ± 0.3 eV for
B, it was concluded that the rate determining step is the same for both

A4.

species and may consist of removal of a LaB_6 precursor, from the surface followed by immediate dissociation. The authors do not, however, explain why the surface should be relatively rich in lanthanum.

Oshima, Horiuchi and Kawai[19], 1974, agree that polycrystalline LaB_6, in thin form, evaporates almost stoichiometrically at 1600 - 2200°C; their figures for the work function are:

$$\emptyset_{TH} = 2.61 \pm 0.05 \text{ eV}$$

Richardson Constant = 41 Amperes $cm^{-2}K^{-2}$.

Further work from the same laboratories (Oshima et al[20], 1977) gives results for different faces of LaB_6 single crystals.

Crystal Plane	$\emptyset_{TH}$ eV	Richardson Constant Amperes $cm^{-2}K^{-2}$
(100)	2.86 ± 0.03	82
(110)	2.68 ± 0.03	57
(111)	3.4 ± 0.2	71

A photoelectron spectroscopic measurement of $\emptyset$ for a clean (100) plane (Aono et al[21], 1974) gave $\emptyset_{FE}$ 2.41 ± 0.1 eV and simultaneously permitted a chemical characterisation of the emitting surface. It was found that exposure of the clean surface to oxygen altered the surface and gave $\emptyset_{FE}$ a value of 4.0 ± 0.1 eV. Initial oxydation is said to be compound formation and not physical adsorption. The same authors (Aono et al[22], 1977) argue that low $\emptyset$ is due to electric dipole moments produced by surface ions. (See also a review by Oshima and Kawai,[23], 1976.).

To sum up: there is still not a general agreement as to the processes which assist or retard electron emission in LaB_6 under field or thermionic conditions. Avdienko and Malev[24], 1976, associate reduction in cathode emissions with poisoning by residual gases, e.g. heavy hydrocarbons and organic solvent vapours. An increase in the partial pressure of carbon dioxide increases emission stability by preventing formation of carbides of boron or lanthanum. Hosoki et al[25], 1974, state on the basis of Auger electron spectroscopy and Auger emission micrography that one hour at 1500°C and 10^{-8} torr will remove

adsorbates and contaminants. Kuznetsova and Kudintseva[26], 1973, argue from observations of thermionic emission by LaB_6 with traces of W, Mo, Re, La or Ti that at 1100 - 1500K LaB_6 can be either active or inactive. A brief treatment at $1400°C$ activates it. The emission rate is governed by access of the active component, said to be La, to the surface and a copious flow can be ensured by the introduction of metallic activating additives.

Vikhrev et al., 1971(14) found that with 10% weight of Re, Mo or Ta, LaB_6 had virtually the same thermionic properties in the temperature range 1150 - 1600°C.

Material	ϕ effective, eV	Current Density, Acm^{-2}	Richardson Constant, $Acm^{-2}K^{-2}$	Temp. Coeff. $eV\ deg^{-1}$
LaB_6+10%Re	2.55 - 2.75	0.42 - 21.3	17.8	6.25×10^{-4}
LaB_6+10%Mo	2.58 - 2.76	0.31 - 20.0	33.2	5.72×10^{-4}
LaB_6+10%Ta	2.55 - 2.77	0.42 - 19.5	31.4	5.27×10^{-4}

A recent publication (Berrada[27] et al., 1978) summarises the opposing views on the mechanism of emission in lanthanum hexaboride. On the basis of systematic original measurements by photo-electron and Auger spectroscopy it is concluded that emission is an intrinsic property of the material and that the hypothesis attributing low work functions (which they measure by the Kelvin method) to a layer of lanthanum atoms on the LaB_6 surface is not confirmed.

5. VAPOUR PRESSURES AND STABILITY

The thermodynamic properties of lanthanium hexaboride have been investigated by Gordienki et al., 1968[28]. By means of mass spectrometry and conventional effusion measurements, the partial vapour pressure of lanthanum over the hexaboride was measured from 2045 to 2300K. The heat content of lanthanum hexaboride was determined by the method of mixing in the range of 1340 - 2300K. The thermodynamic parameters were calculated in the range 298 - 2500K and the standard heat of formation, $\Delta H_{298}°$ found to be -24.9 ± 1.5 k cal $mole^{-1}$.

Calculations by Barry and Chart[29], 1977 and based on data by Fesenko et al[30], 1966, gave the following values for the reaction pressure of lanthanum in the reaction.

$$LaB_6 \rightleftharpoons La(g) + 6B(s)$$
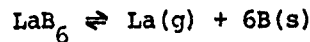
Log_{10} (Reaction Pressure) of La, atmospheres

1000K	2000K
-20.6	-5.9

The pressures are somewhat higher than those of carbides and nitrides at similar temperatures.

As is now well-known, the stoichiometric compound can be grown as single-crystals by various melt techniques. Takagi and Ishii[31], 1977 have shown that single crystals of LaB_6 prepared by a floating zone method contain inclusions identifiable as LaB_4. These inclusions are also present in the feedstock and do not form by vaporization. The formation of LaB_4 from feedstock can be entirely eliminated by control of power input so as to maintain a constant zone height (and hence a constant temperature). Their view that vaporization is congruent is supported by several sources quoted previously[18,20]. Verhoeven et al.,[32], 1976 describing another zone technique, commented that in spite of the high vapour pressure in the molten state evaporation is congruent and, under the experimental conditions which include Ar gas (not He) stoichiometry is preserved to 6.00 ± 0.15. The compound LaB_4 itself is believed to lose lanthanum preferentially on heating[33,34].

6. FABRICATION AND PERFORMANCE OF CATHODES FROM LANTHANUM HEXABORIDE

The extensive literature on thermionic LaB_6 cathodes will not be reviewed here. However, in addition to the references quoted earlier on their application in the thermionic or in the field mode, it may be mentioned (Verhoeven and Gibson[35], 1976) that in the thermionic mode, combined with a Faraday cage, LaB_6 gives a brightness fifteen to twenty times that of tungsten under 40h life conditions and that single crystal cathodes are more reliable for high brightness. Futamoto[36] et al., 1977 have reported that (100) oriented single crystals, thermally

cleaned have current fluctuations under field emission conditions larger than those of tungsten sources. At 1550°C and 3kV a single-crystal LaB$_6$ cathode was operated at 7W for over 200h[37]. Schmidt et al[38] state that at 1545°K the <110> orientation has an emission ten times that of <100> for pointed single crystals. A flux 100 times that of tungsten is anticipated. Under test conditions similar to those of Verhoeven and Gibson[35], 1976, the brightness has been determined as a function of purity and orientation[39].

Investigations in the field mode are fewer and less systematic. A review has noted that tungsten and molybdenum are the most frequently studied, with and without adsorbates[40]. Windsor[41], 1969 has developed an acid-spray method for preparing single-crystal field emitter points which have a current density of over $10^5 Acm^{-2}$ and life-times of several hundred hours at 10^{-9} torr. Switching tests indicate a good resistance to catastrophic failure caused by vacuum arcing. Tip radii are 1000 - 6000 Å. An electron emission method of machining LaB$_6$ is described in reference[42]. There are a number of other papers describing the fabrication of LaB$_6$ cathodes but it appears from the ESA (Recon) computer search that no experiments on the fabrication of needle arrays have been carried out. Similarly the literature in the phase equilibria of LaB$_6$ with other elements (in effect La-B-X) is somewhat sparse and no cases are known of pseudo-binary eutectic equilibria LaB$_6$ - X wherein unidirectional solidification to produce rod morphologies would be possible.

Fortunately papers have been found which allow one to infer the possibilities of suitable pseudo-binary equilibria. Aita et al[43] have grown crystals in needle form, <110> growth direction and also plates and cubes, with the {100} planes prominently in evidence, by heating lanthanum and boron in the correct proportions in aluminium at 1500°C for 8h. and cooling to room temperature at 30 deg. h^{-1}. The crystals are removed by dissolving the aluminium matrix in acid. A further study of the method (Futamato et al.[44], 1975) showed that cooling rates of 6.2 - 7.5 deg. h^{-1} gave prodominantly <110> needles of size 0.1 - 0.5mm square cross-section and 5mm long. The crystals,

A8.

identifiable as LaB_6, a = 4.1564 ± 0.0001 Å, contained less than
0.01 weight % impurity. It may be concluded that Al and LaB_6 do
not dissolve in one another in the solid phase. Since they are
miscible in the liquid phase it is likely that a pseudo-binary
equilibrium, possibly eutectic, will be found for LaB_6 - Al.

7. OUTLINE METHOD FOR PREPARING LaB_6 AS DSE MATERIAL

Information on phase equilibria for LaB_6 is very sparse but does
suggest that, at first instance, systems based on postulated pseudo-
binary eutectic equilibria.

$$Al - LaB_6 \rightleftharpoons Liquid$$
$$Cr - LaB_6 \rightleftharpoons Liquid$$
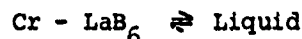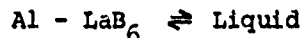
should be tried. A survey of other elements chosen primarily for
their suitability as matrices would included Hf and Ta.

It is suggested that by using differential thermal analysis (DTA)
the liquidus of the above four systems could be checked, followed
by microstructural examination of cooling curve ingots to confirm
that the desired pseudo-binary reactions have occurred.

Directional solidification could be attempted using crucible materials
chosen from the following:

pyrolytic graphite[11]
borated tantalum[45]
carbonized tantalum[1]

REFERENCES

1. J.M. Lafferty, Boride Cathodes, J. Appl. Phys. 1951, $\underline{22}$ (3),
    299- 309.

2. R.W. Johnson and A.H. Daane, The Lanthanum-Boron System,
    J. Phys. Chem., 1961, $\underline{65}$, 909 - 915.

3. G.V. Samsonov, Ju. B. Paderno and V.S. Fomenko, Poroshk, Metall,
    1963, (6), 449 - 454.

4. P. Blum and F. Bertaut, Contribution a L'Etude des Borures a
    Teneur Elevee de Bore, Acta Cryst., 1954, $\underline{7}$, 81 - 86.

5. G.A. Meerson, R.M. Manelis and V. Kh. Nurmukhamedov, Preparation
    of Very Pure Stiochiometric Lanthanum Hexaboride, Izv. Akad. Nauk
    SSSR, Neorg. Mat., 1970, $\underline{6}$, (7), 1219 - 1223.

6. N.N, Zhuravlev, R.M. Manelis, I.A, Belousova and V. Kh Nurmukhamedov,
    Izv. Akad. Nauk SSSR, Neorg.Mat., 1973, $\underline{9}$, (7), 1162 - 1165.

7. V.P. Bondarenko,V.V. Morozov and L.V. Chernyak, Interaction of
    LaB_6 and CeB_6 with Refractory Metals, Poroshk. Metall., 1971, (1)
    73 - 78.

8. A.I. Kondrashov, Interaction of LaB_6 with the Carbides and Borides
    of Refractory Metals, Poroshk. Metall., 1974, (11), 58 - 60.

9. G.V. Samsonov, A.I. Kondrashov, L.M. Ochremchuk, I.A. Podchernayeva
    and V.S. Fomenko, Thermoemission Properties of LaB_6 Solid Solutions
    with Refractory Compounds and Nickel. Poroshk. Metall., 1976 (4)
    89 - 91.

10. Yu. B. Kuz'ma, N.S. Bilonizhko and E.M. Nimlovich, the La-Ni-B
    System, Dop. Akad. Nauk. Ukrain, R.S.R. 1973 (A), (10), 939 - 941.

11. G.F. Stepanchikova, Crystal Structures of Compounds in the
    La-Co-B System. Tezisy Dokl., 2nd Vses.
    Konf. Kristallochim-Intermet., 1974, $\underline{71}$, (R.M. Rykhal, Ed.)
    L'vov.

12. Yu. B. Kuz'ma, S.I. Svarichevskaya and N.N. Fomenko, La-Cr-B
     and Ce-Cr-B Systems, Izv. Akad, Nauk, SSSR, Neorg. Mat., 1973,
     9 (9), 1542 - 1545.

13. S.I. Svarichev'ska and Yu. B. Kuz'ma, The La-Mo-B and La-W-B
     Systems, Vestn. L'vov Univ., 1972 (Khim), (14), 24 - 27.

14. Yu. I. Vikhrev, G.W. L'vov, V.P. Savchenko and F.A. Fekhretdinov,
     An Investigation of Composite Thermionic Emitters Based on LaB_6,
     Izv. Leningrad Elektrotekh Inst., 1971, 104, 132 - 136.

15. A.A. Kosyachkov, A.N. Stepanchuk and V. Ya Shlyuko, A Comparison
     of the Properties of Cast and Sintered Lanthanum Hexaboride (casting
     using consumable electrodes),Poroshk, Metal, 1974, 13, (3), 74 - 76.

16. V.S. Fomenko,Handbook of Thermionic Properties (G.V. Samsonov, Ed.)
     Transl. and Pub. Plenum Press Data Division New York 1966.

17. H. Ahmed and A.N. Broers, Lanthanum Hexaboride Electron Emitter, J
     Appl.Phys., 1972, 43, (5) 2185 - 2192.

18. L.W. Swanson and T. Dickinson, Single Crystal Work Function and
     evaporation Measurements of Lanthanum Hexaboride. Appl. Phys.
     Letters., 1976, 28, (10), 578 - 580.

19. C. Oshima, S. Horiuchi and S. Kawai, Thin Film Cathodes of
     Lanthanum Hexaboride, Proc. 6th Int. Vac. Congr. 1974, 281 - 284.

20. C. Oshima, E. Bannai, T.Tanaka and S. Kawai, Thermionic Work
     Function of Lanthanum Hexaboride Single Crystals and Their
     Surfaces, J. Appl. Phys., 1977, 4b , (9), 3925 - 3927.

21. M. Aono, T. Tanaka, E. Bannai and S. Kawai, Structure and
     Initial Oxidation of the Lanthanum Hexaboride (001) Surface,
     Appl. Phys., Letters, 1974, 31, (5), 323 - 325.

22. M. Aono, T. Tanaka, E. Bannai, C. Oshima and S. Kawai, Surface
     States of Lanthanum Hexaboride (001) as Revealed by Angular-
     Resolved Ultra-Violet Photoelectron Spectroscopy, Phys., Rev. B.,
     Solid State, 1977, 16 (8), 3489 - 3492.

23. C. Oshima and S. Kawai, Thermionic Emission of Lanthanum
     Hexaboride Single Crystals and their Surfaces, Oyo Butsuri,
     1976, 45 (7), 600 - 606.

24. A.A. Avdienko and M.D. Malev, Poisoning of Lanthanum Hexaboride
     Cathode, Sov. Phys. Tech. Phys., 1976, 21. (10), 1230 - 1234.

25. S. Hosoki, S. Yamamoto, K. Hayakawa and H. Okano, Surface
     Condition and Thermionic Emission of Lanthanum Hexaboride, Proc.,
     6th Int. Vac. Cong., 1974, 285 - 288.

26. G.M. Kuznetsova and G.A. Kudintseva, Mechanism of Emission from
     Lanthanum Hexaboride Cathodes, Izv. Akad. Nauk. SSSR, 1973, (Fiz.),
     37 (12), 2508 - 2512.

27. A. Berrada, J.F. Mercurio, J. Etourneau, F. Alexandre, J.B. Theeton,
     and Tran Minh Duc, Thermionic Emission Properties of LaB_6 and CeB_6
     in Connection with their Surface States, Examination by XPS, Auger
     Spectroscopy and the Kelvin Method, Surface Science, 1978, 72,
     177 - 188.

28. S.P. Gordienki, E.A. Guseva and V.V. Fesenko, An Investigation of
     the Thermodynamic Properties of Lanthanum Hexaboride, Teplofizika
     Vysokikh Temperatur, 1968, (5), 821 - 825.

29. T. Barry and T.G. Chart, National Physical Laboratory,1977, Private
     Communication.
30. V.V. Fesenko, A.S. Bolgar and S.P. Gordienko, Rev. Hautes Temper.
     Refract., 1966, 3 , 261 - 271.

31. M. Takagi and M. Ishii, Growth of LaB_6 Single Crystals by a
     Laser-Heated Floating Zone Method, J. Cryst. Growth, 1977,
     40, 1 - 5.

32. J.D. Verhoeven, E.D. Gibson, M.A. Noack and R.J. Conzemus,
     J. Cryst. Growth, 1976, 36, 115 - 120.

33. P.K. Smith and P.W. Gilles, US At. Energy Comm. COO-1140-103.,
     1964. Quoted by F.A. Shunk in "The Constitution of Binary
     Alloys', M. Hansen and K. Anderko, Second Supplement, 1969.

34. A. Deacon and S.E.R. Hiscocks, On the Growth and Properties of Single-Crystal Lanthonum Tetraboride, LaB_4, J. Mat. Sci., 1971, 6 (4) 309 - 312.

35. J.D. Verhoeven and R.D. Gibson, Evaluation of a LaB_6 Cathode Electron Gun, J. Phys. E.: Sci. Instr., 1976, 9 (1), 65 - 69.

36. M. Futamoto, S. Hosoki, H. Okano and U. Kawabe, Field Emission and Field-Ion Miscrocopy of LaB_6, J. Appl. Phys., 1977, 48, (8), 3541 - 3546.

37. R. Shimizu, T. Shinike, S. Kawai and T. Tanaka, Stability of Beam Current of Single-Crystal LaB_6, Cathode in High Vacuum , J. Jap. Appl. Phys., 1977, 16 (4) 669 - 670.

38. P.H. Schmidt, D.C. Joy, L.D. Longinotti, H.J. Leamy and S.D. Ferris, Anisotropy of Thermionic Electronic Emission Values for LaB_6 Single Crystal Emitter Cathodes, Appl. Phys. Letters, 1976, 29, (7), 400 - 401.

39. J.D. Verhoeven, E.D. Gibson and M. Nock, Influence of Crystallography and Purity on Brightness of LaB_6 Cathodes, J. Appl. Phys., 1976, 47, (11), 5105 - 5106.

40. J.W. Gadzuk and E.W. Plummer, Field Emission Energy Distribution, Rev. Mod. Phys., 1973, 45 (3), 487 - 548.

41. E.E. Windsor, Construction and Performance of Practical Field Emitters from LaB_6. Proc. Inst. Elec. Eng., 1969, 166, (3), 343 - 350.

42. W.W. Blair and R. Lane, Controlled Method of Melting LaB_6 Cathodes Prior to Fabricating Fine Tips, IBM Technical Disclosure Bulletin, 1972, 15 (1), 162.

43. T. Aita, U. Kuwabe, Y Honda, Single Crystal Growth of Lanthanum Hexaboride in Molten Aluminium, Jap. J. Appl. Phys., 1974, 13, (2), 391.

44. M. Futamoto, T. Aita, and U. Kawabe, Crystallographic Properties of LaB_6 formed in Molten Aluminium, Jap. J. Appl. Phys., 1975, 14, (9), 1263 - 1266.

45. H. Yamauchi, K. Takagi, I. Yuito and U. Kawabe, Work Function of Lanthanum Hexaboride, Appl. Phys. Letters, 1976, 29 (10), 638-640.
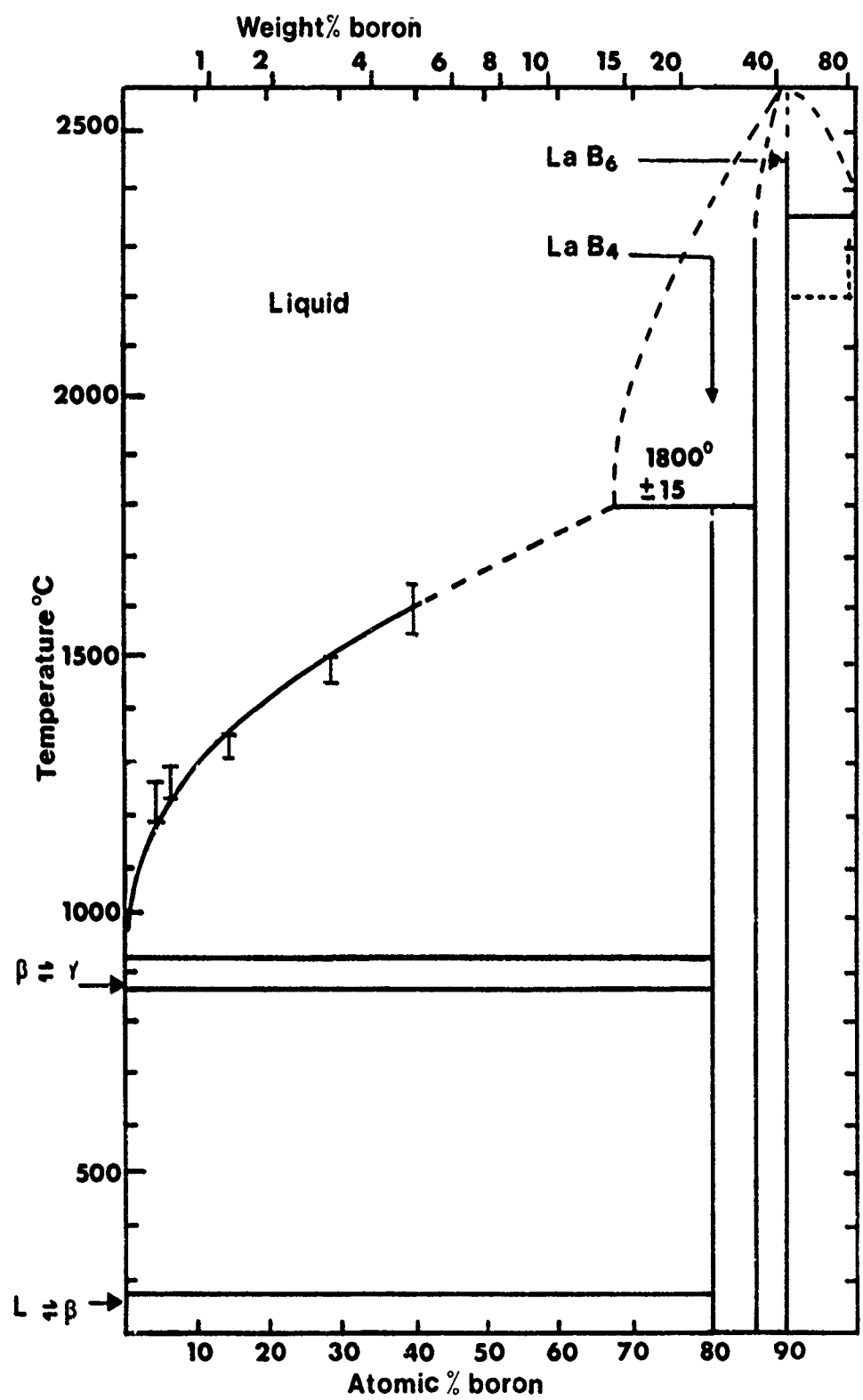
Figure 1. Phase diagram proposed for the lanthanum – boron system

(Johnson and Daane, ref. 2 1961)

Figure 2. Crystal structure of LaB_6 : Cubic, Space Group O_H^I P_M 3_M
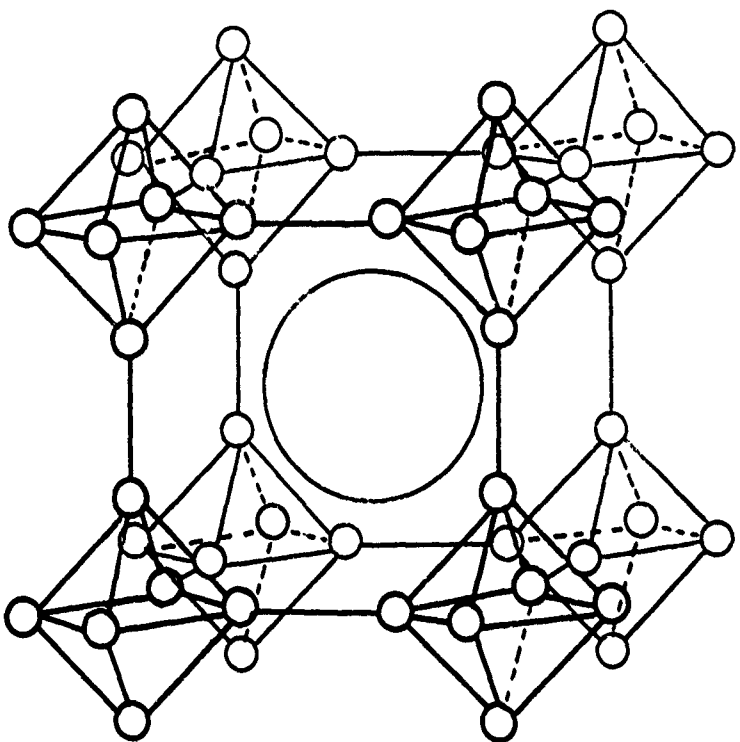
La sites: $\frac{1}{2}$ $\frac{1}{2}$ $\frac{1}{2}$

B sites: $x00$; $0x0$; $00x$;
$\bar{x}00$; $0\bar{x}0$; $00\bar{x}$
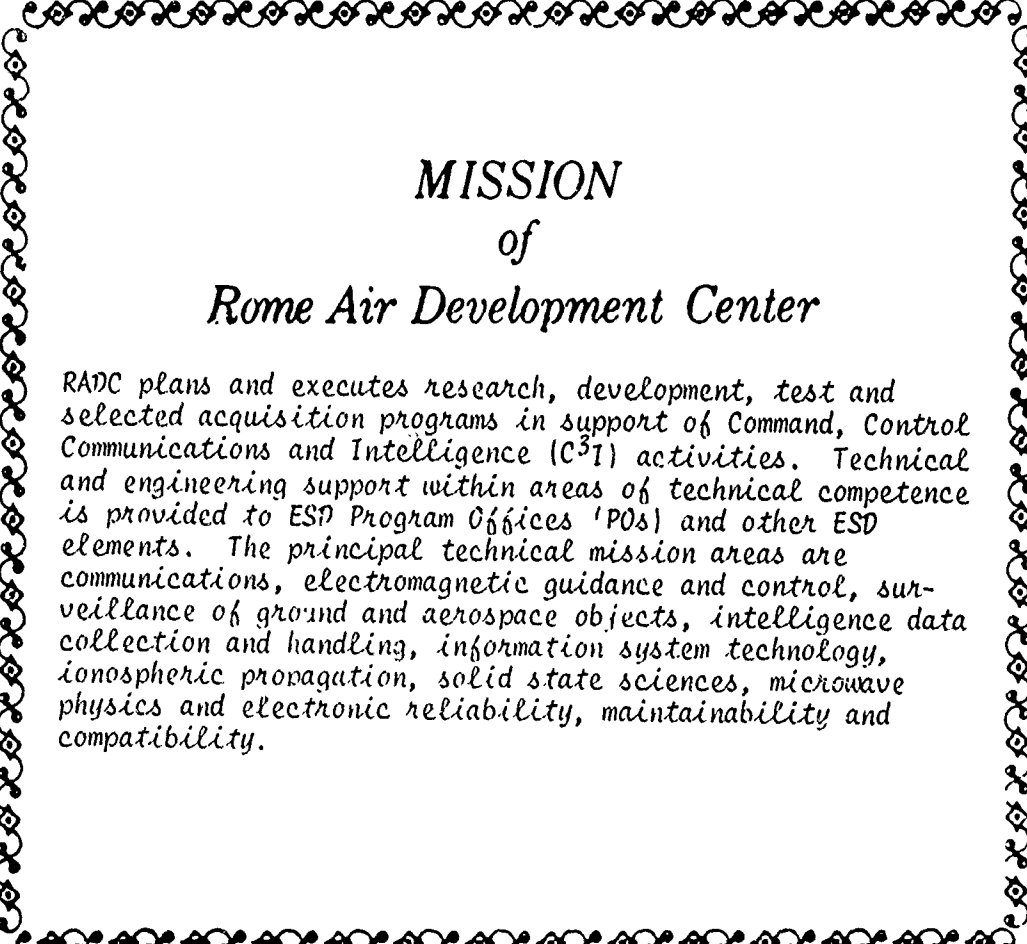
MISSION
of
Rome Air Development Center

RADC plans and executes research, development, test and selected acquisition programs in support of Command, Control Communications and Intelligence (C^3I) activities. Technical and engineering support within areas of technical competence is provided to ESD Program Offices (POs) and other ESD elements. The principal technical mission areas are communications, electromagnetic guidance and control, surveillance of ground and aerospace objects, intelligence data collection and handling, information system technology, ionospheric propagation, solid state sciences, microwave physics and electronic reliability, maintainability and compatibility.